



# CMOS MAPS: Design Challenges and State of the Art

Lucio Pancheri

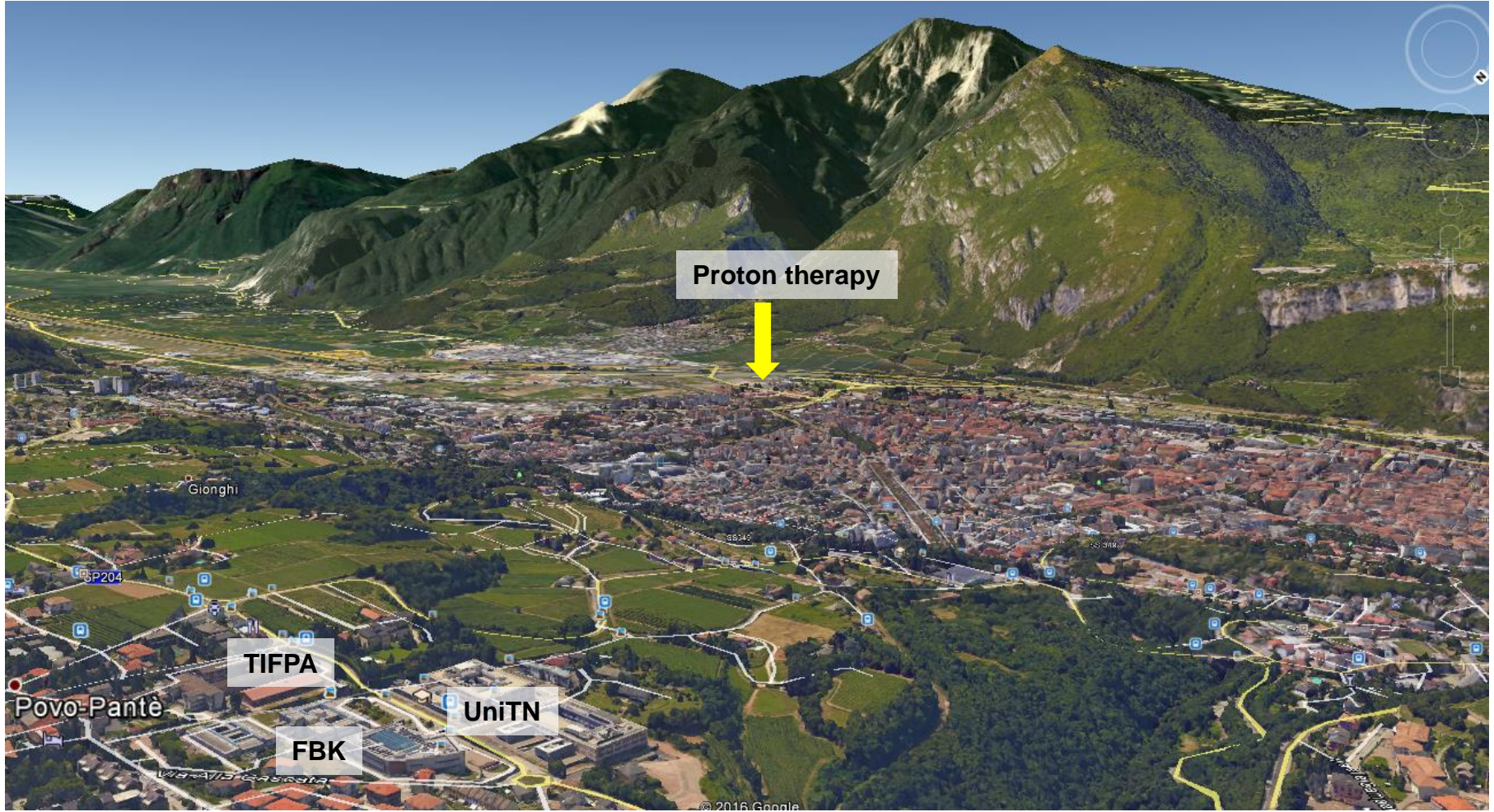
Department of Industrial Engineering, University of Trento  
TIFPA – INFN, Trento

Cogne, 12- 16 February 2018



# Research on silicon detectors in Trento

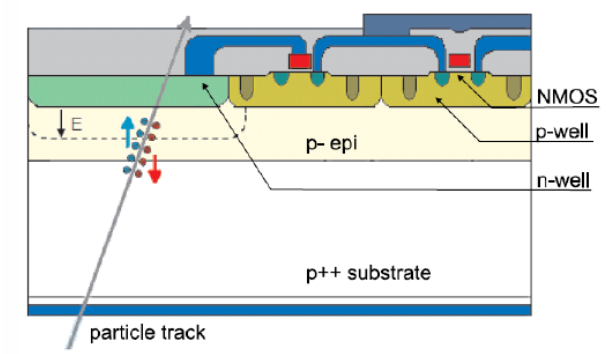
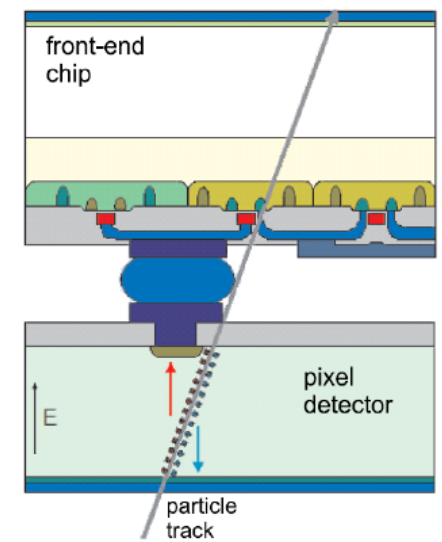






# Pixel detectors for tracking in HEP

- **Hybrid Pixel Sensors**
  - Adopted in major experiments at LHC (ATLAS, CMS, ALICE)
  - Detectors and electronics are developed and optimized separately
  - Excellent radiation damage tolerance
- **Monolithic Active Pixel Sensors (MAPS)**
  - Detectors and electronics fabricated on the same substrate
  - Emerging, still not widespread in HEP



L. Gonella, Particle Physics Seminar, 2017



# MAPS development - motivation

---

- Adoption of MAPS in HEP applications:
  - Higher spatial resolutions
  - Lower material budget
  - Cost
  
- Synergies outside HEP tracking applications:
  - X-ray imaging
  - IR imaging
  - Medical imaging with particles
  - Space



# Outline

---

- Radiation detection in silicon
- CMOS technologies: characteristics, opportunities and challenges
- Monolithic active pixels for photon imaging
- MAPS: design approaches and research directions
- SEED project overview



# Outline

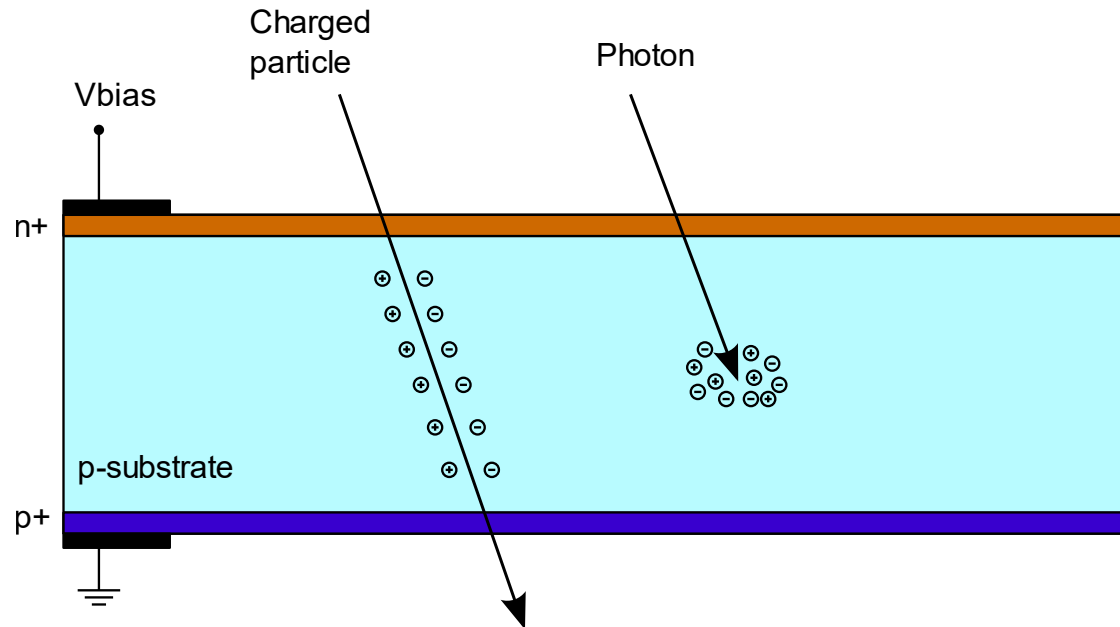
---

- Radiation detection in silicon
- CMOS technologies: characteristics, opportunities and challenges
- Monolithic active pixels for photon imaging
- MAPS: design approaches and research directions
- SEED project overview



# Radiation signal detection

- Charge generation
- Charge collection
- Amplification – analogue processing (shaping)
- Recording (Signal Amplitude, Thresholding, Time of arrival, Signal Width)

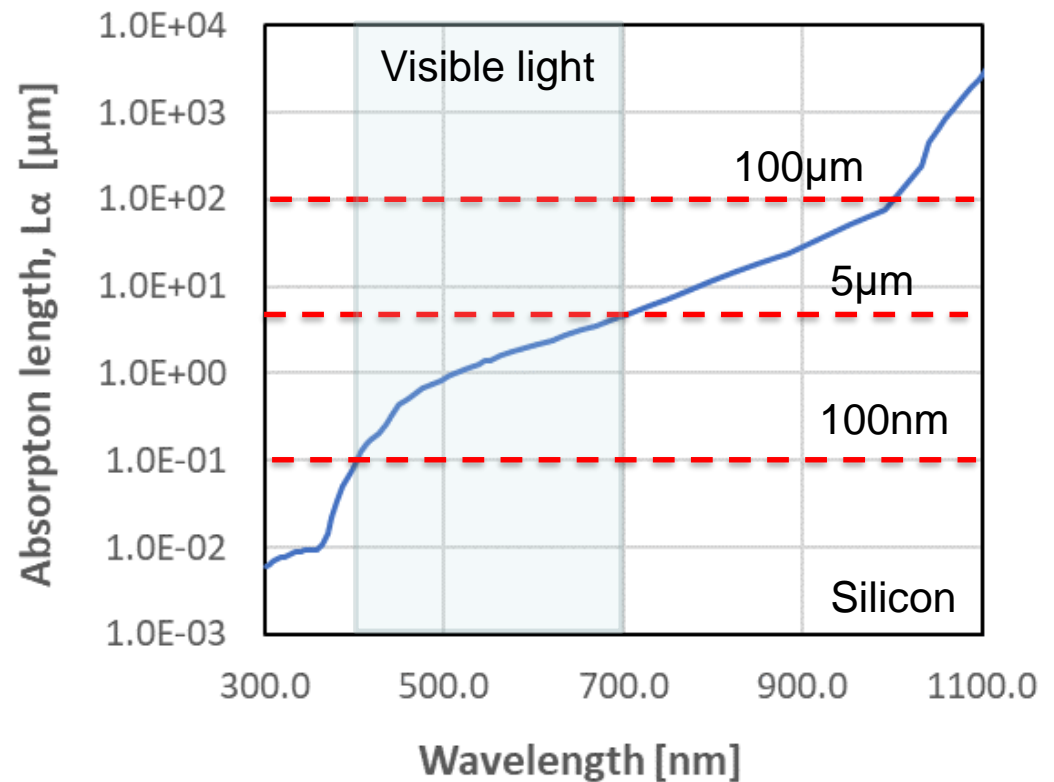
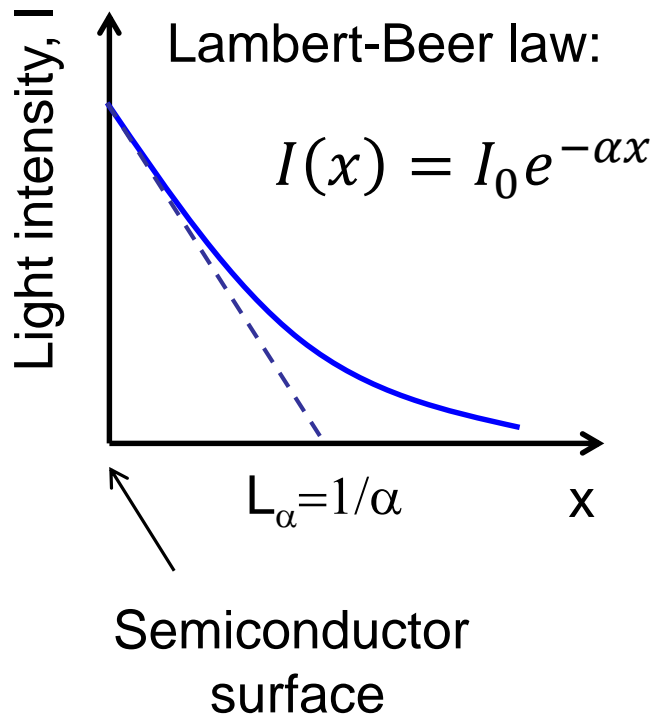






# Photons: absorption length

NUV – Visible – NIR light: 1 e-h pair per photon





# X-rays

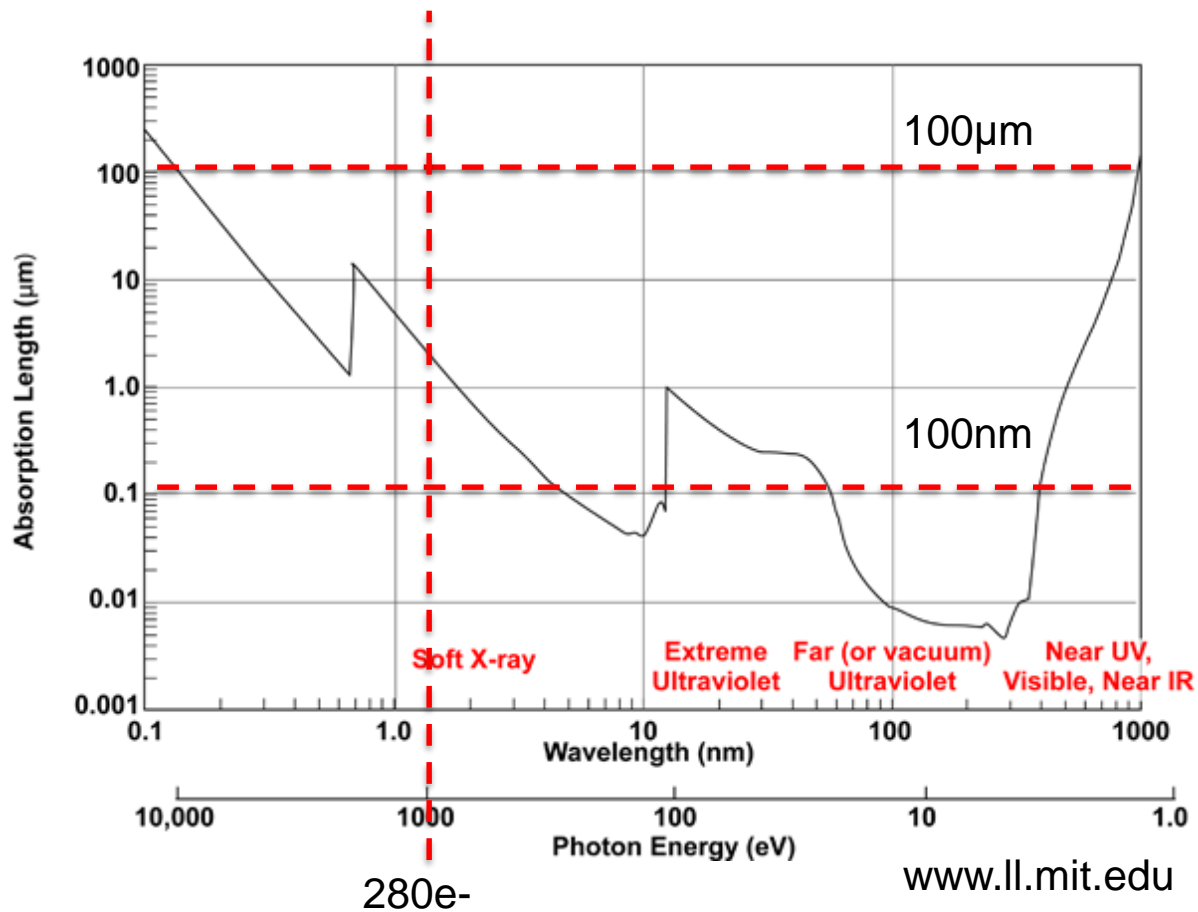
EUV, X-rays: “Point-like” interaction with the production of many e-h pairs in a small region, a few μm wide.

Average number of e-h pairs:

$$n_{e-h} = \frac{E_{ph}}{E_{ion}}$$

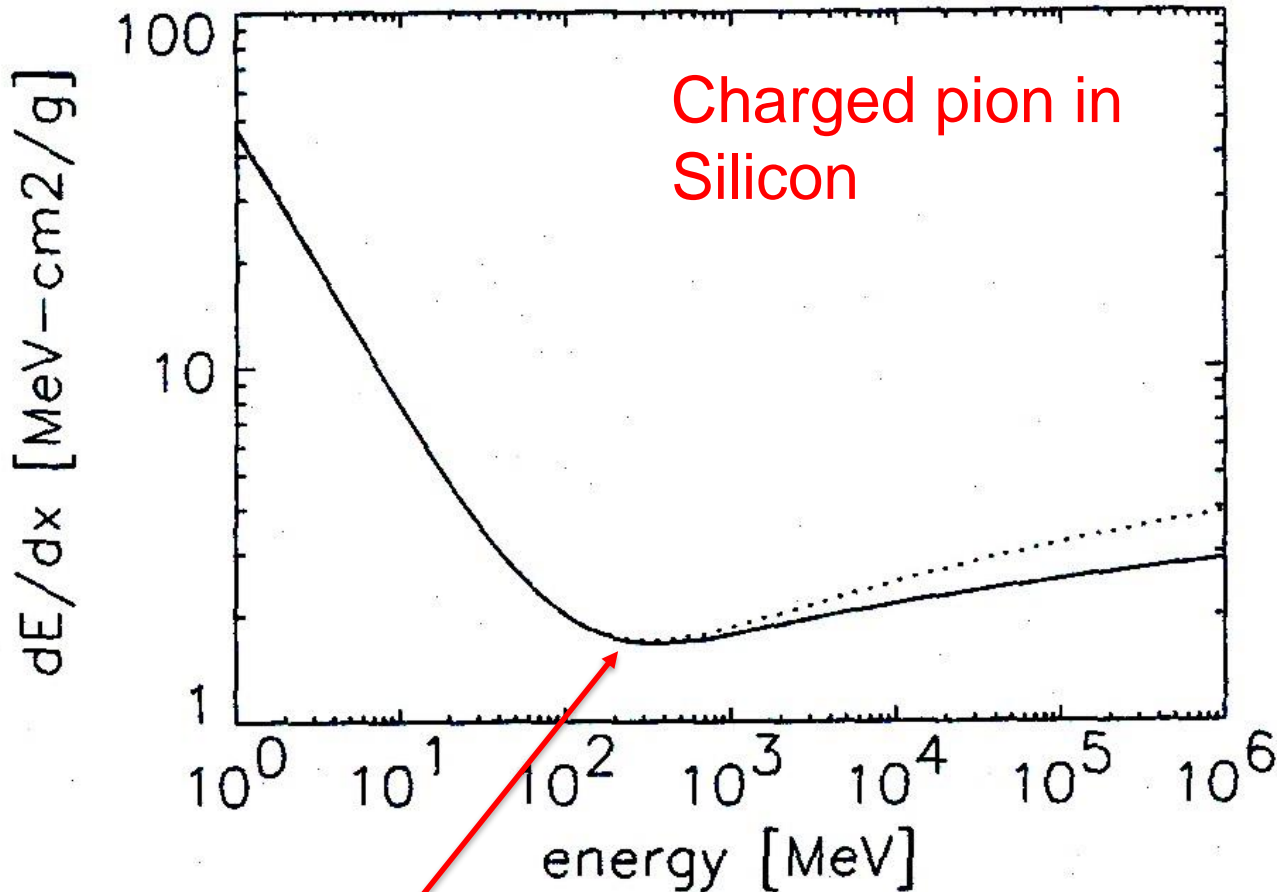
Si ionization energy

$$E_{ion} = 3.6\text{eV}$$





# Charged particles: ionization energy loss in Si



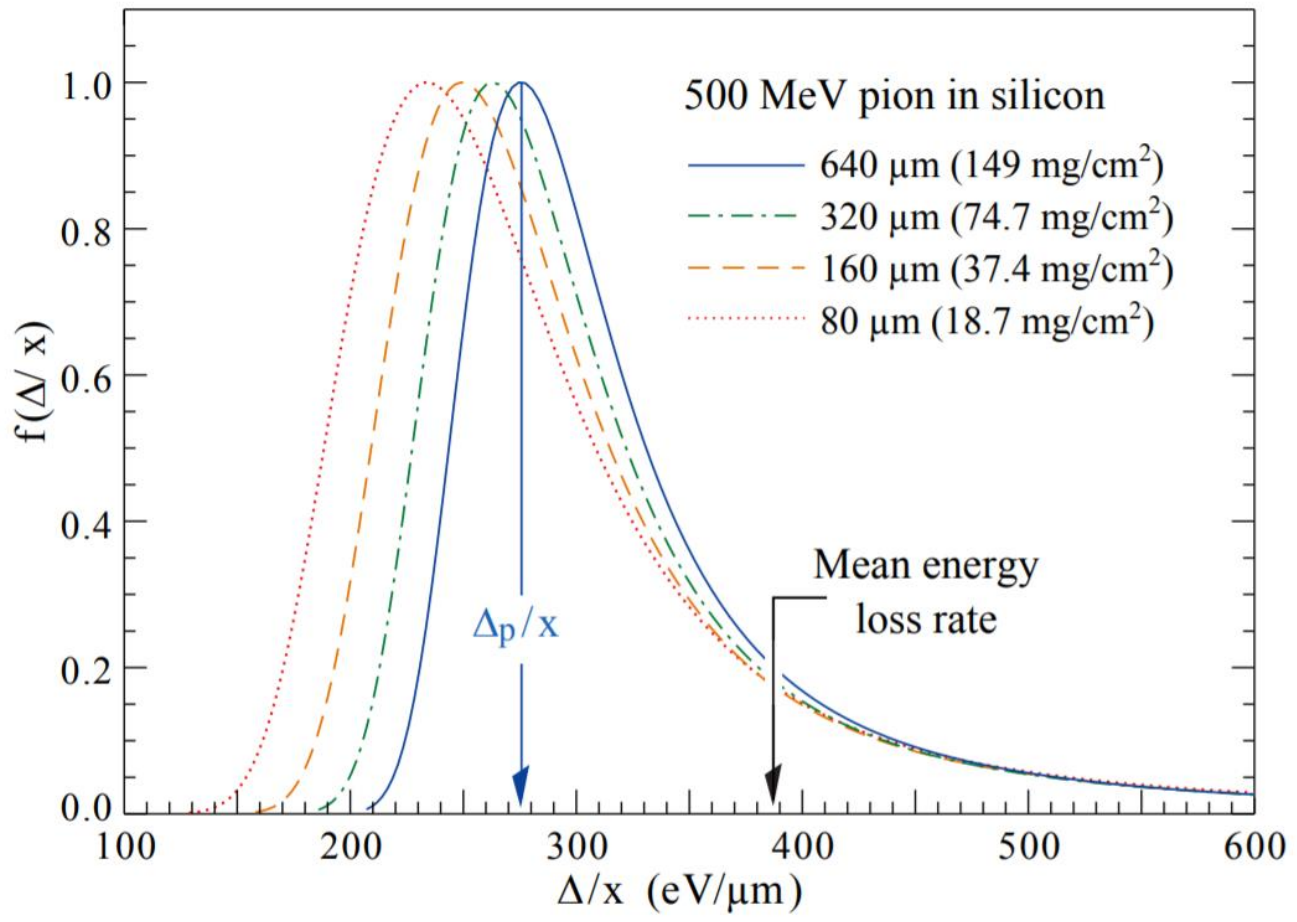
Charged pion in Silicon

Minimum Ionizing Particle (MIP)

G.Lutz, Semiconductor Radiation detectors, Springer, 1999



# Energy loss distribution in silicon

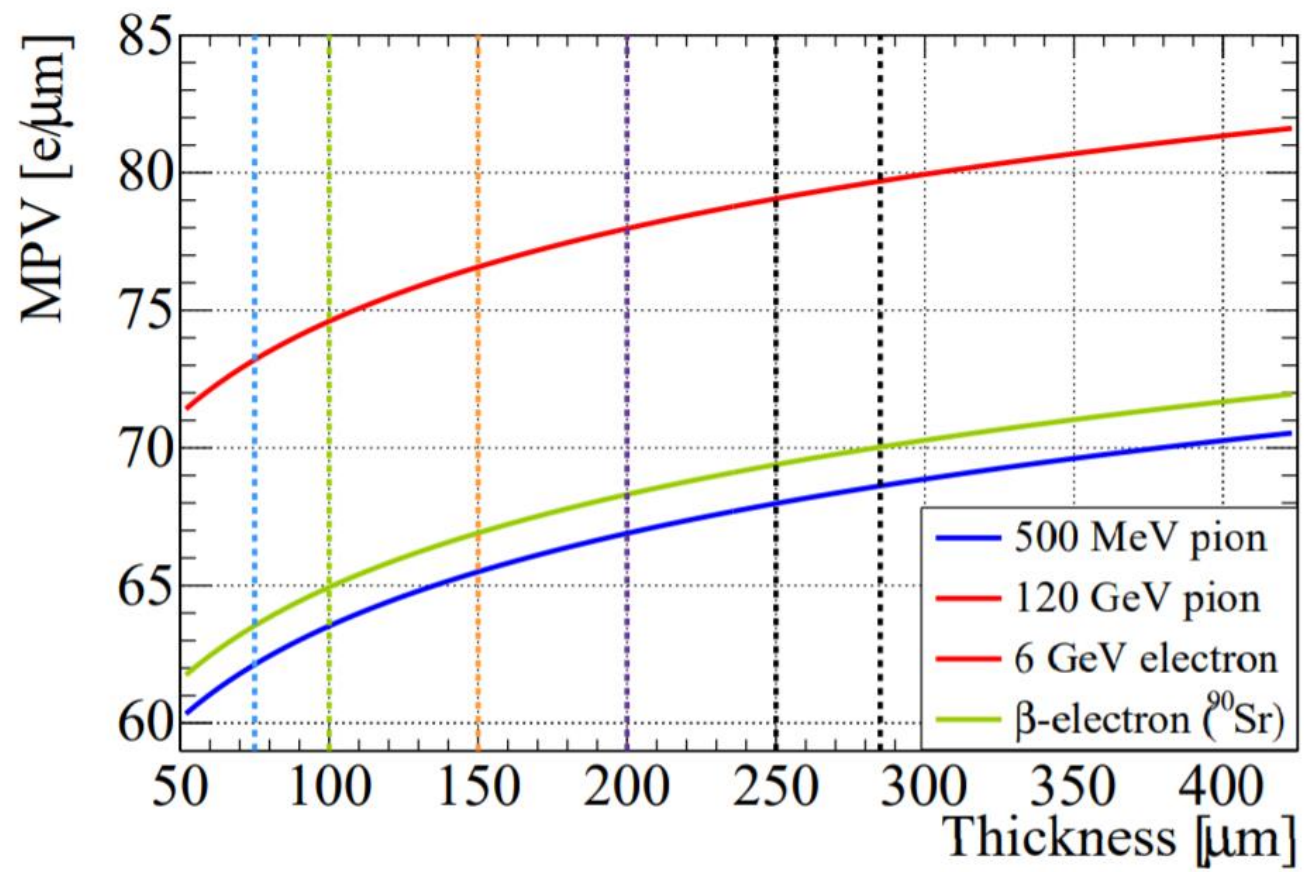


**Landau distribution**

S.Terzo, PhD thesis, MPI, 2015



# Generated electrons vs. thickness



S.Terzo, PhD thesis, MPI, 2015

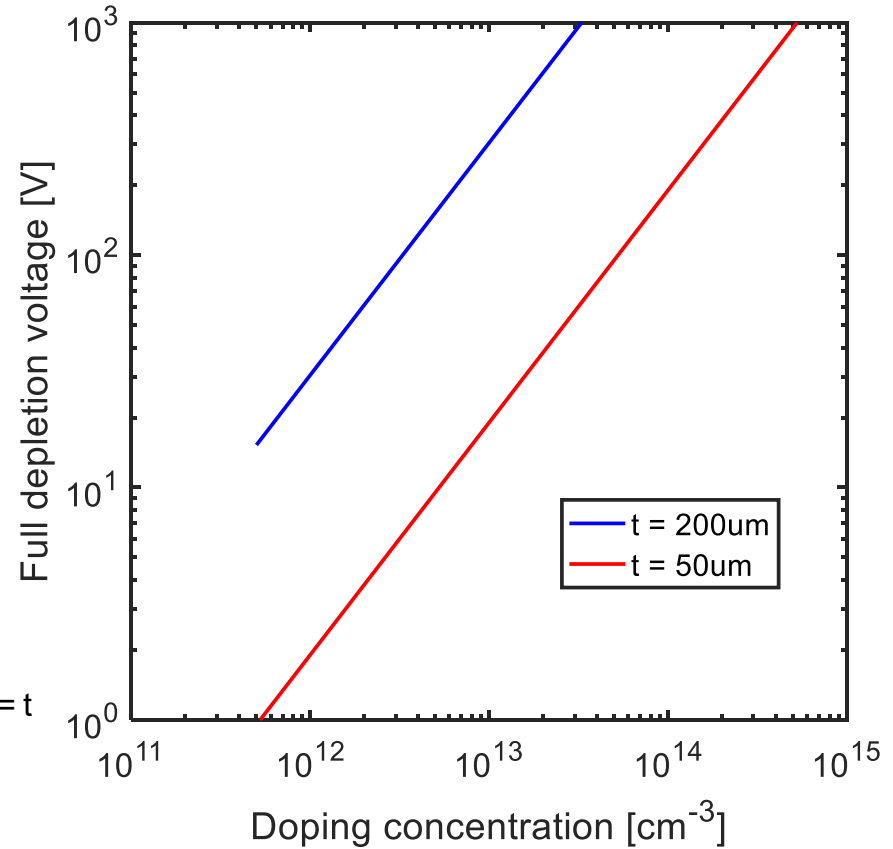
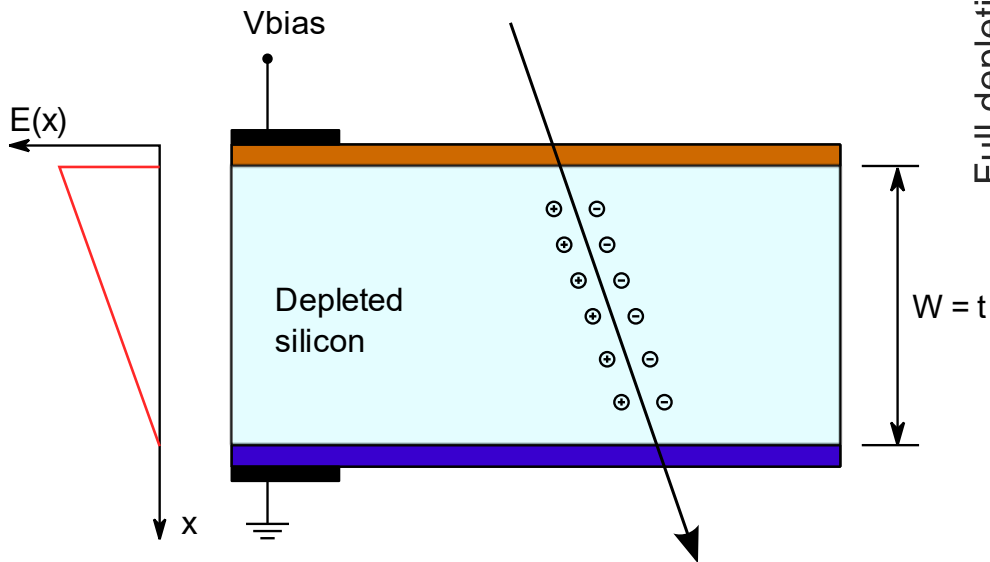


# Detector bias

Minimum bias voltage for full depletion:

$$V_{bFD} \cong \frac{qNt^2}{2\epsilon_s}$$

N: detector doping  
t: detector thickness

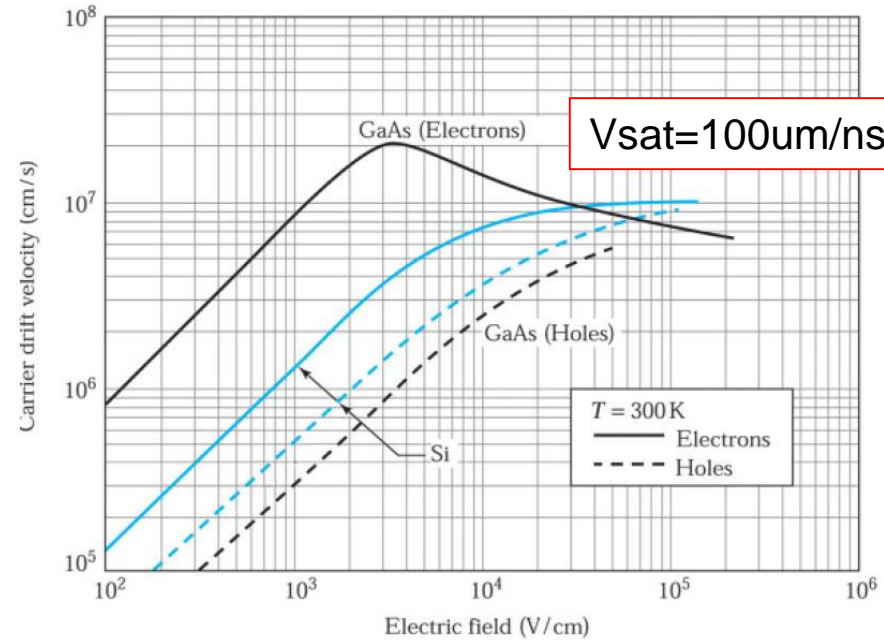
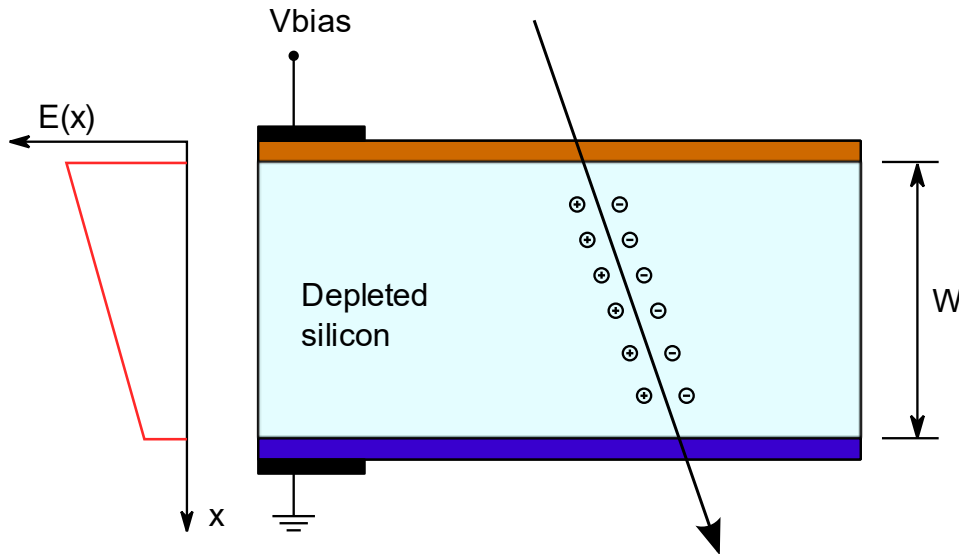




# Charge collection

In a **fully depleted** detector, collection speed depends on carrier transit time in the depleted region ( $W$ )

$$t_1 = \frac{W}{v} = \frac{W^2}{\mu V_{bias}} \geq \frac{W}{v_{sat}}$$



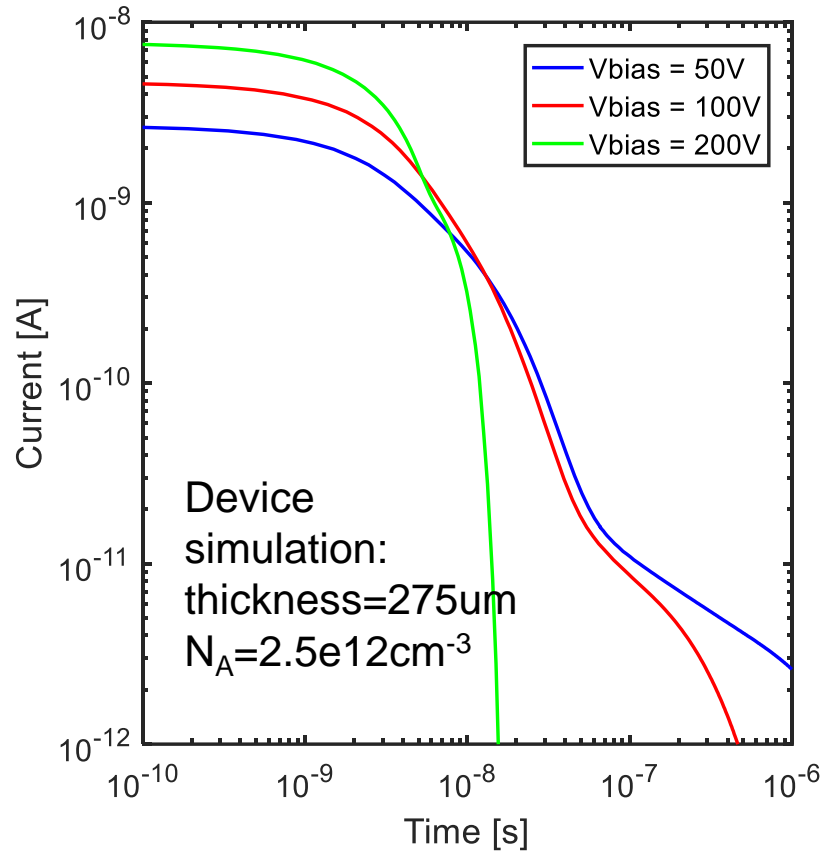
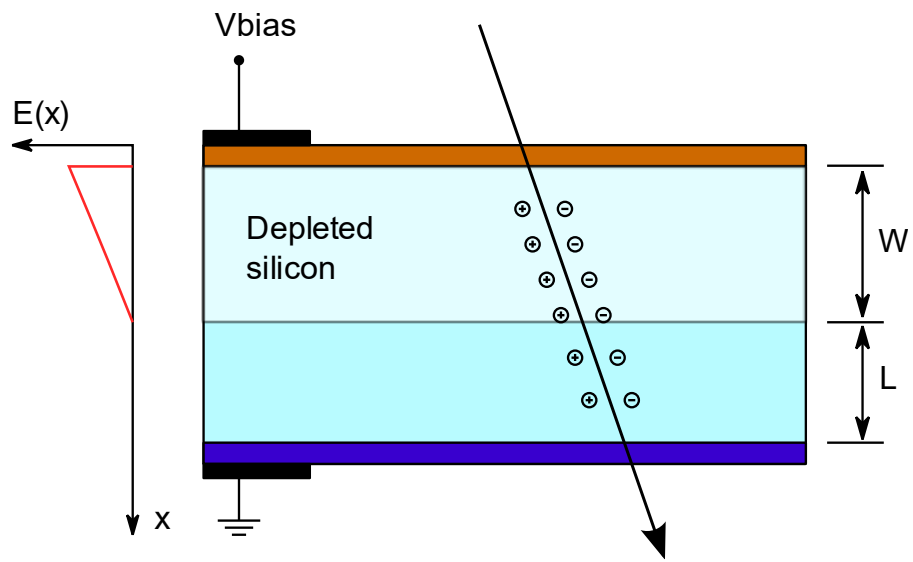
Sze, Semiconductor devices, Wiley & Sons, 2012



# Charge collection

In a **partially depleted** detector, there is a contribution of diffusion time in the non-depleted region ( $L$ )

$$t_2 = \frac{L^2}{2D}$$

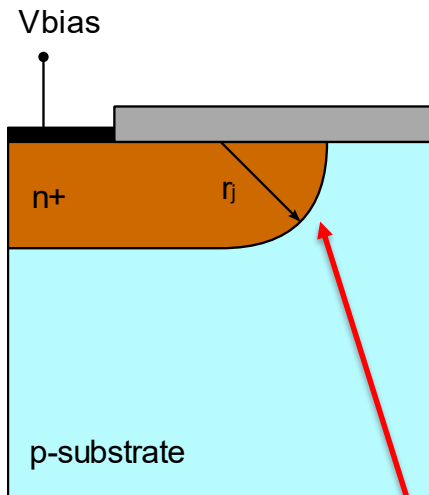




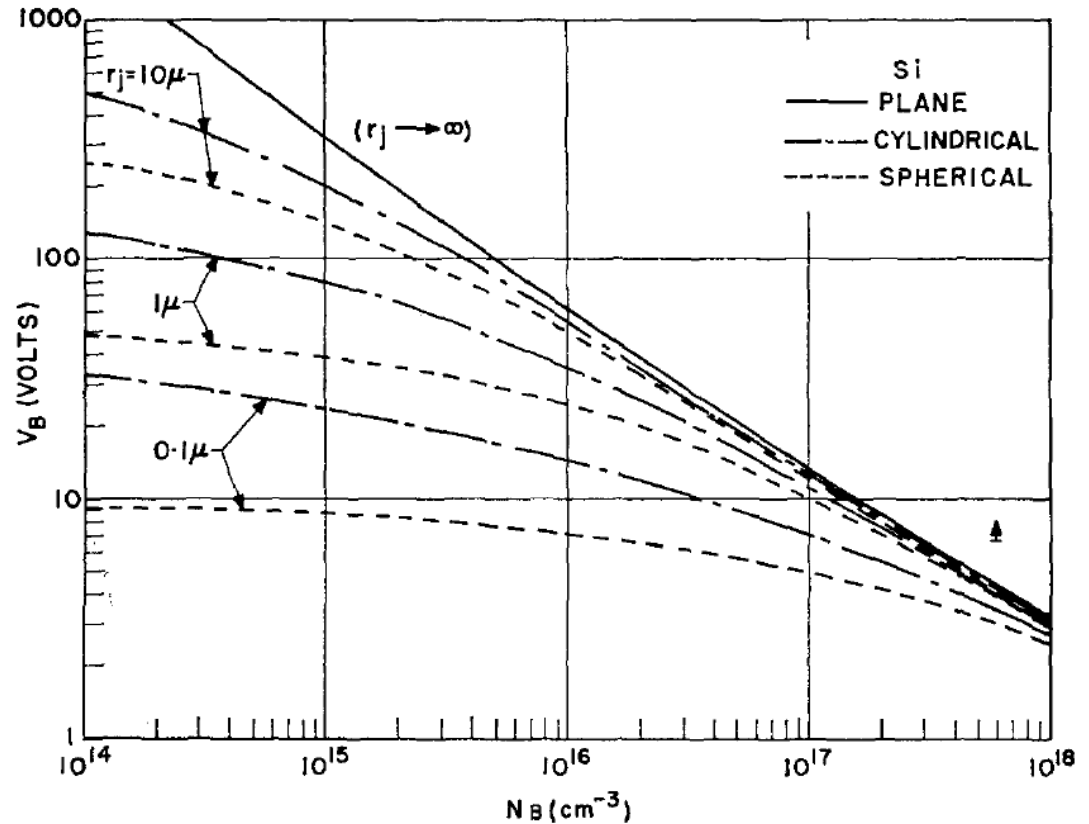


# Detector bias

Early breakdown at the junction borders



Electric field intensification



Sze and Gibbons, Solid-state Electron., 1966



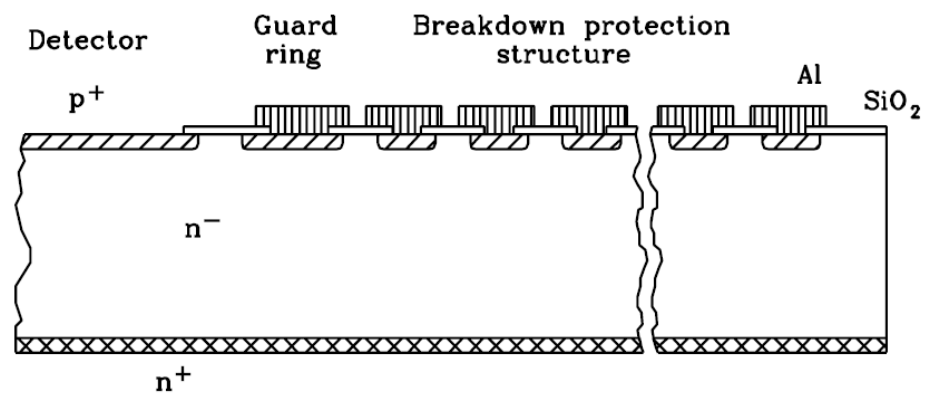


# Detector bias

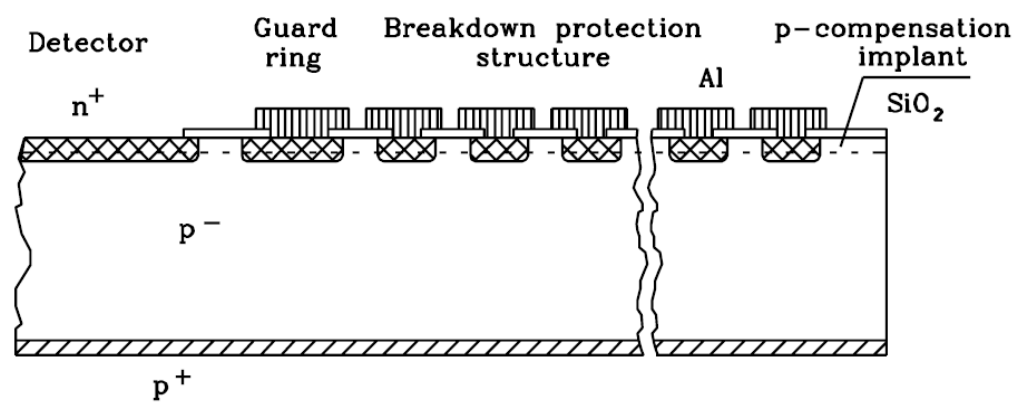
Handling Large Bias Voltages:

- Deep implantations or diffusion (large  $r_j$ )
- Multiple guard rings protection structures

p-on-n



n-on-p



G.Lutz, Semiconductor Radiation detectors, Springer, 1999

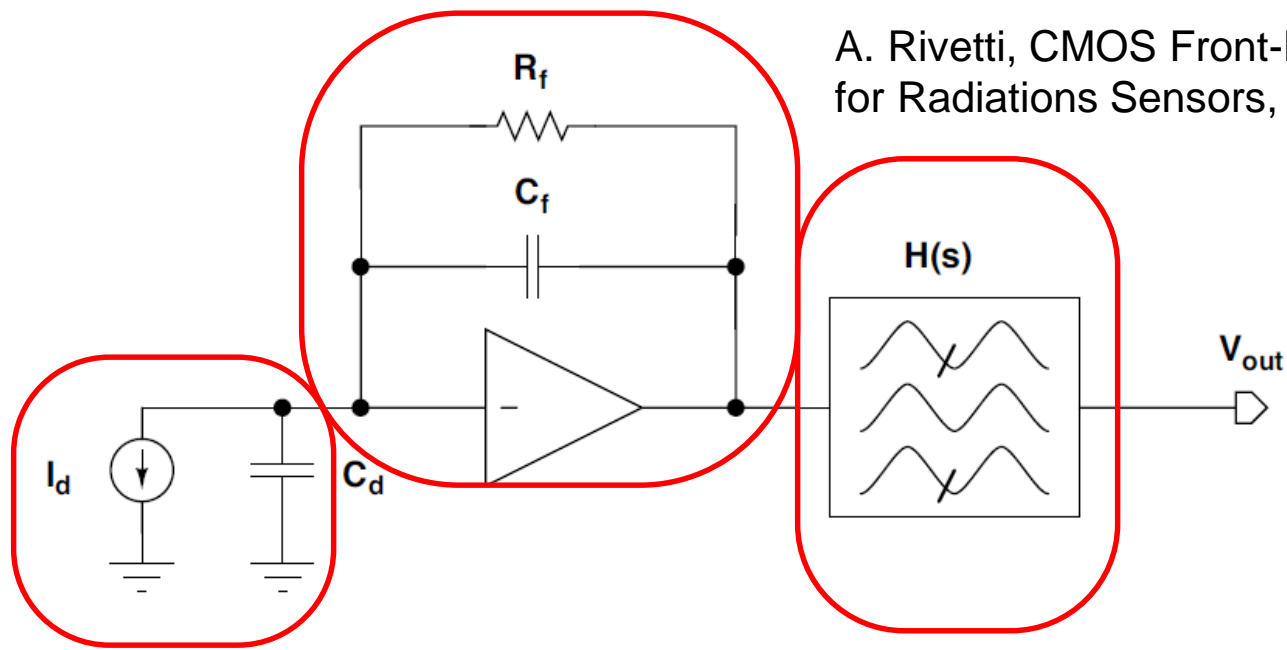


# Readout electronics

## Preamplifier:

Charge to voltage conversion

$$\text{gain: } 1/C_f$$



A. Rivetti, CMOS Front-End Electronics for Radiations Sensors, CRC Press, 2015

## Detector:

provides current signal

## Shaper (band-pass filter):

optimized SNR  
(minimizes ENC)

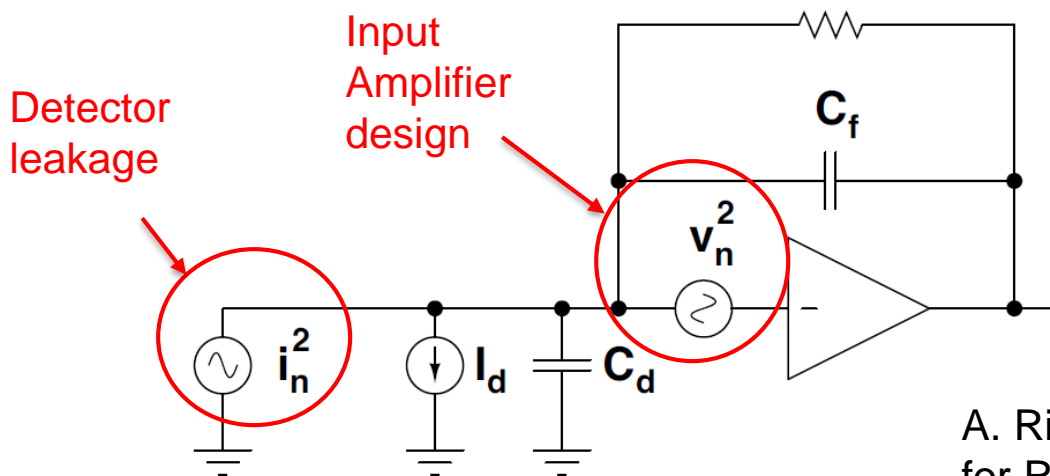


# Requirements for low-noise

- Low **detector** and amplifier input **capacitance**
- Low detector **leakage current**
- Optimized amplifier design
- Optimized shaping filter

Total noise summarized with the **Equivalent Noise Charge (ENC)**

$$ENC^2 = (C_d + C_{in})^2 \left( A_w \underbrace{v_n^2}_{\text{red circle}} \frac{1}{T_p} + A_f K_f \right) + A_p \underbrace{i_n^2}_{\text{red circle}} T_p$$



A. Rivetti, CMOS Front-End Electronics for Radiations Sensors, CRC Press, 2015



# Radiation damage in detectors

---

Two general types of radiation damage to the detector materials:

- 1) **Surface damage** due to **Ionizing Energy Loss (IEL)**:  
accumulation of positive charge in the oxide ( $\text{SiO}_2$ ) and at the  $\text{Si}/\text{SiO}_2$  interface
- 2) **Bulk (Crystal) damage** due to **Non Ionizing Energy Loss (NIEL)**:  
displacement damage, built-up of crystal defects

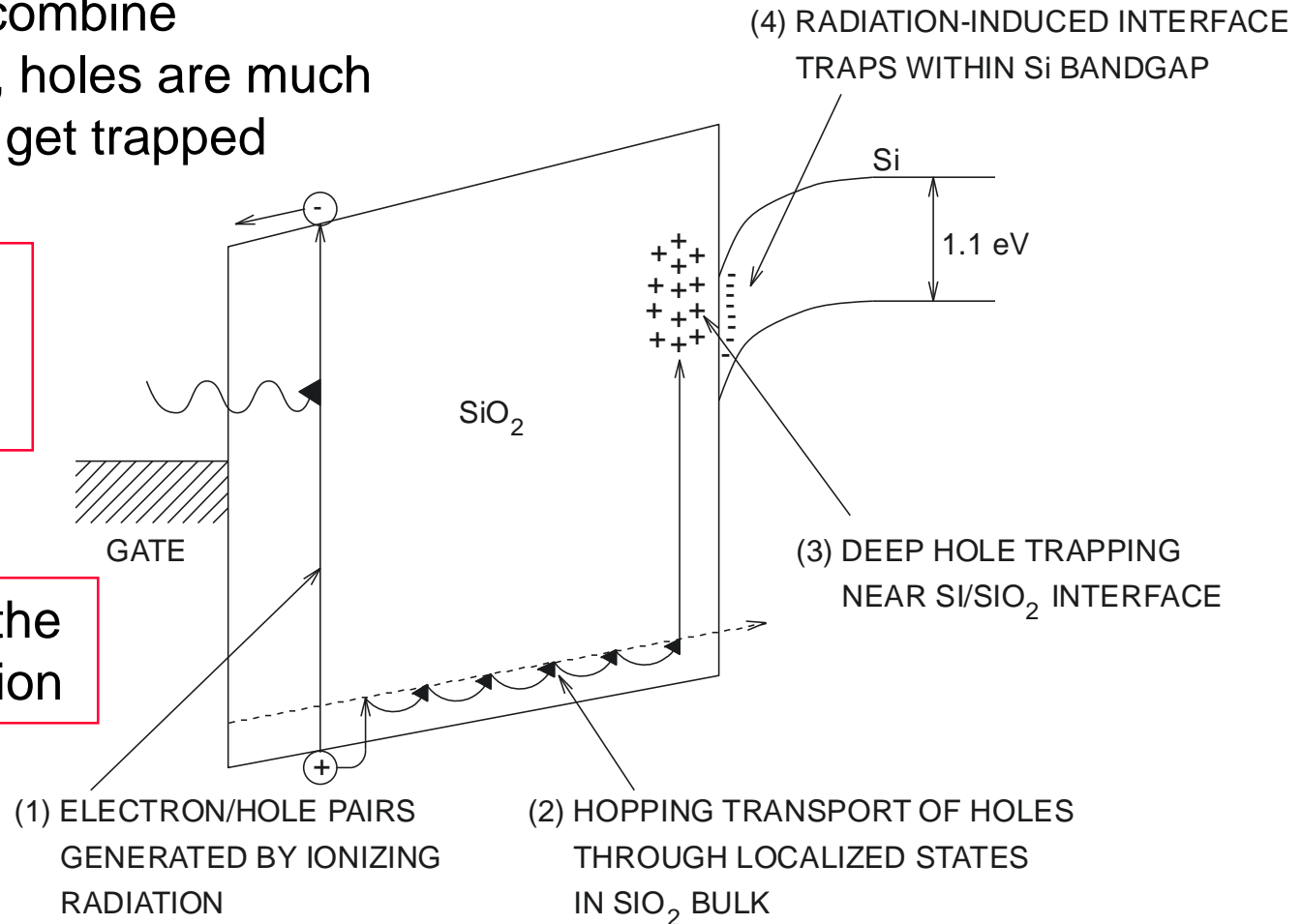


# Surface radiation damage

- Most e-h pairs recombine
- Electrons escape, holes are much slower and finally get trapped

$\text{SiO}_2$ :  
 $\mu_n \sim 20 \text{ cm}^2/(\text{Vs})$ ,  
 $\mu_p \sim 2 \times 10^{-5} \text{ cm}^2/(\text{Vs})$

- Strong effects of the bias during irradiation



T.R. Oldham, Ionizing radiation effects in MOS oxides, World Scientific, 1999



# Consequences for detectors

---

1. Positive fixed oxide charge density induces a negative charge at the Si-SiO<sub>2</sub> interface, which affects:
  - a) isolation between n<sup>+</sup> regions;
  - b) parasitic capacitance between adjacent regions (→ noise);
  - c) electric fields at surface: breakdown;
  
2. Surface generation/recombination leads to increased surface leakage current;

Radiation effects may vary with detector structure ...

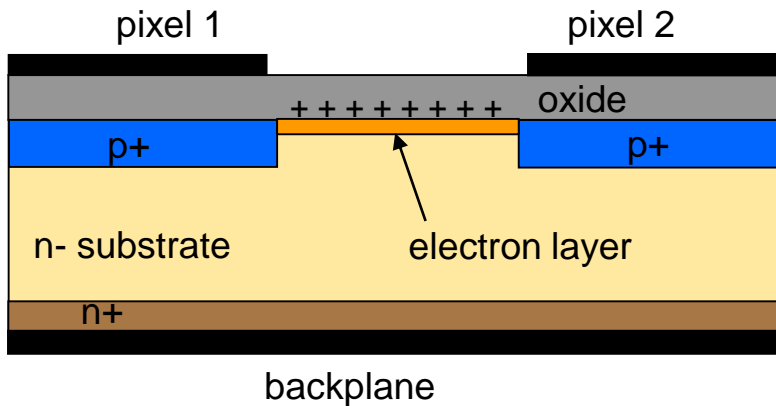




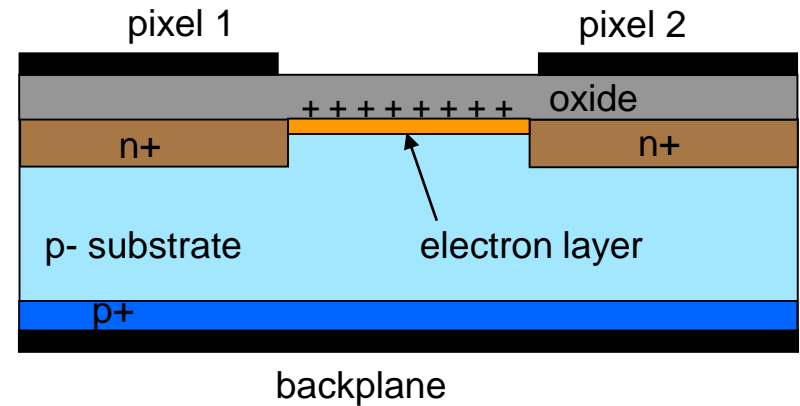
# P-on-N vs N-on-P

With reference to pixel detectors

## P-on-N



## N-on-P (N-on-N)



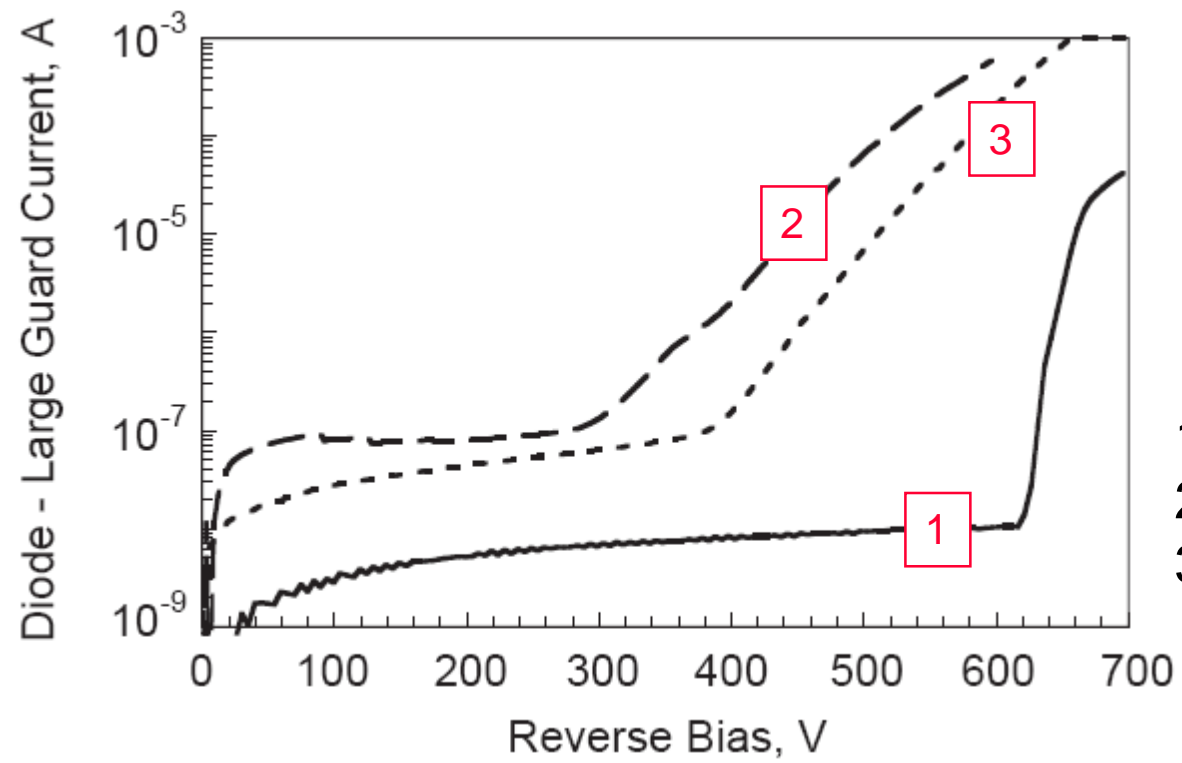
- Pixels are “**self-isolated**”
- Increase of oxide charge density further improves isolation, but:
  - reduces **breakdown** voltage
  - increases inter-pixel **capacitance**

- Pixels are connected by electrons
- Need for **isolation structures**



# P-on-N: edge breakdown

Irradiation: CNR Bologna,  $^{60}\text{Co}$  gamma source, 200krad(Si)



- 1. pre-irradiation
- 2. soon after irradiation
- 3. four days after irradiation

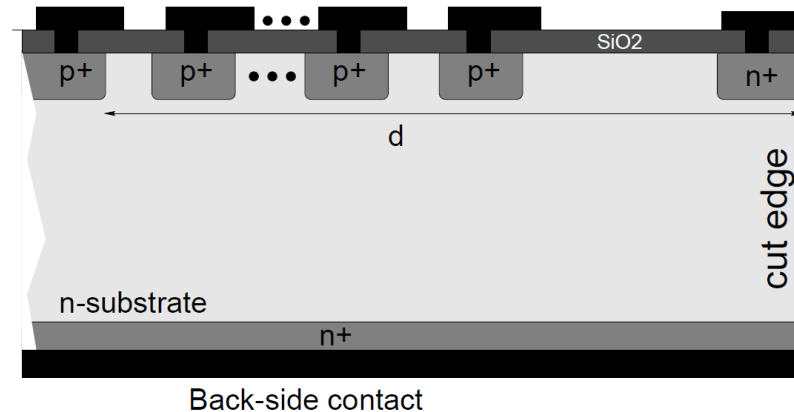
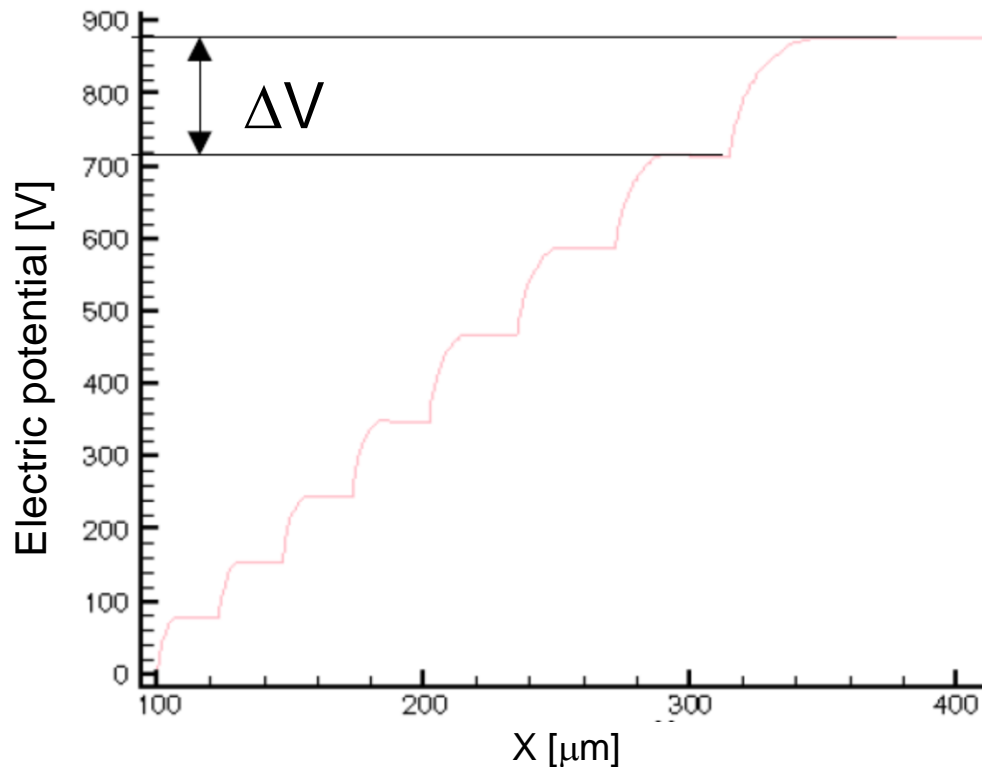
M. Da Rold, et al., IEEE TNS 44(3) (1997) 721

Breakdown voltage decreases after irradiation, and is slightly recovered with room temperature annealing



# Multiple rings with field plates

- Guard ring potential scales according to punch-through spreading
- The potential (field) can be evenly distributed enhancing the breakdown voltage, at the expense of dead area at the edges
- Main design parameters: ring spacing, FP size, oxide thickness



M. Da Rold, et al., IEEE TNS 46(5)  
(1999) 1215, and references therein



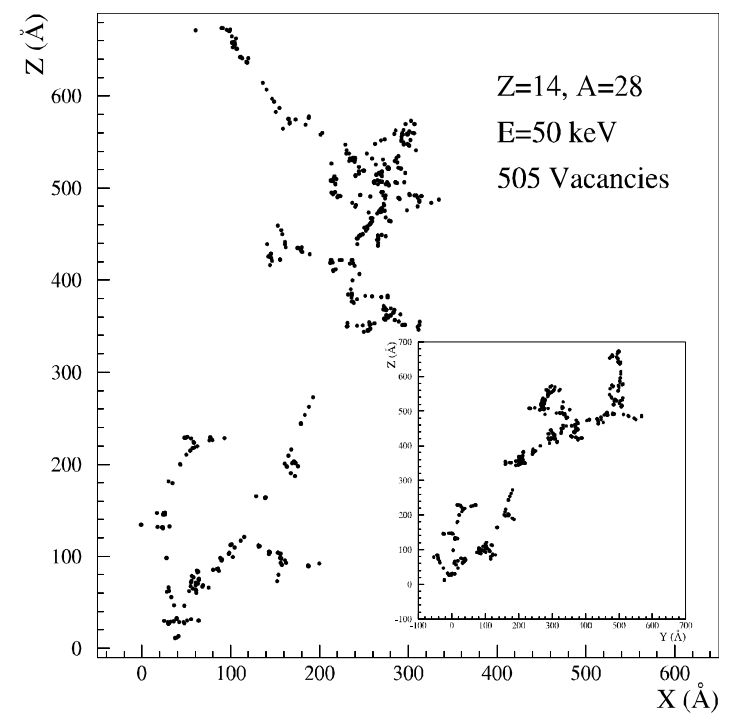
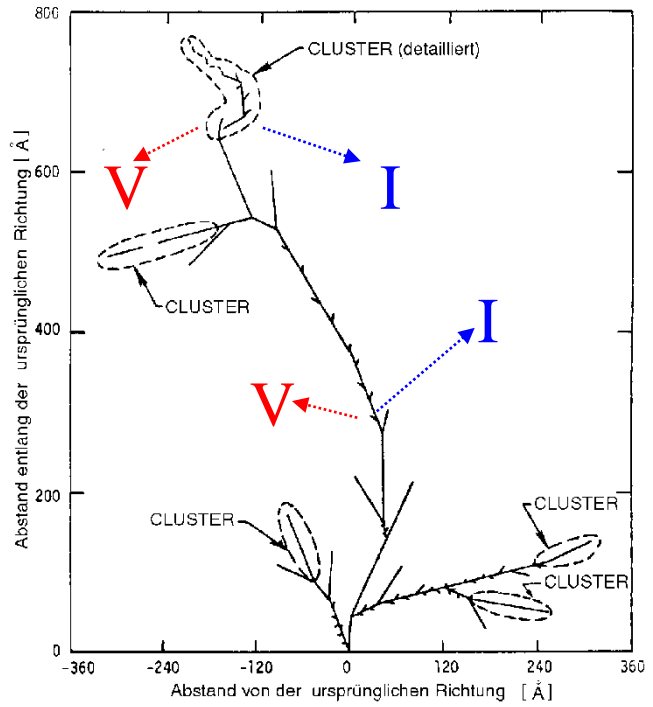
# Radiation Damage – Bulk Effects

Spatial distribution of vacancies created by a 50 keV Si-ion in silicon.

(typical recoil energy for 1 MeV neutrons)

M.Huhtinen 2001

van Lint 1980

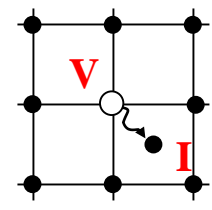


particle



$E_K > 25 \text{ eV}$

$E_K > 5 \text{ keV}$



Vacancy + Interstitial

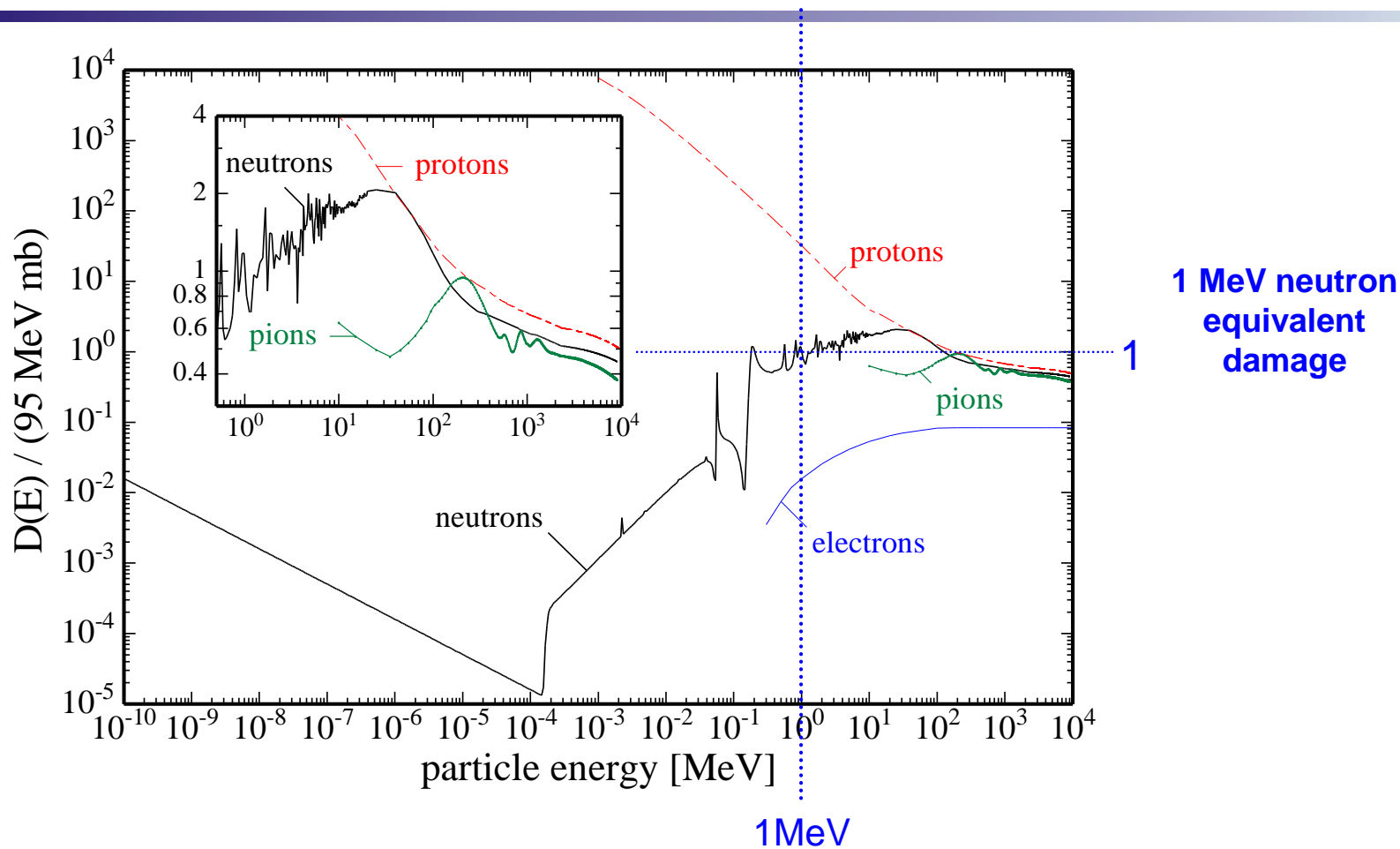
point defects (V-O, VV, ..)

point defects and clusters of defects

Michael Moll – MC-PAD Network Training, Ljubljana, 27.9.2010



# NIEL - Displacement damage functions



NIEL - Hypothesis: Damage parameters scale with the NIEL  
(! does not hold for all particles & damage parameters)

Michael Moll – MC-PAD Network  
Training, Ljubljana, 27.9.2010



# Effect on detector properties

---

## Bulk (Crystal) damage due to Non Ionizing Energy Loss (NIEL)

1. Increase of **leakage current** (increase of shot noise)
2. Change of **effective doping concentration** (higher depletion voltage, under- depletion)
3. Increase of **charge carrier trapping** (loss of charge)

Impact on detector performance and **Charge Collection Efficiency**



# Outline

---

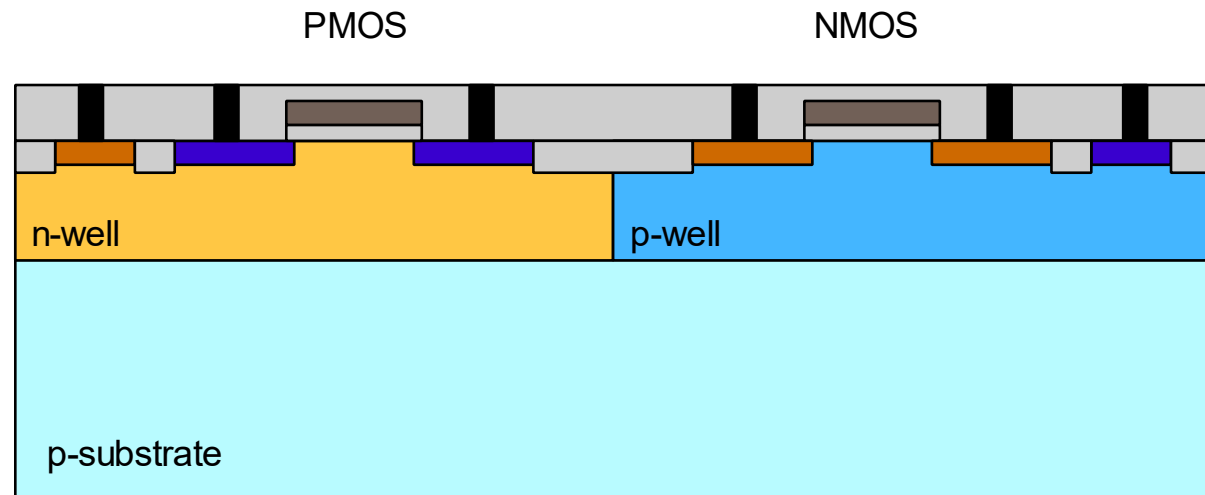
- Radiation detection in silicon
- CMOS technologies: characteristics, opportunities and challenges
- Monolithic active pixels for photon imaging
- MAPS: design approaches and research directions
- SEED project overview



# CMOS process

- Twin-tub process: industrial standard for digital electronics
- Standard CMOS process includes p/n junctions that can be used for radiation detection
- Commercial development of CMOS optical image sensors started in the 1990s

Standard CMOS process - simplified cross section



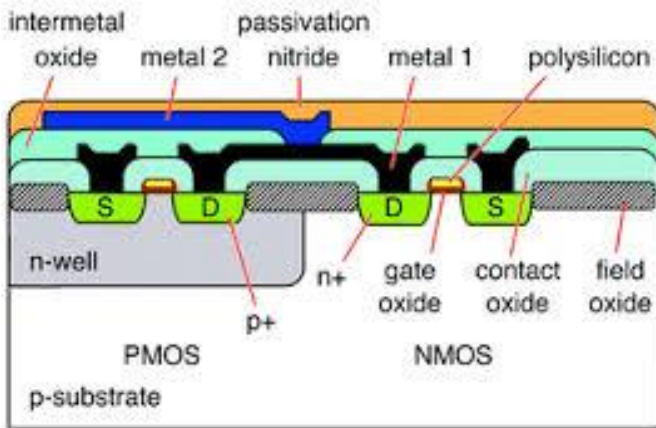




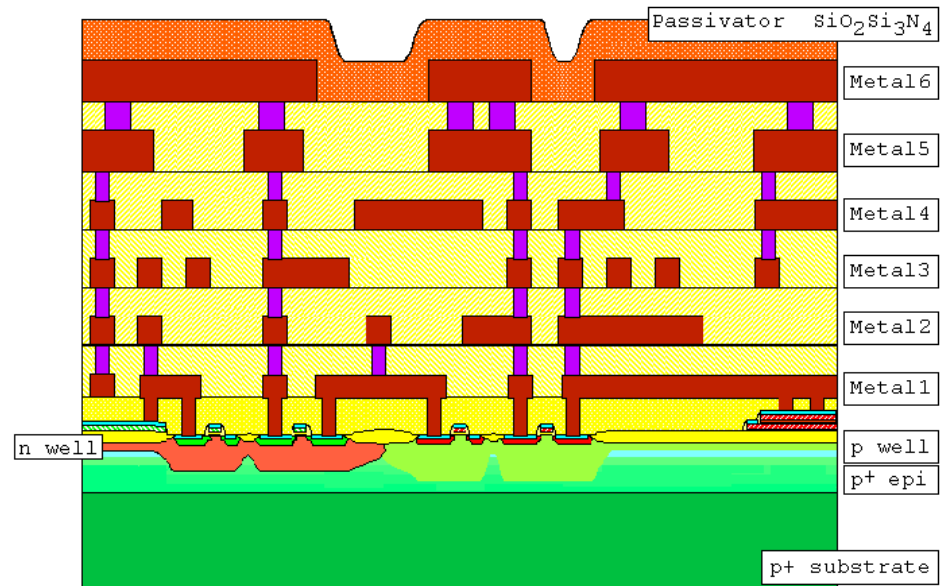
# CMOS process layer stack

In standard CMOS, stack thickness increases with technology advancement

2-metal process:  
Passivation stack:  $< 1\mu\text{m}$



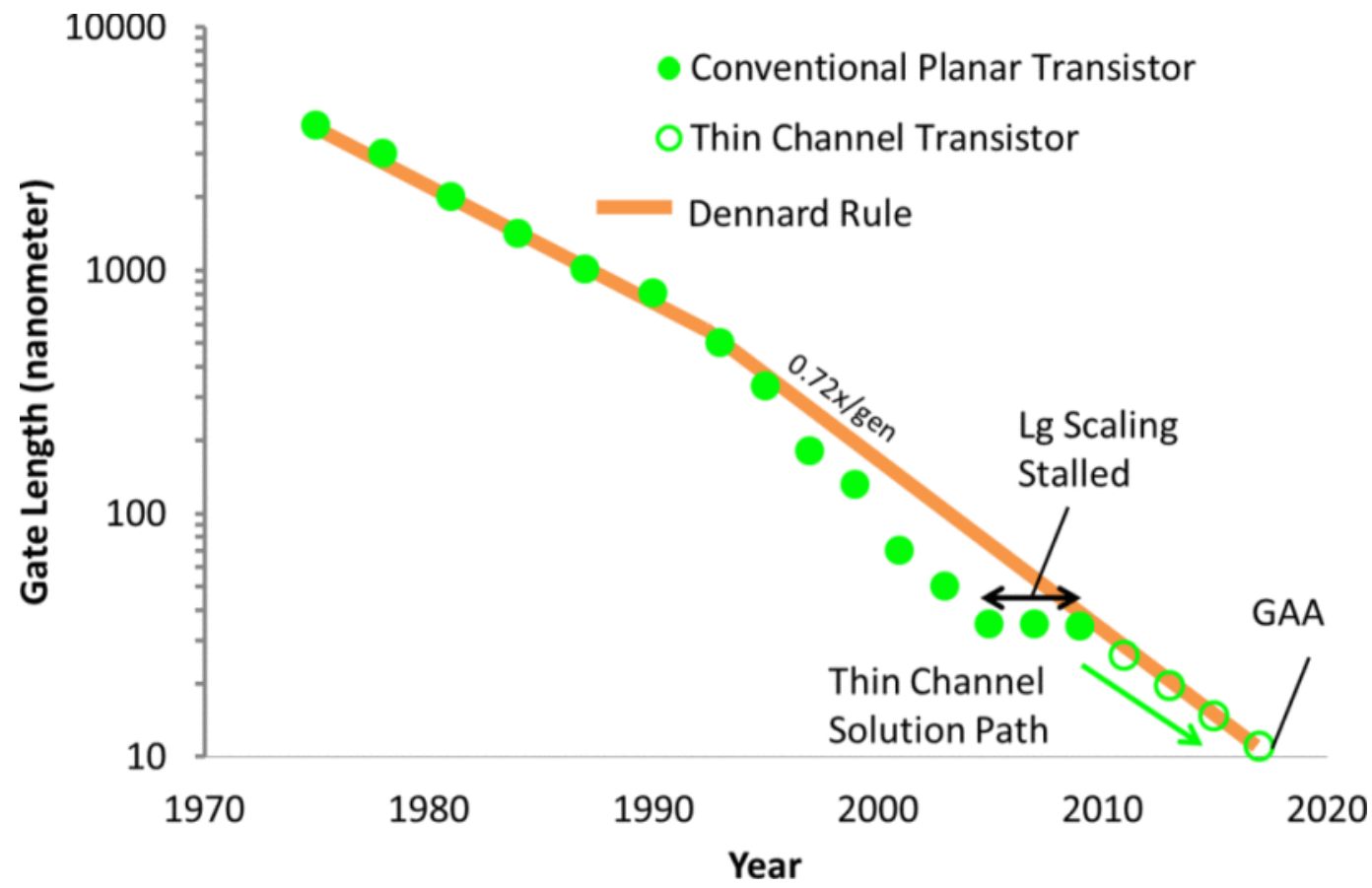
6-metal process  
passivation stack thickness:  $3-5\mu\text{m}$





# CMOS technologies

## MOSFET gate length scaling







K. Schuegraf, IEEE J. Electron Devices Society, 2013



# CMOS technology roadmap

Date Production Part Available\*

Foundry	2012	2013	2014	2015	2016	2017	2018	2019	2020
	28HPM		20SoC 28HPC	16FF-T 16FF+	16FFC	10FF	7FF	7HPC	5nm
			20LPE	14LPE	14LPP	10LPE	10LPP		7nm
					14LPP	22FDX		7nm 12FDX	
	22nm	22SoC	14nm	14SoC	14nm+	10nm 10SoC			7nm

\*risk production and qualification start is typically 1 year ahead



[www.techinsights.com](http://www.techinsights.com)



# Digital mainstream

## How transistors are evolving

No end in sight for logic scaling

ASML

Public  
Slide 17  
November 2014



**N 20**

**Bulk CMOS:**  
Complementary  
Metal Oxide  
Semiconductor

**N 20 / N 14**

**SOI:** Partially  
depleted Silicon  
on insulator

**N10**

**SOI:** Fully depleted  
Silicon on insulator

**N 20 / N 7**

**Bulk FinFet :**  
fin field effect  
transistor

**N 7 / N 5**

**SOI FinFet :**  
silicon on insulator  
fin field effect  
transistor, III-V

**N 5 / N 3.5**

**Gate-all-around  
transistor**

[www.sec.gov](http://www.sec.gov)



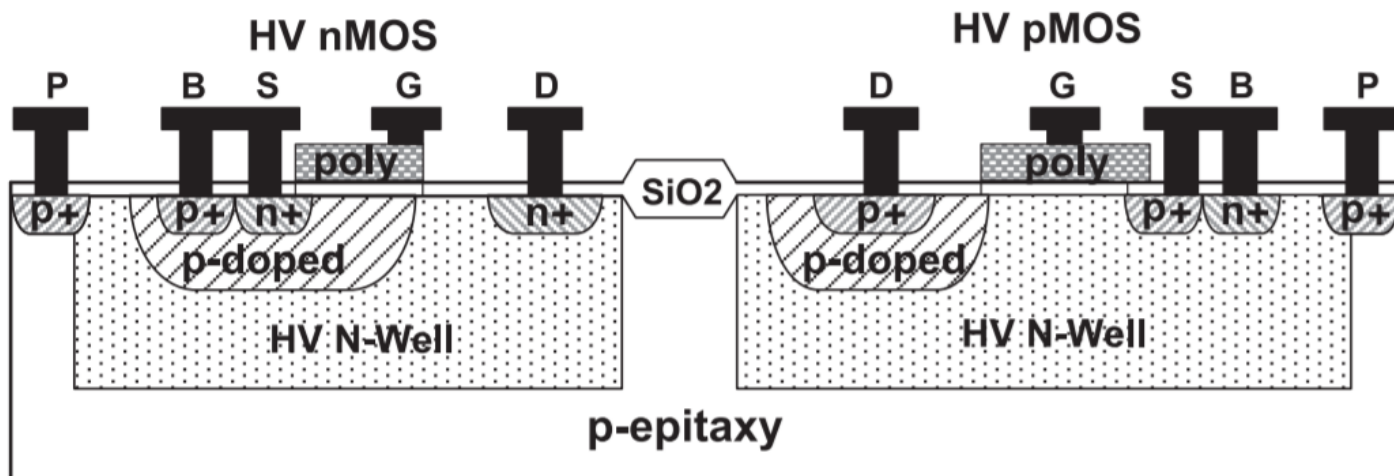
# Add-ons to standard CMOS

---

- Supply voltage reduces with CMOS node size: advanced digital nodes not ideal for analog design:
  - Low input/output voltage range
  - Low headroom for cascode stages
- Technology add-ons for **analog circuits**:
  - 3.3V – 5V transistors
  - Different thresholds: high – low – 0 threshold
  - Metal capacitors

# High-Voltage CMOS

- Power electronics: high voltage MOSFETS
- Low-doped substrate or epitaxial layers
- Deep n-wells and p-wells in addition to regular n-well and p-wells

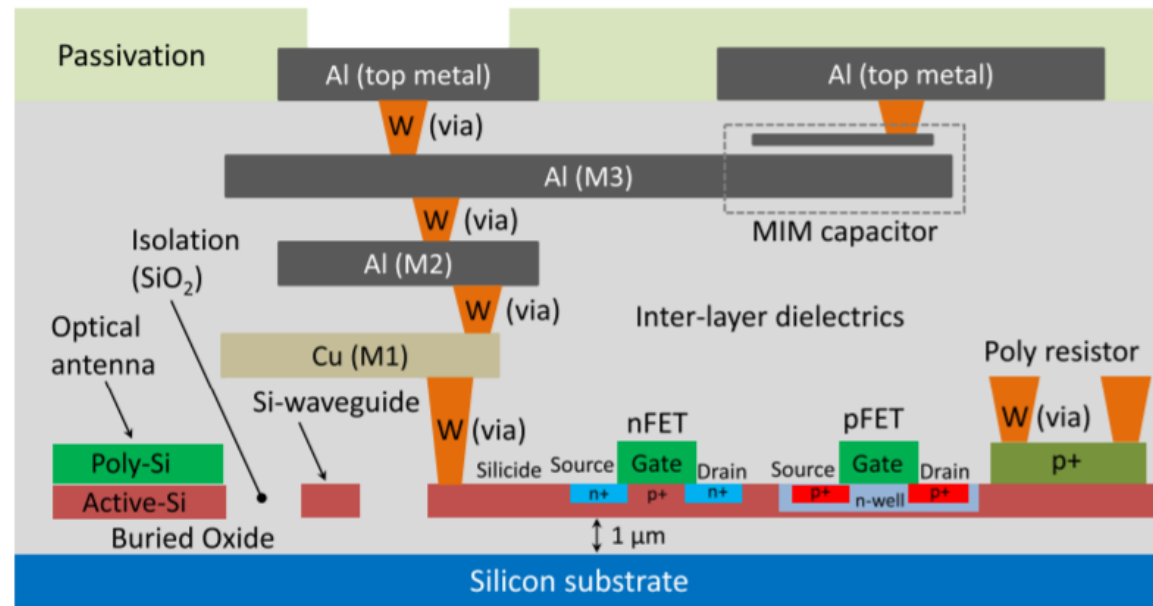


S. Dai, IEEE TCAS I, 2015



# SOI processes

- Insulator substrate: SiO<sub>2</sub> buried oxide or sapphire
- Low parasitics (RF applications, high speed)
- Higher substrate costs



S. Chung, IEEE J. Solid-State Circuits, 2018



# Research on hybrid bonding

	3D-SIP			3D-SIC	3D-SOC		3D-IC		
3D Technology	“PoP”	“Chip last”	“Chip first”	Die stacking	Parallel W2W		Sequential FEOL		
3D-Wiring level	Package I/O	Chip I/O Interposer I/O	Chip I/O	Global	Semi-global	Intermediate	Local	FEOL	
				Chip BEOL Wiring Hierarchy					
Partitioning	Functional unit	subsystem	Embedded die	Die	Blocks of standard cells		Standard cells	Transistors	
Technology	Package-to- Package reflow	Multi-die SIP 3D/2.5D stack	FO-WLP Embedded die	3D D2D, D2W 2.5D Si-interposer	Wafer-to-Wafer bonding Hybrid bonding		Via-last	Active layer transfer or deposition	
2-tier stack Schematic									
Characteristic	Solder ball Stack	• C4, Cu-pillar Si-Organic • Through- Mold-vias	• Bumpless • Si-RDL • Through- Package-vias	• μbump • Si-to-Si • Through- Silicon-Via	BEOL between 2 FEOL layers			FEOL stack	
					Overlay 2 <sup>nd</sup> tier defined by W2W alignment/bonding		Overlay 2 <sup>nd</sup> tier defined by litho scanner alignment		
Contact Pitch	400⇒350⇒300μm	120⇒80⇒60μm	60 ⇒40 ⇒20μm	40 ⇒20 ⇒10⇒5μm	5μm ⇒ 1 μm	2 μm ⇒ 0.5 μm	200nm ⇒ 100nm	< 100 nm	
Relative density:	1/100⇒1/77⇒1/55	1/9⇒1/4 ⇒1/2.3	1/2.3 ⇒ 1 ⇒ 4	1 ⇒ 4 ⇒16⇒ 64	64 ⇒ 1600	400 ⇒ 6400	4 10 <sup>4</sup> ⇒ 1.6 10 <sup>5</sup>	> 1.6 10 <sup>5</sup>	

Eric Beyne, IMEC, January 2018





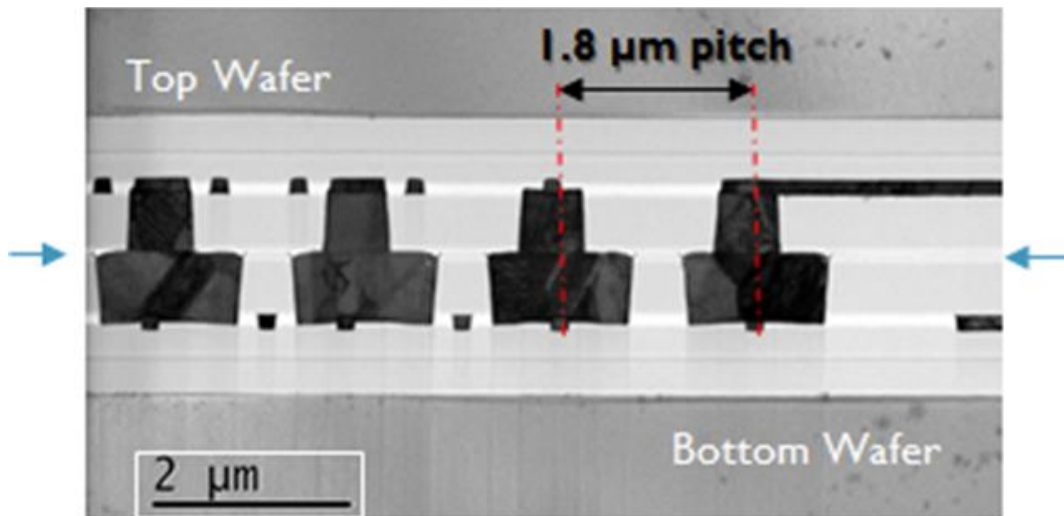
# Hybrid bonding – State of the Art

By David Manners 24th January 2017

Electronics  
Weekly.com

## Imec, EVG demo superior overlay accuracy for wafer-to-wafer bonding

Imec and EVG have demonstrated 1.8 $\mu\text{m}$  pitch overlay accuracy for wafer-to-wafer bonding.



[https://www.evgroup.com/en/about/news/2017\\_01\\_imec/](https://www.evgroup.com/en/about/news/2017_01_imec/)



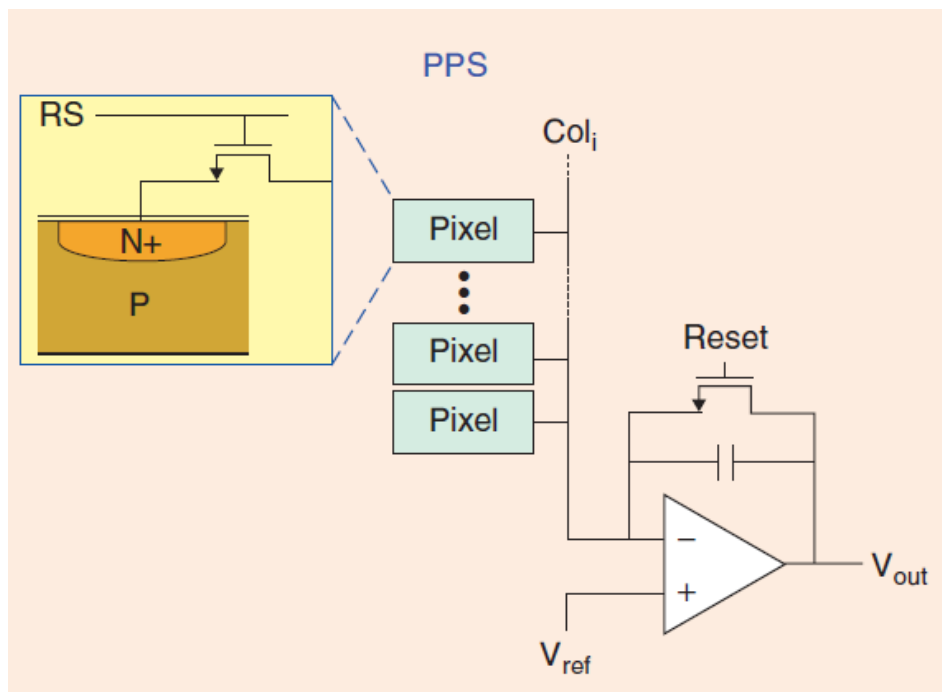
# Outline

---

- Radiation detection in silicon
- CMOS technologies: characteristics, opportunities and challenges
- **Monolithic active pixels for photon imaging**
- MAPS: design approaches and research directions
- SEED project overview



# Passive Pixel Sensor (PPS)



- The PPS consists of a photodiode and just one transistor TX.
- TX is used as a charge gate, switching the contents of the pixel to the charge integration amplifier (CIA).

First introduced by G. Weckler in 1967:

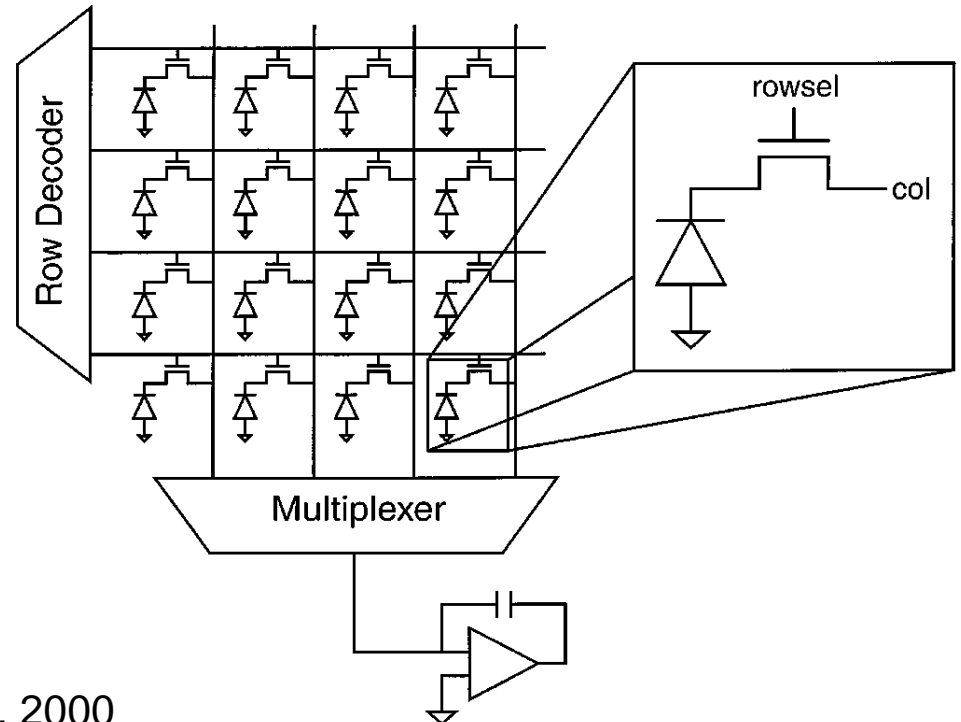
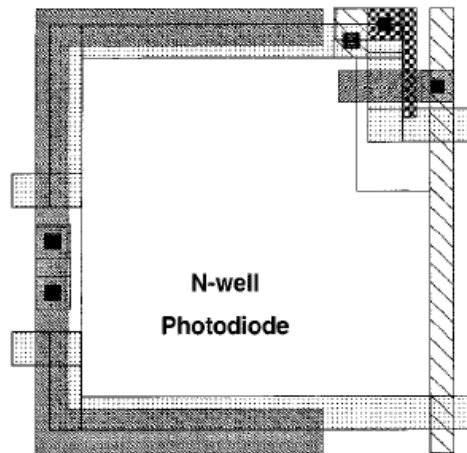
G. P. Weckler, IEEE J. Solid-State Circuits, vol. SC-2, pp. 65–73, 1967.

A. El Gamal, "CMOS Image Sensors", IEEE Circuits and Devices Magazine, pp. 6 – 20, 2005.



# Passive Pixel Sensor (2)

- Advantage: high fill factor – each pixel has only one transistor.
- Architecture: 1 amplifier per chip or 1 amplifier per column



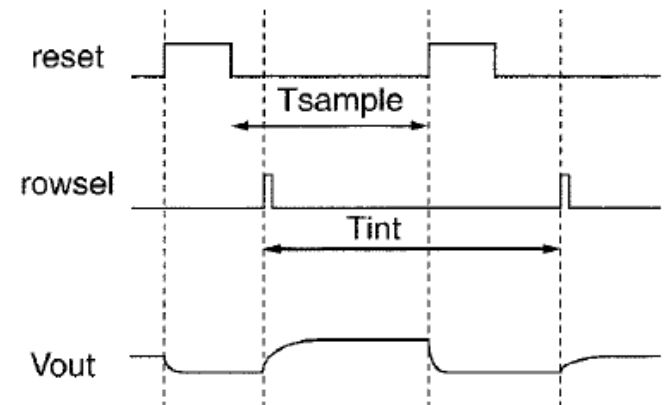
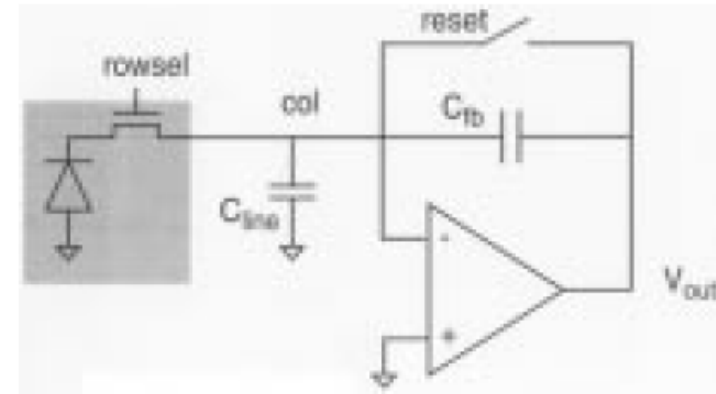
I. L. Fujimori, IEEE J. Solid-State Circuits, 2000



# Passive Pixel Sensor (3)

Major problem: large capacitive loads (metal lines):

- High **readout noise**  
250 electrons rms typically
- Low readout speed in large pixel arrays.





# Active Pixels

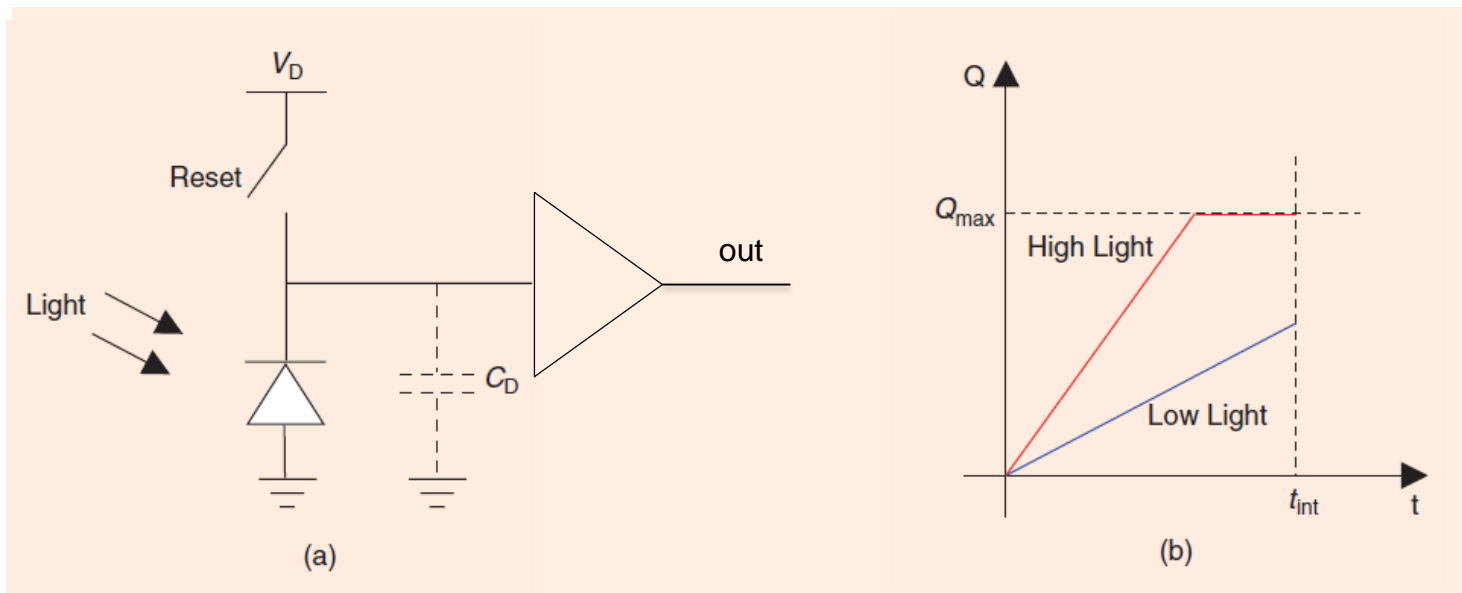
---

- Buffer amplifier in the pixel
- Origins: end of the 1960s
- Optical imaging applications
- CCDs were much more reliable at the time. Active pixel emerged in the 1990

- P.J.W. Noble, "Self-Scanned Silicon Image Detector Arrays". IEEE Tran. Electron Dev. Vol. 15, pp. 202–209, 1968.
- S. G. Chamberlain, "Photosensitivity and Scanning of Silicon Image Detector Arrays". IEEE Journal of Solid-State Circuits vol. 4 pp. 333–342, 1969.

# Active Pixel Sensor

- Charge is integrated on photodiode capacitance
- Output of the photodiode is buffered using in-pixel follower

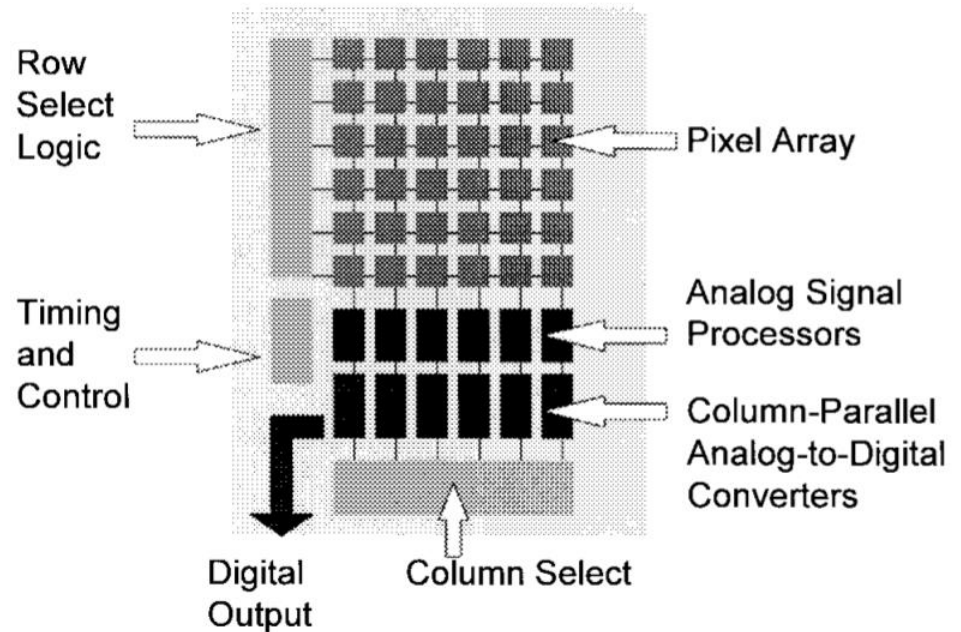
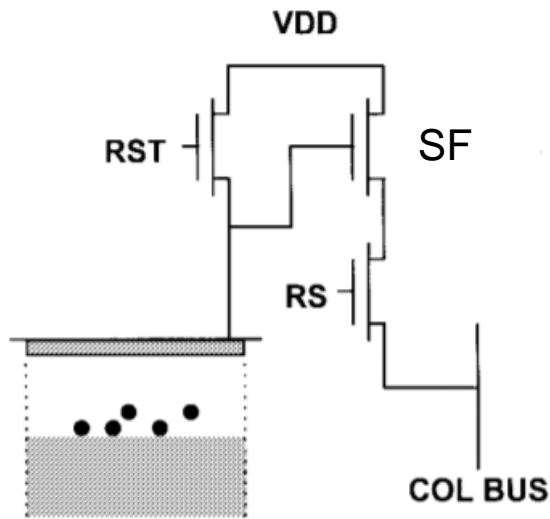


A. El Gamal, IEEE Circuits and Devices Magazine, 2005.



# Active Pixel Sensor (3T - APS)

Conversion gain depends on the total capacitance at the SF gate: PD + parasitic capacitances

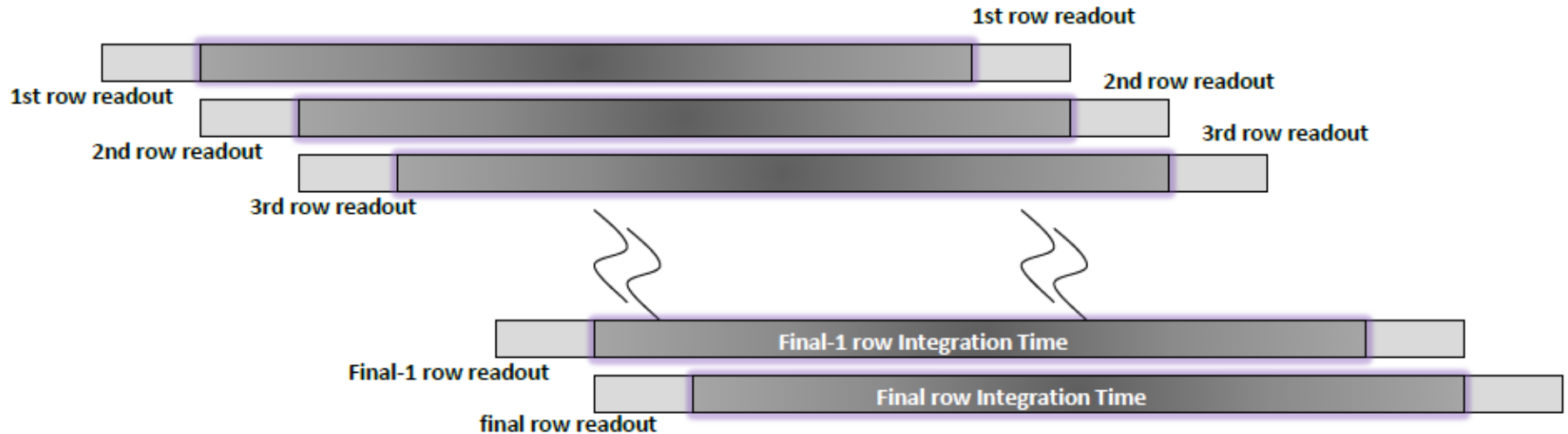


E. R. Fossum, "CMOS image sensors :electronic camera-on-a-chip", IEEE Trans. On Electron Devices 44 (10) (1997)





# Array readout: rolling shutter



- Pixel voltage is read out one row at a time
- Row integration times are staggered by row/column readout time
- The progressive scanning of the image cause artifacts (distortion) when the scene is changing fast.

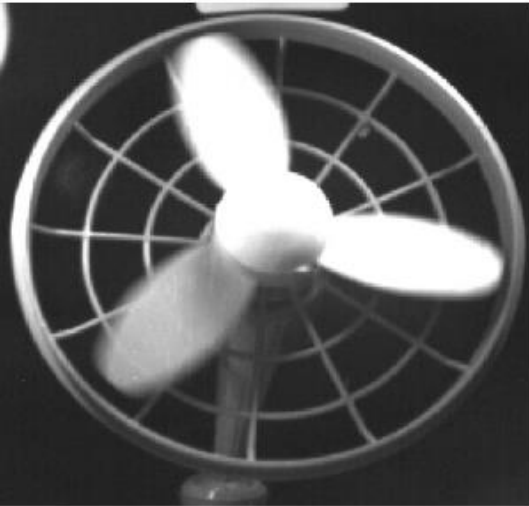
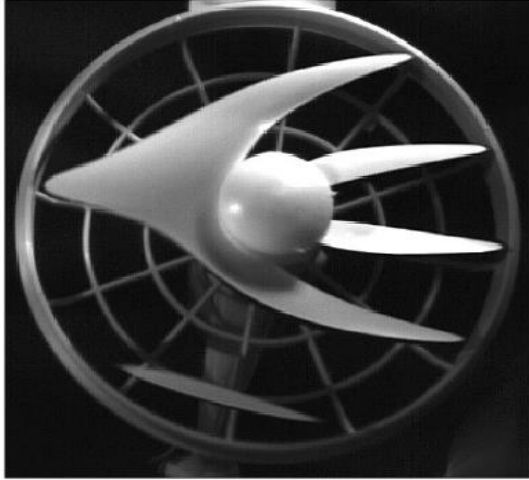


# Rolling shutter effects

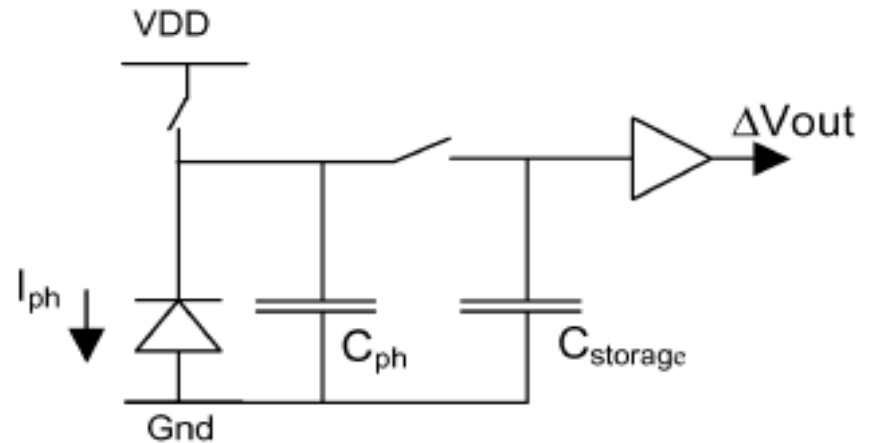




# Global shutter pixels



- In-pixel Sample-and Hold
- Problem: GS adds complexity and reduces the Fill Factor



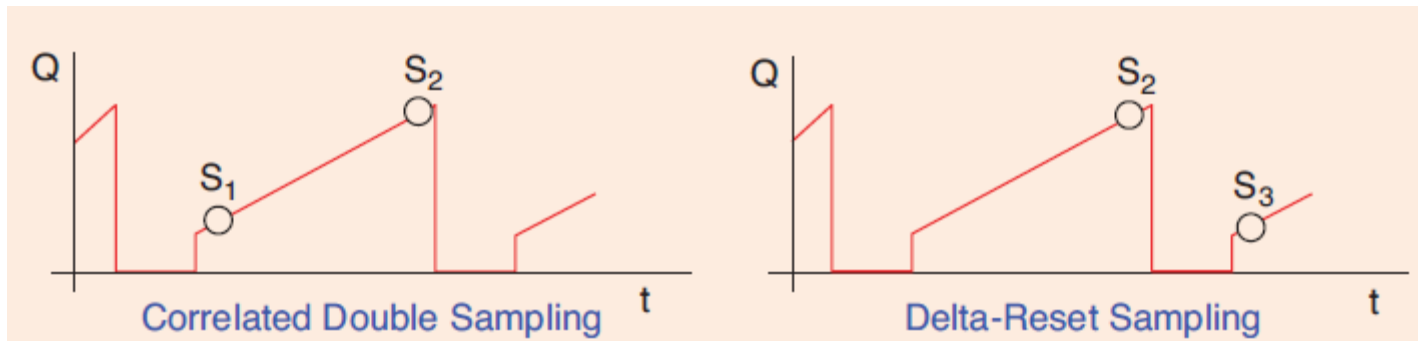
Ref: IEEE Transactions on Electron Devices, Vol. 50, No. 1, Jan. 2003



# 3T – APS: signal sampling

Two different sampling schemes:

- **Correlated double sampling (CDS):**
  - eliminates reset noise
  - Samples are separated in time
- **Delta-reset sampling:**
  - Does not eliminate reset noise
  - samples are close in time

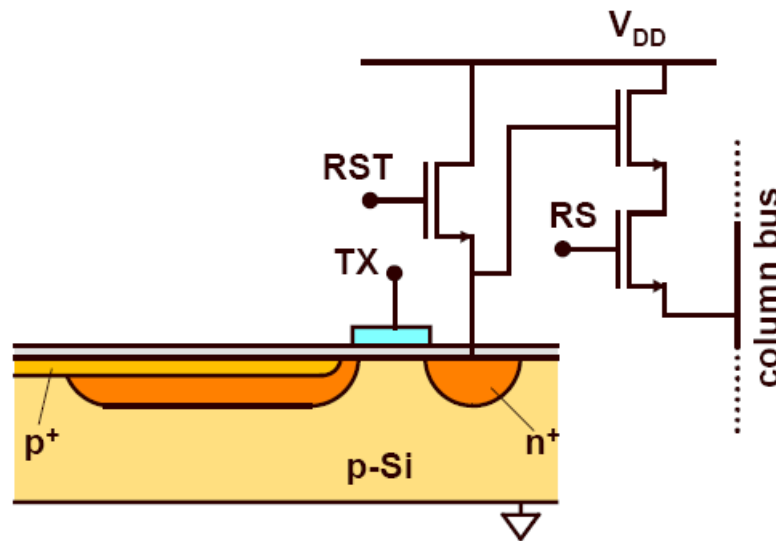


A. El Gamal, IEEE Circuits and Devices Magazine, 2005.



# Pinned – photodiode APS (4T – APS)

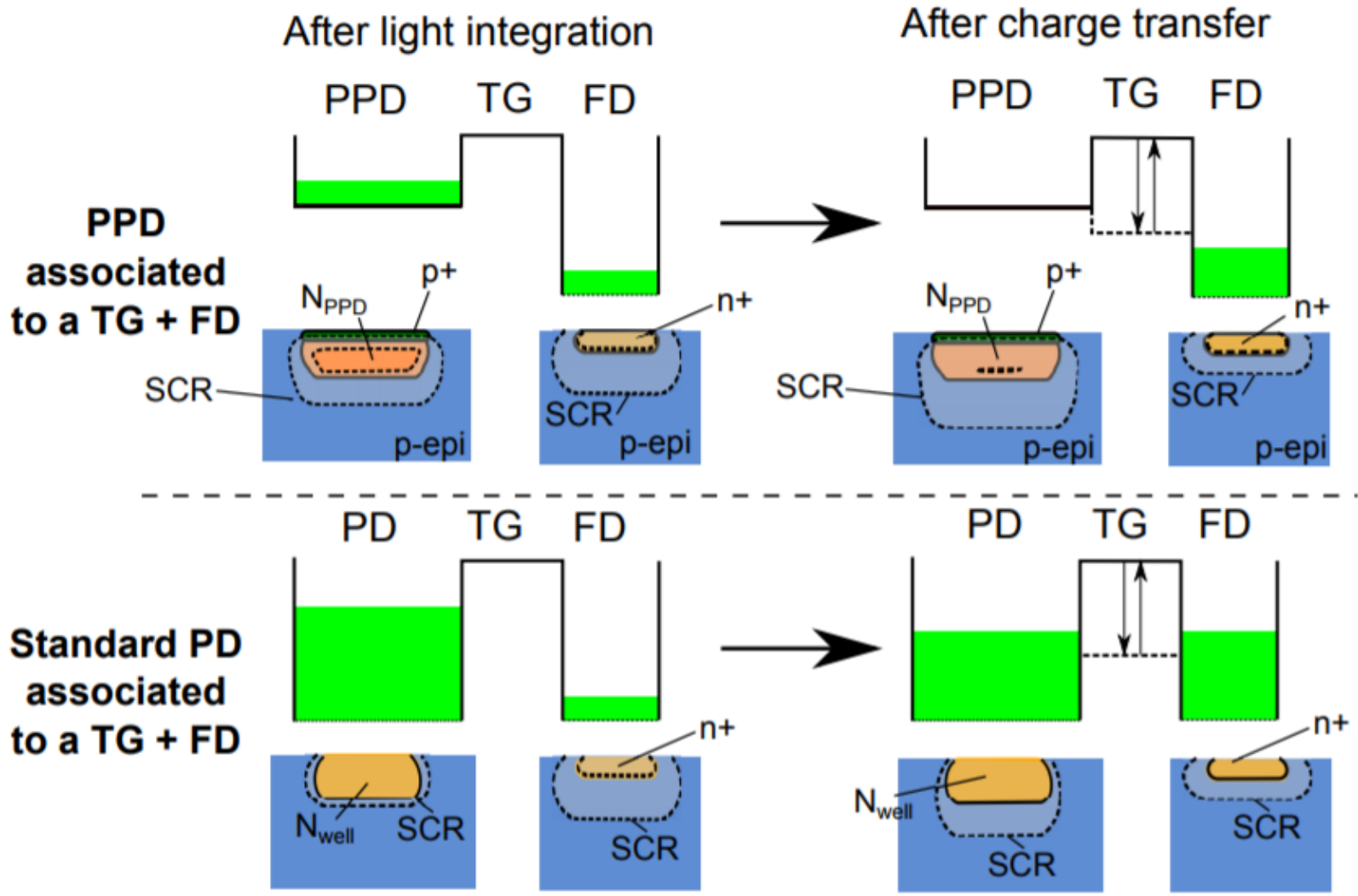
- **Pinned photodiode:** buried  $p^+/n/p$  photodiode that can be fully depleted of electrons
- First introduced in CCDs, later ported to CMOS image sensors



A. Theuwissen, Proc. IEEE ESSDERC 2007



# Pinned photodiode operation



A. Pelamatti PhD Thesis, University of Toulouse, 2015

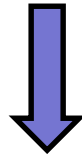


# 4T-APS vs 3T-APS

---

## Advantages:

- Conversion gain ( $q/C_{FD}$ ) is independent of detector, 4T-APS can achieve higher conversion gain than photodiode APS
- Lower noise: reset noise cancellation and lower dark current



Higher performance (SNR) for low-light imaging

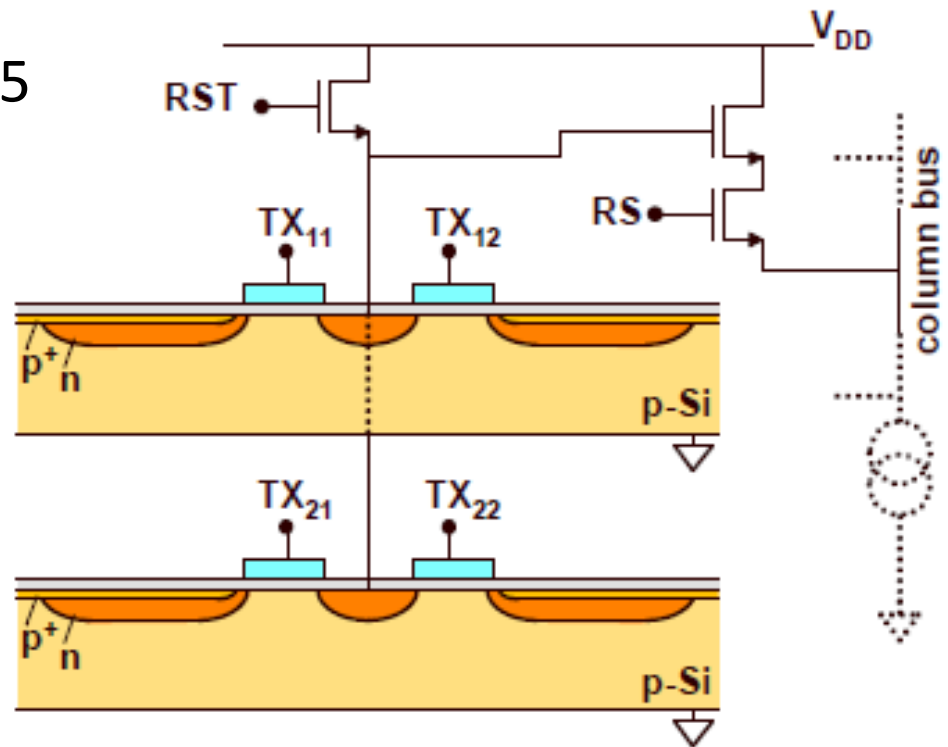
## Disadvantages:

- More devices than 3T-APS (lower Fill Factor)
- Destructive readout



# Transistor sharing

- A group of pixels (typically 4) can share some transistors (reset, SF, row select).
- Total number of transistors in 4 pixels: 4 + 3
- Transistors x pixel:  $7/4 = 1.75$
- Other sharing schemes can be implemented



A. Theuwissen, Proc. IEEE ESSDERC 2007



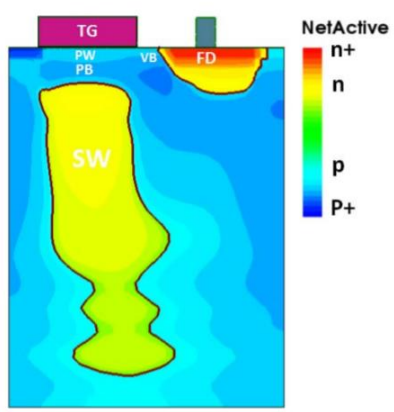


# Noise reduction

Sub-electron noise reduction by

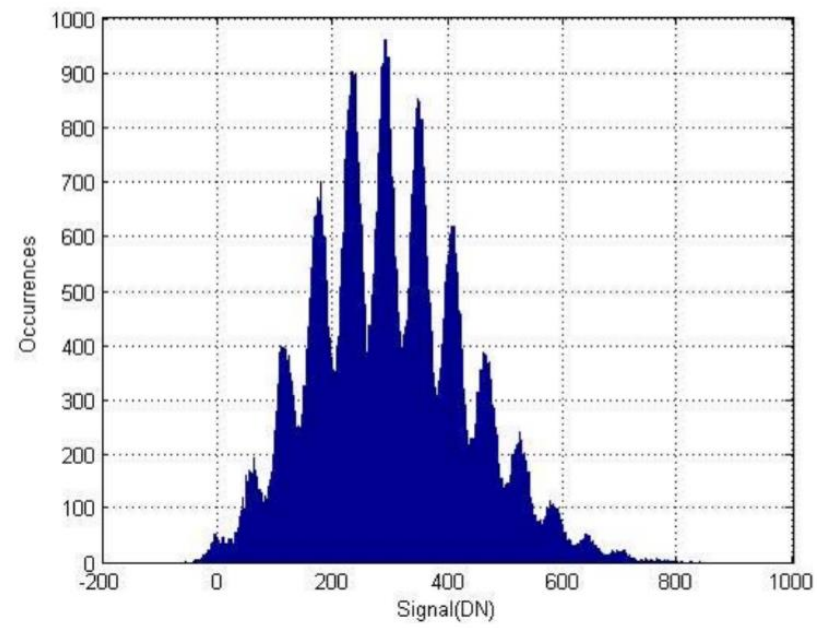
- Boosting conversion gain
- Implementing advanced filtering techniques
- Optimizing process

} Photon counting



Pixel pitch: 1.4um  
Conversion gain:  
400uV/e-  
Noise rms: 0.34e-

Output signal histogram

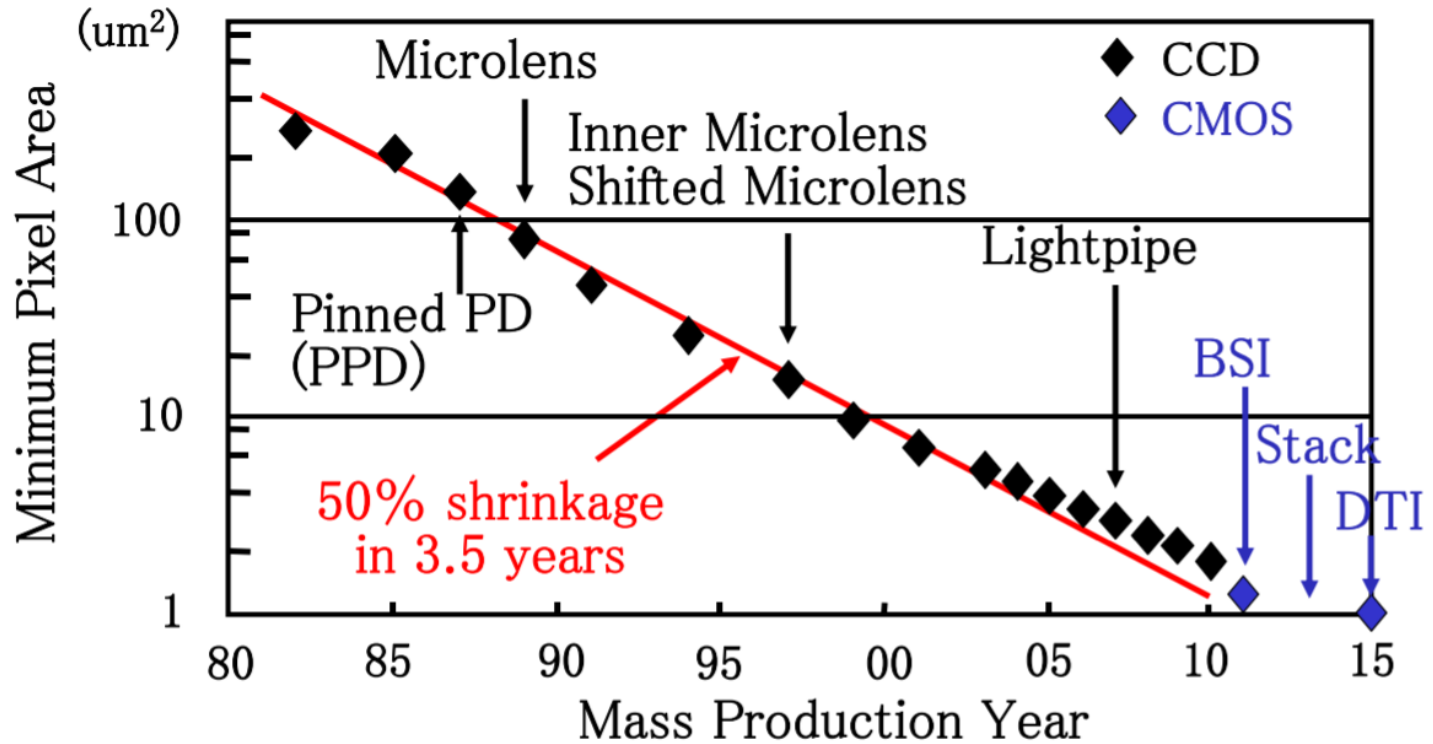


J. Ma and E. Fossum, IEEE Electron Device Letters, 2015



# Pixel size scaling

- Commercial products with 0.9 $\mu\text{m}$  pixels are entering the market
- Current research: deep sub- $\mu\text{m}$  pixels (0.4 – 0.7 $\mu\text{m}$  pitch)

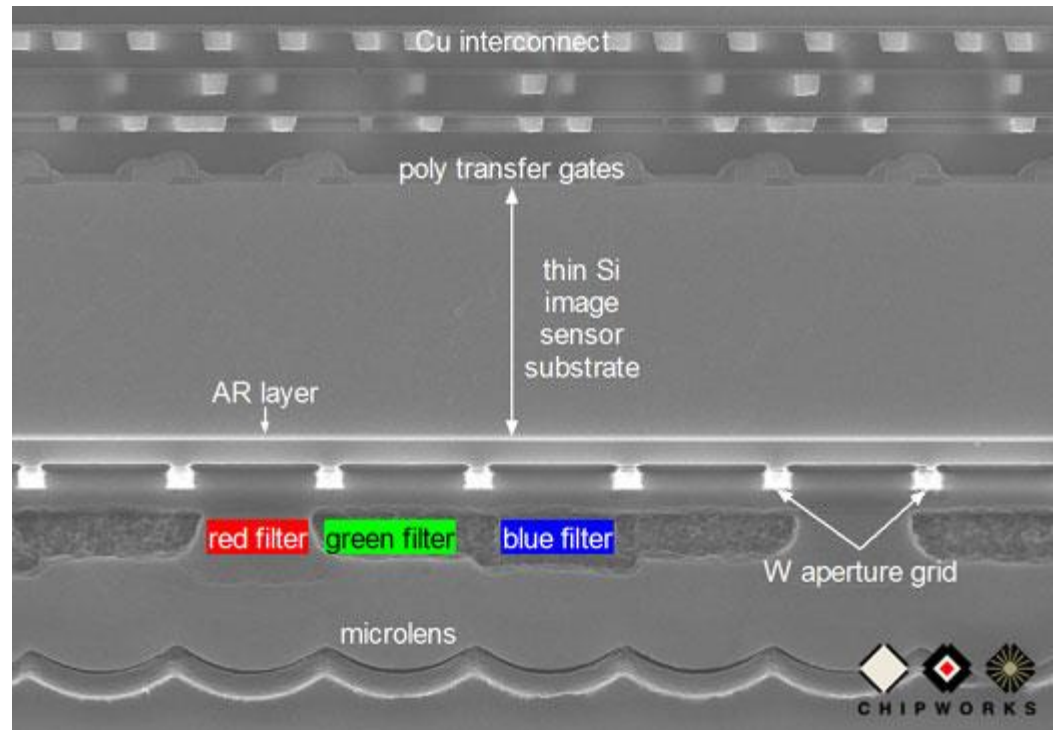


N. Teranishi – FFE 2016



# CIS processes: backside illumination

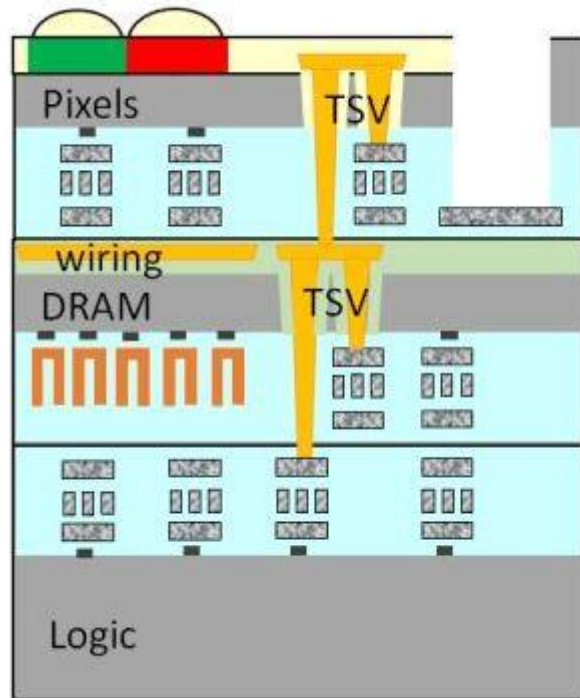
- Thinning down to 2.5 $\mu\text{m}$  – 3 $\mu\text{m}$
- Backside processing
- Color filters
- Microlenses



<http://image-sensors-world.blogspot.it>

# CIS processes: 3D stacking

- State of the art: Sony 3-layer stacked image sensor



Sony, IEDM 2017

- Upper TSV connects pixels and DRAM chips
- Lower TSV connects DRAM and logic chips
- TSV wiring is located on DRAM backside

TSV diameter:  $2.5\mu\text{m}$   
pitch:  $6.3\mu\text{m}$

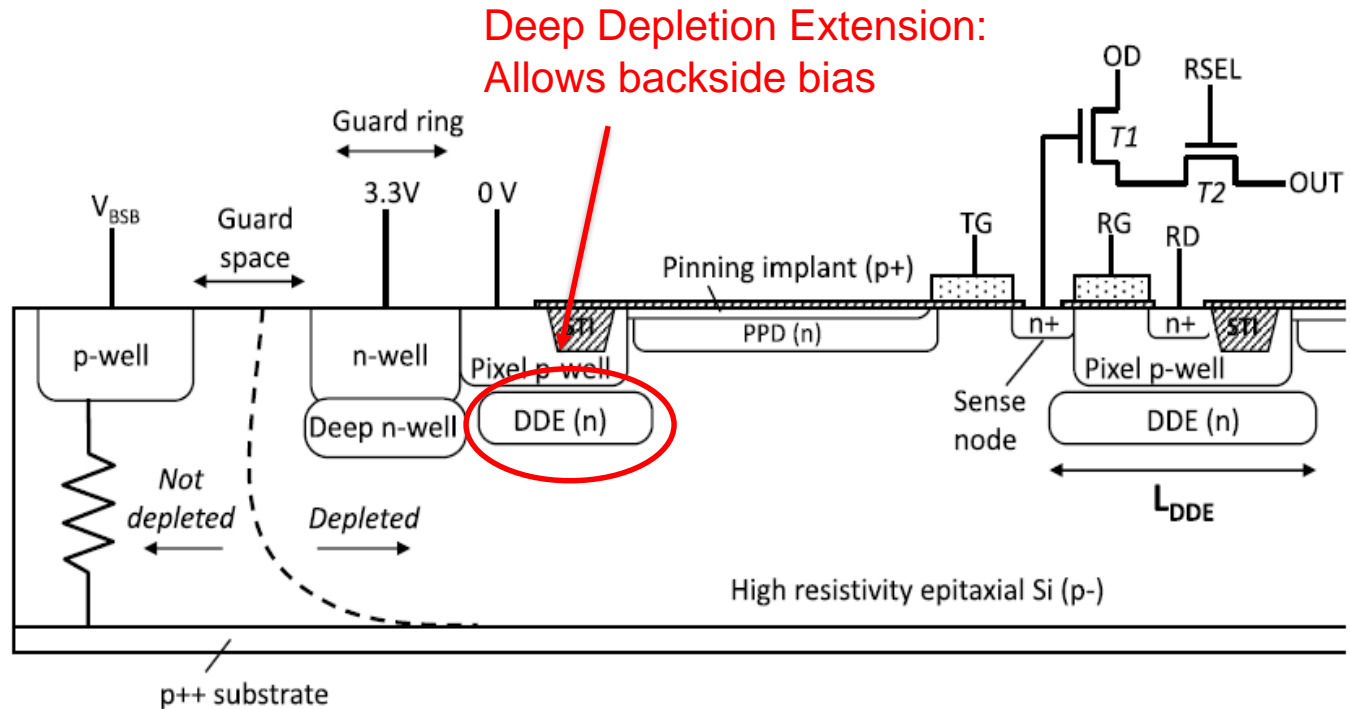


# Deep Depletion PPD sensors

18  $\mu\text{m}$  thick,  $1\text{k}\Omega\cdot\text{cm}$  epitaxial silicon

180nm CMOS process

Goal: low-noise IR imaging



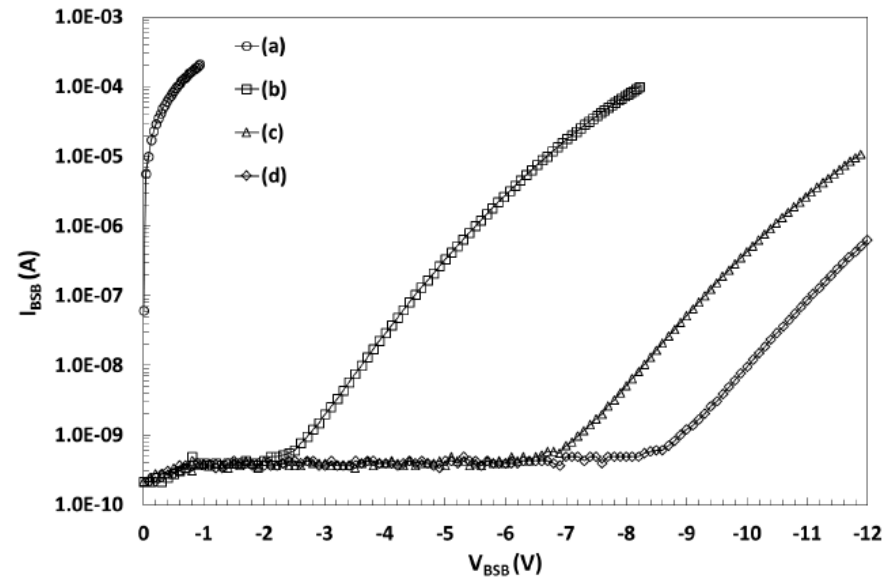
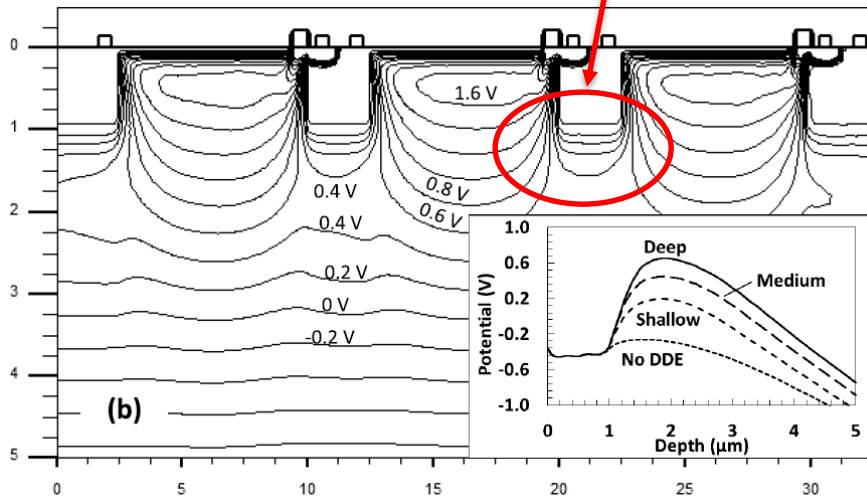
K.D. Stefanov, IEEE Electron Dev. Lett., vol. 38, no. 1, pp. 64-66, Jan. 2017.



# Deep Depletion PPD: backside bias

## Backside current vs. DDE implant dose

Barrier potential





# Outline

---

- Radiation detection in silicon
- CMOS technologies: characteristics, opportunities and challenges
- Monolithic active pixels for photon imaging
- **MAPS: design approaches and research directions**
- SEED project overview



# MAPS applications in HEP

---

Few example applications in HEP so far:

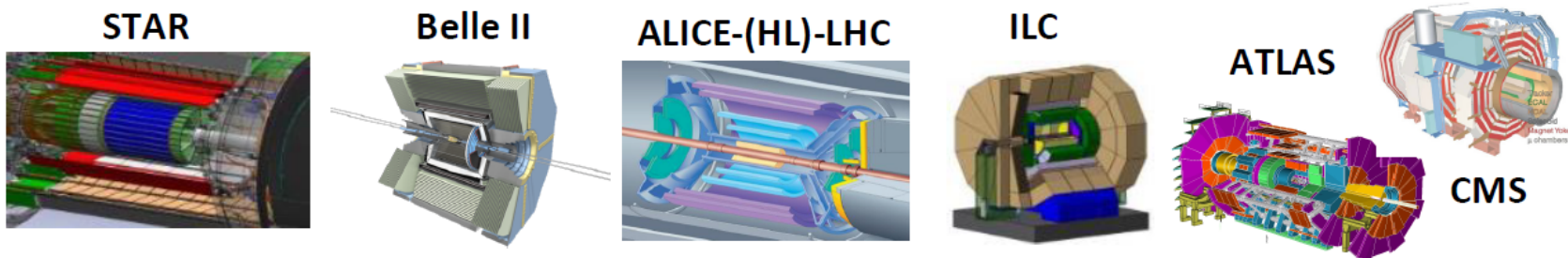
- STAR: detector area =  $0.15 \text{ m}^2$ , data taking started in 2014
- ALICE: detector area =  $12 \text{ m}^2$ , to be installed in 2020
- Promising for precision experiments (ILC)
- R&D for outer pixel layers at HL-LHC





# Pixel detectors for HEP

## Rate and Radiation Levels



Numbers for innermost layers ( $r \approx 5\text{cm}$ , ) -> scale by 1/10 for typical strip layers ( $r > 25\text{cm}$ )

	STAR	Belle II	ALICE-LHC heavy ion	ILC	LHC pp	HL-LHC-pp	
						Outer	Inner
BX-time (ns)	110	2	20 000	350	25	25	25
Particle Rate (kHz/mm <sup>2</sup> )	4	400	10	250	1 000	1 000	10 000
$\Phi$ (n <sub>eq</sub> /cm <sup>2</sup> )	few 10 <sup>12</sup>	3 x 10 <sup>12</sup>	> 10 <sup>13</sup>	10 <sup>12</sup>	2x10 <sup>15</sup>	10 <sup>15</sup>	2x10 <sup>16</sup>
TID (Mrad)*	0.2	20	0.7	0.4	80	50	> 1000

\*per (assumed) lifetime  
 LHC, HL-LHC: 7 years  
 ILC: 10 years  
 others: 5 years

in need for

- much less material
- higher resolution
- thinner strips & monolithic pixels

state of the art

- large area strips
- hybrid pixels

- even larger area
- radhard sensors
- higher rates R/O
- R&D of new types

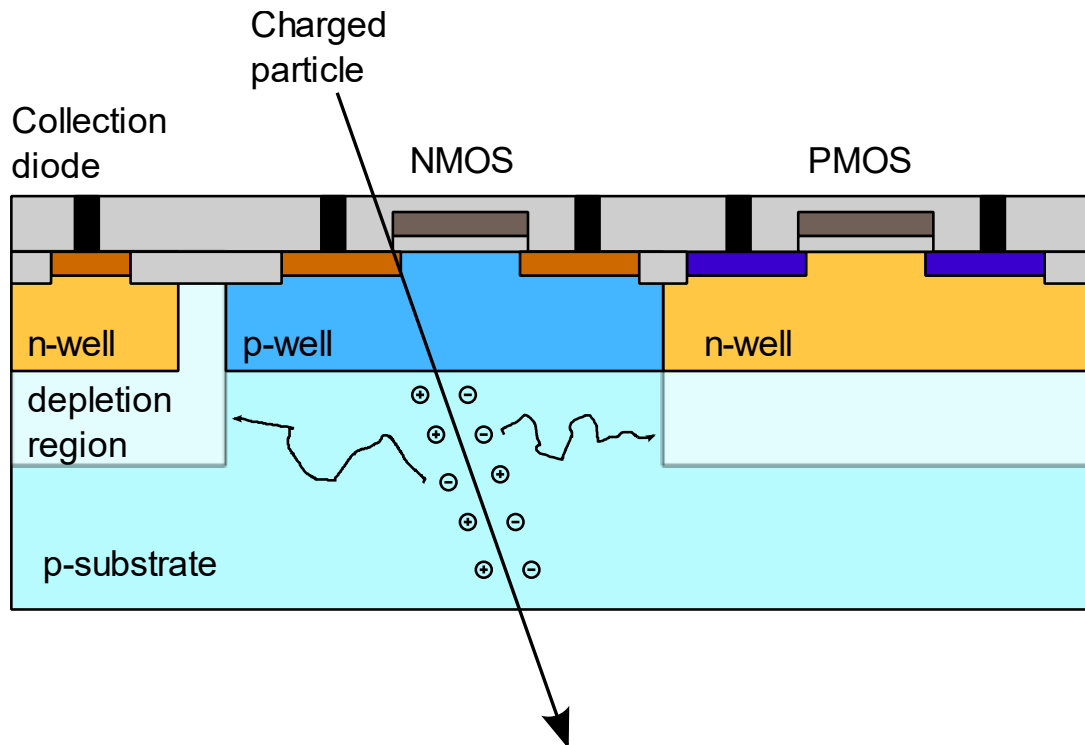
N. Wermes, 14th VCI Wien, 2/2016



# Monolithic sensors

Standard CMOS has problems:

- Collection speed: slow diffusion in undepleted substrate
- Competitive collection by nwell: low efficiency





# Solutions

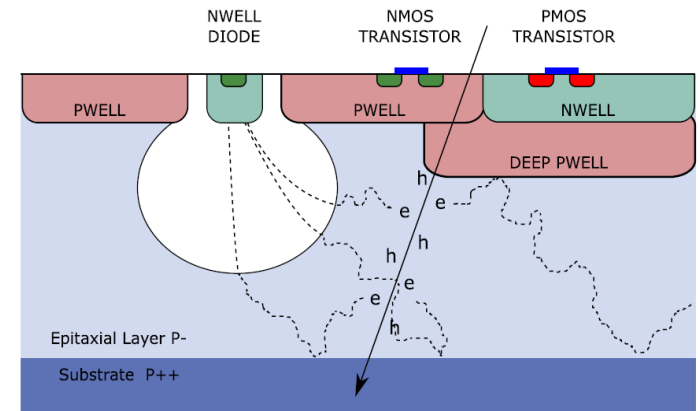
---

- Lowering substrate doping: high resistivity silicon
- High bias voltage
- Avoid competitive charge collection. Three approaches:
  1. Isolating n-wells other than collection electrodes with deep p-well
  2. Put CMOS electronics inside the collection electrode
  3. Isolate the electronics from the detectors with a buried oxide layer → SOI

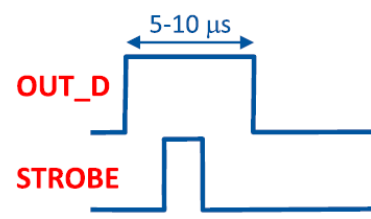
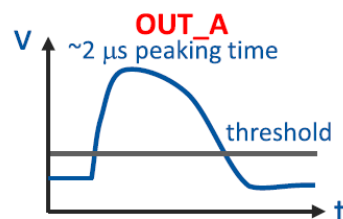
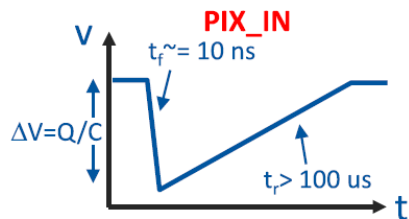
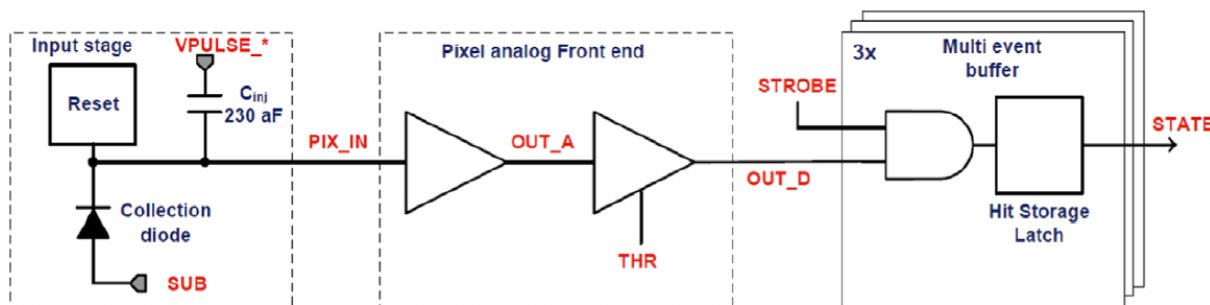


# ALPIDE approach

- Nwell shielded by deep pwell
- High resistivity ( $> 1\text{k}\Omega\text{ cm}$ ) p-type epi-layer with  $25\ \mu\text{m}$  thickness
- $28 \times 28\ \mu\text{m}^2$  pixel size
- Small sensor capacitance  $\rightarrow$  low noise
- Partial depletion: drift and diffusion
- Radiation tolerance (TID) up to 700 krad



J.P. Crooks, et al., IEEE TNS 2007

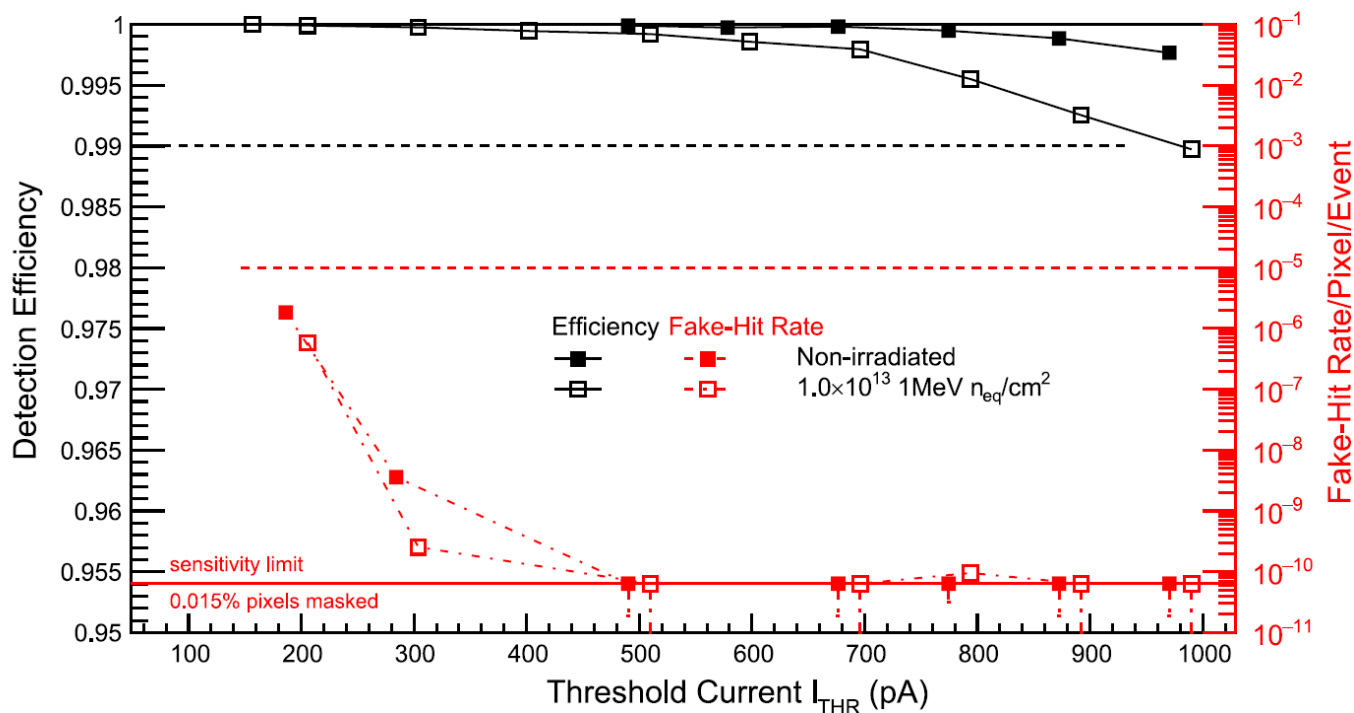


G. Aglieri Rinella,  
NIMA 845 (2017) 583–587



# ALPIDE performance

- Efficiency > 99.5%
- Fake hit rate <  $10^{-5}$  over wide threshold
- NIEL up to  $10^{13}$  (1MeV  $n_{eq}$ )/cm<sup>2</sup>

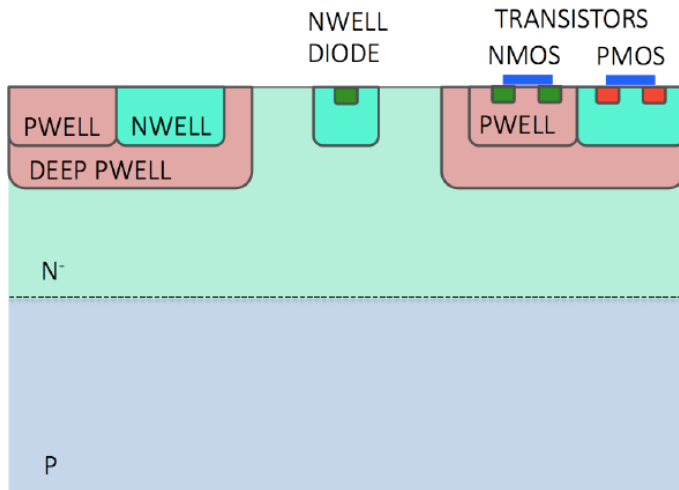


G. Aglieri Rinella, NIMA 845 (2017) 583–587

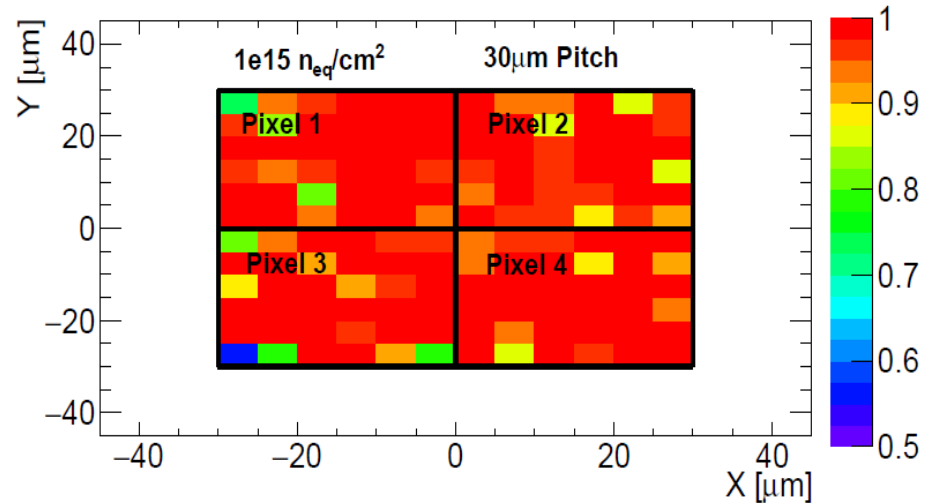


# ALPIDE with n-layer

- Fully depleted n- layer: collection by drift
- Fast charge collection: few ns
- Good efficiency and speed at  $10^{15}$  ( $1\text{MeV } n_{eq}$ )/ $\text{cm}^2$



Efficiency vs. hit position

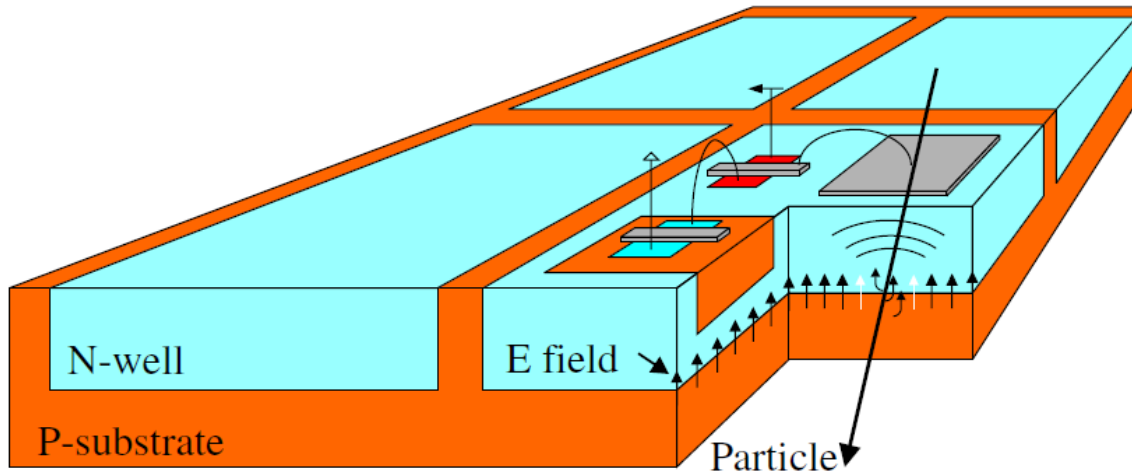


H. Pernegger et al., 2017 JINST 12 P06008



# High Voltage CMOS

- The collection diode is a deep nwell.
- The CMOS electronics (p wells + n wells) is inside the deep nwell
- High voltage bias can be applied



I. Peric et al., NIM A582 (2007) pp. 876-885



# High-Resistivity HV-CMOS

High resistivity substrates  
( $>2 \text{ k}\Omega\text{m}/\text{cm}$ )

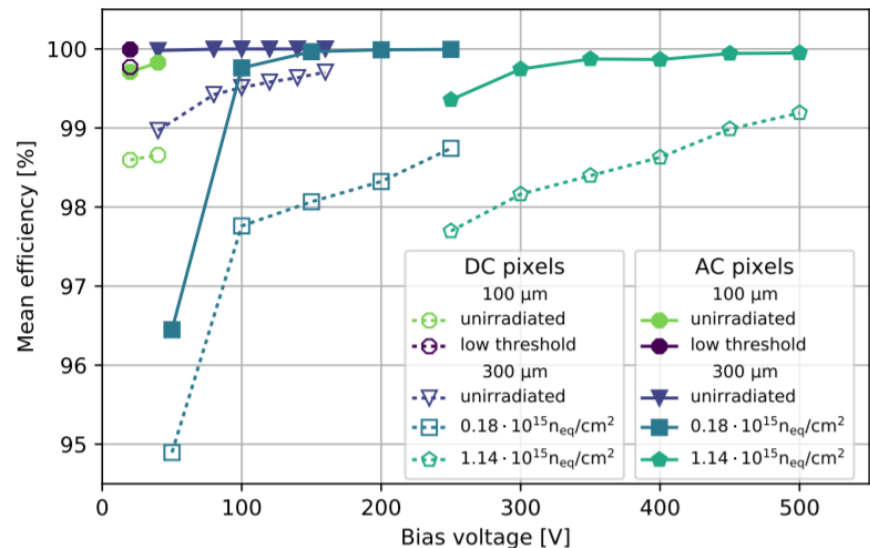
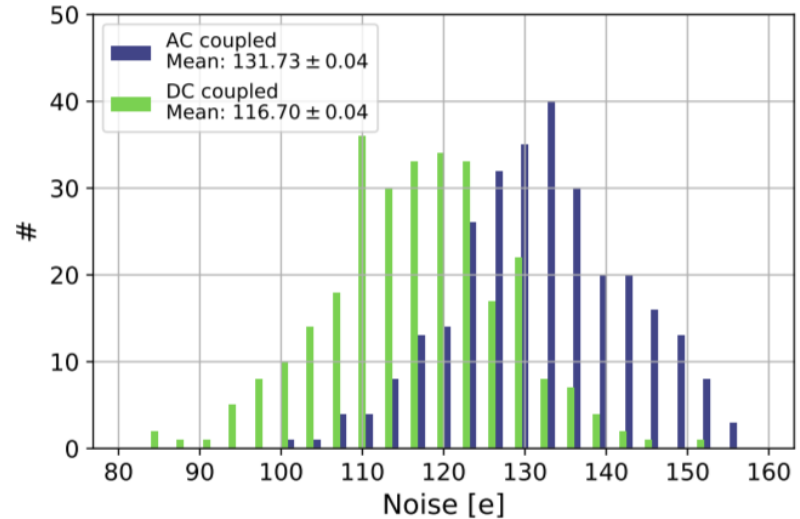
Promising approach:

- Fast charge collection
- High efficiency at fluence  $> 10^{15} \text{ n}_{\text{eq}}/\text{cm}^2$

Main drawback:

- Parasitic capacitance: large noise

D.-L. Pohl, 2017 JINST 12 P06020

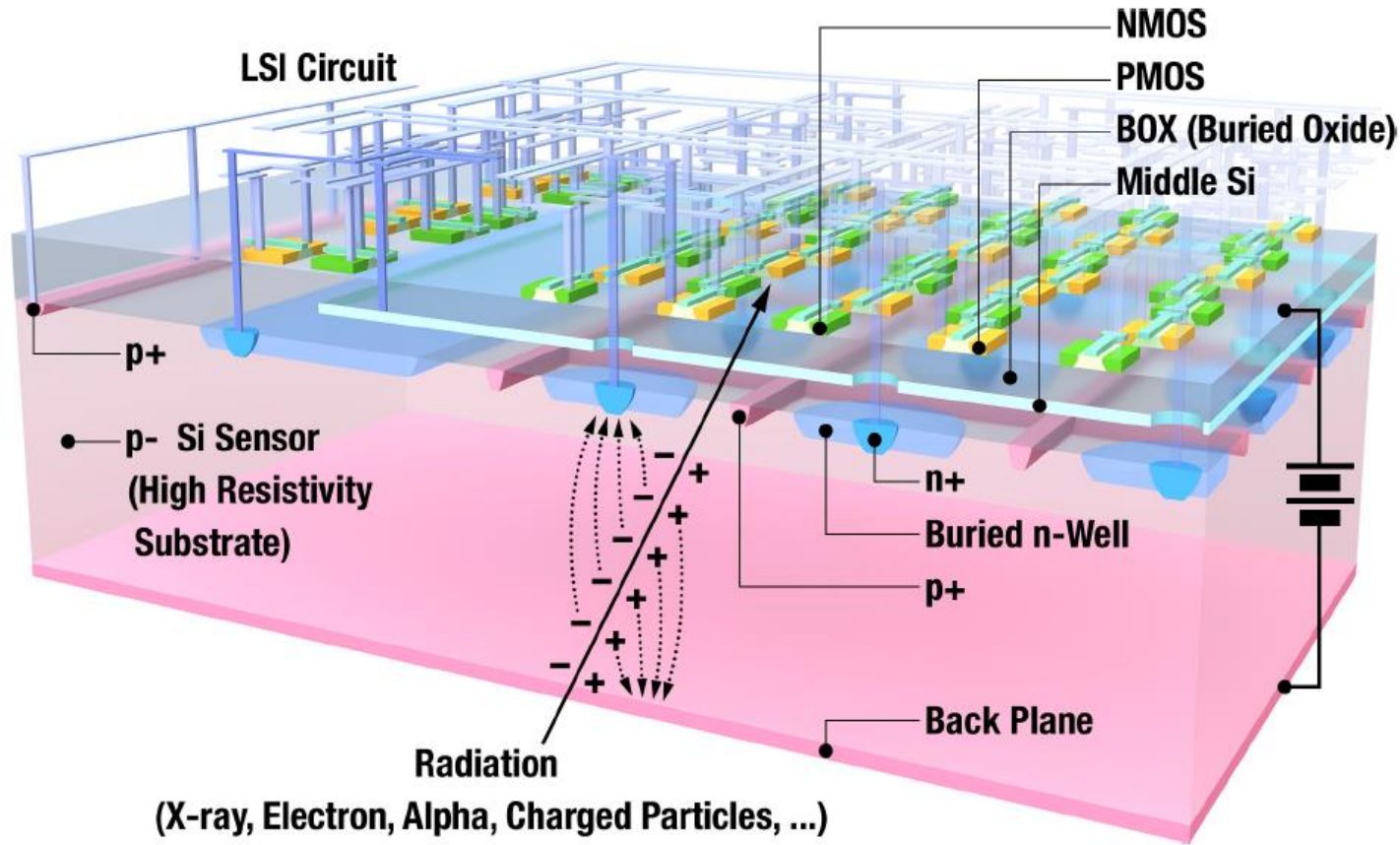






# Fully depleted SOI sensors

Buried oxide: separates detectors from electronics

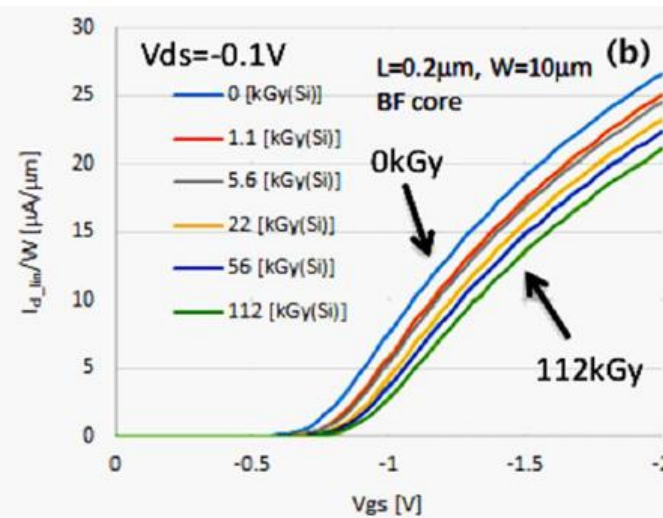
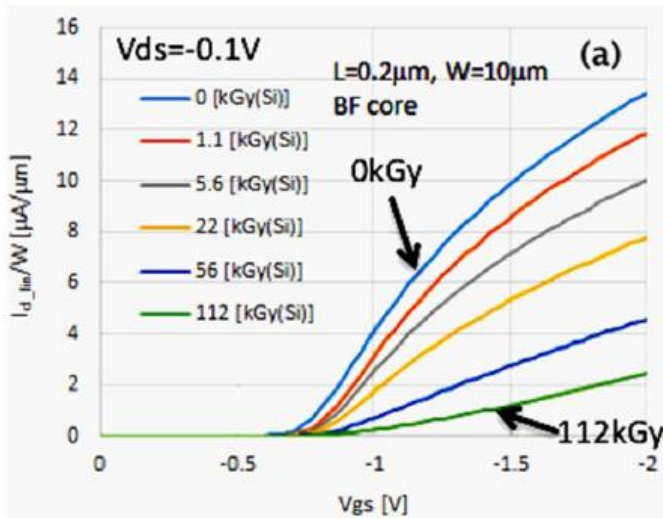
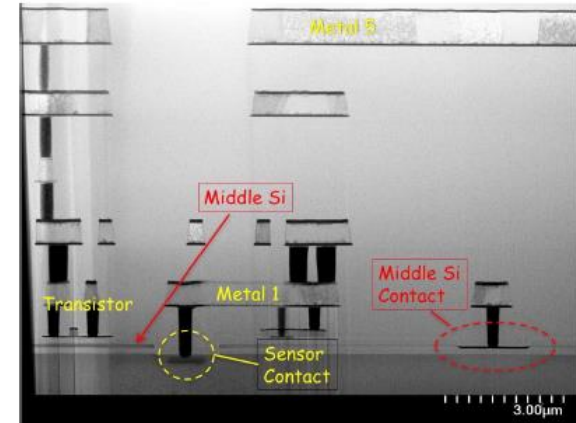


Y. Arai, IEEE IEDM 2017



# FD-SOI progress

- Problem: buried oxide affects electronics → back-gate effect
- Solution: 2 buried oxide layer
- Ionizing radiation tolerance up to 100kGy

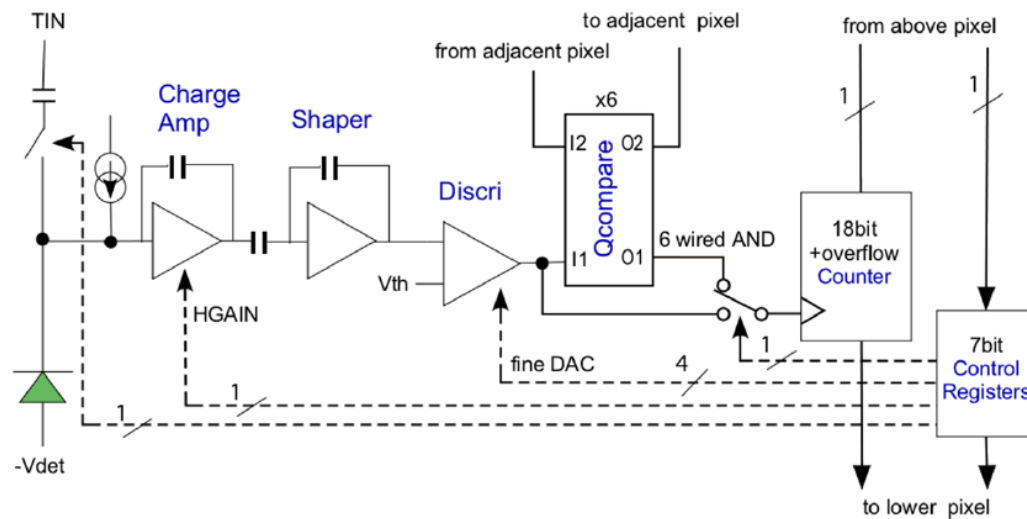
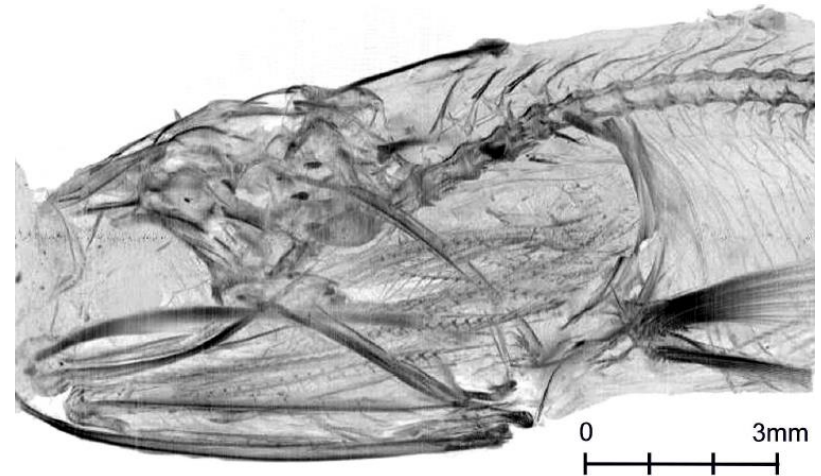


Y. Arai, IEEE IEDM 2017



# FD-SOI: X-ray imaging

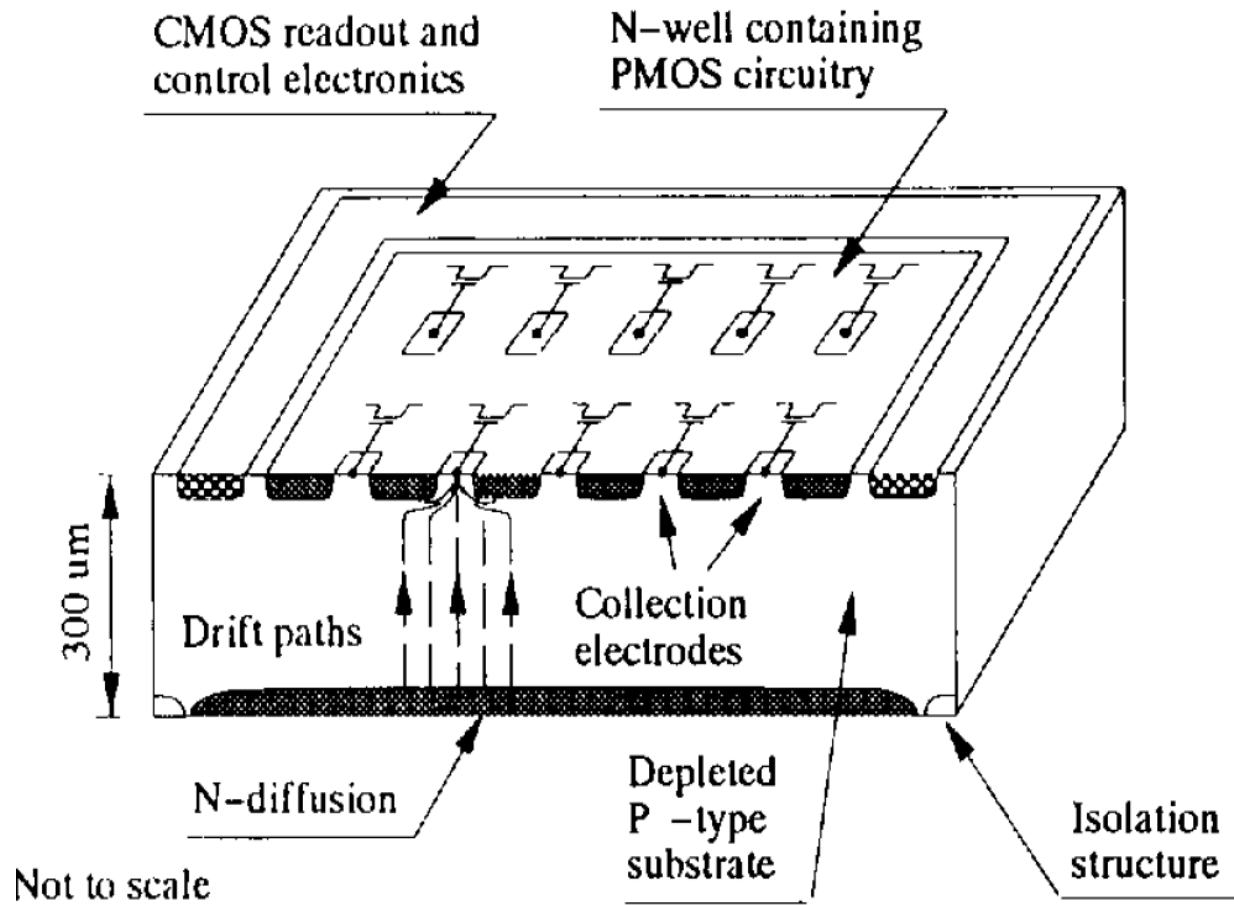
- Pixel size:  $17\ \mu\text{m}$
- Pixel count:  $512 \times 832$
- Substrate thickness  $500\ \mu\text{m}$
- In-pixel photon counting electronics



Y. Arai, IEEE IEDM 2017



# Monolithic pixel array with backside junction



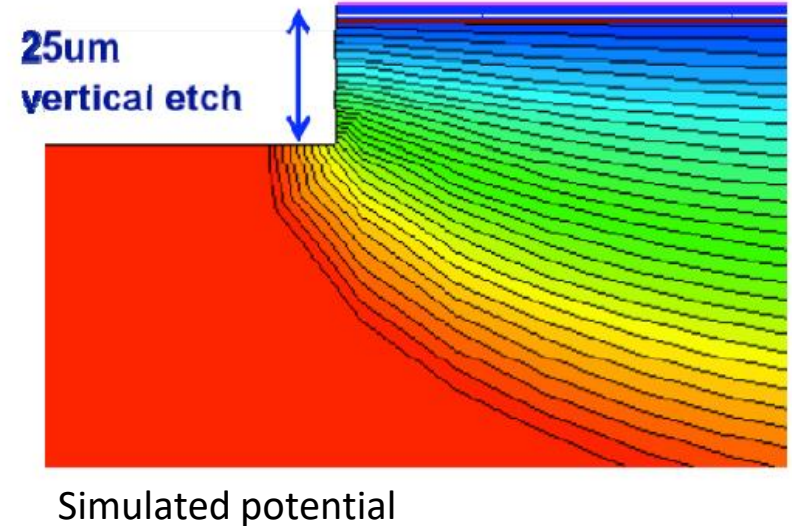
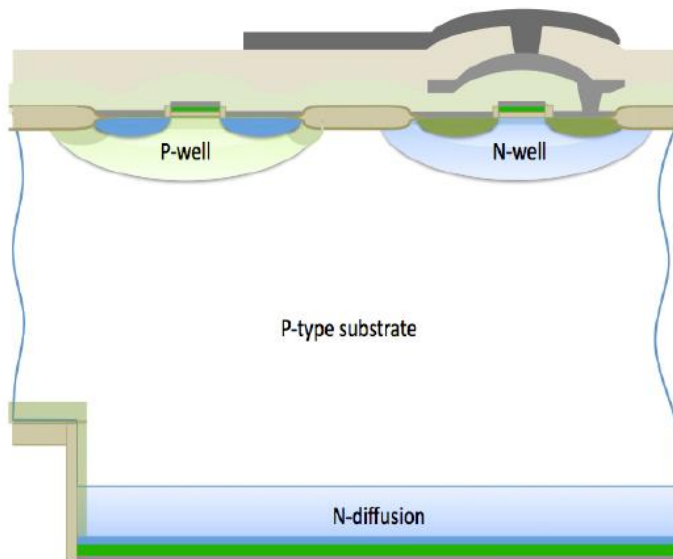
W. Snoeys, IEEE Tran. Electron Dev., 1994

J. D. Segal, IEEE NSS, Knoxville, TN, 2010, pp. 1896-1900.



# Monolithic pixel array with backside junction

- PMOS-only pixel electronics
- BS junction terminates on a trench for breakdown prevention
- Difficult to integrate in a commercial CMOS



J. D. Segal, IEEE NSS, Knoxville, TN, 2010, pp. 1896-1900.



# Outline

---

- Radiation detection in silicon
- CMOS technologies: characteristics, opportunities and challenges
- Monolithic active pixels for photon imaging
- MAPS: design approaches and research directions
- **SEED project overview**



# INFN project SEED project

---

## Sensor with Embedded Electronics Development

- Goal: fully depleted monolithic pixel sensor
- High timing resolution (ns)
- Integrated CMOS pixel electronics
- Process development with an industrial partner (LFoundry)

INFN sections: Torino, Padova, Trento, Frascati, Perugia

**INFN-LFoundry patent pending**

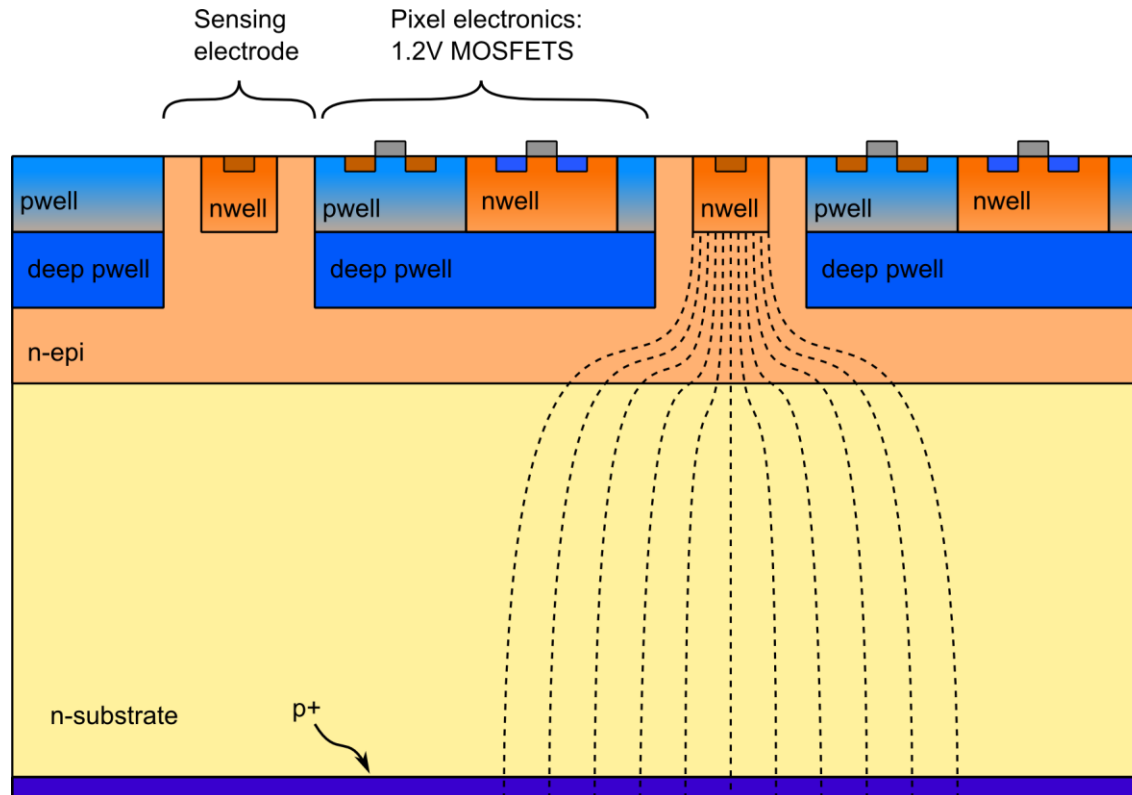


# SEED approach

Starting point: 110nm CMOS process with 1.2V transistors

Substrate thickness: 300um

Substrate doping: n-type, phosphorus,  $2.5 \times 10^{12} \text{ cm}^{-3}$







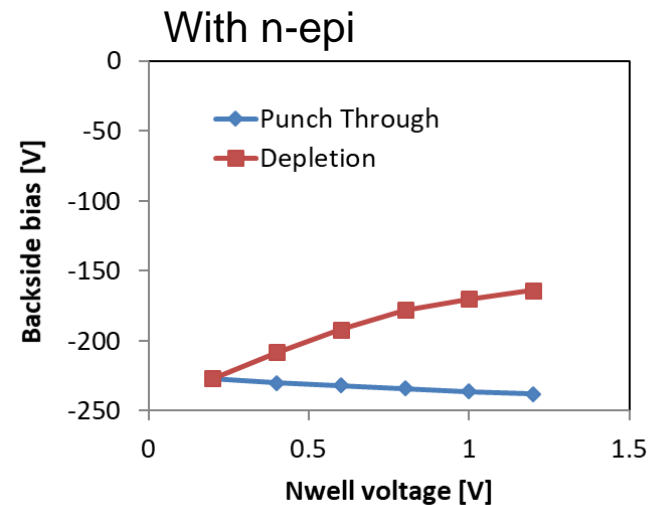
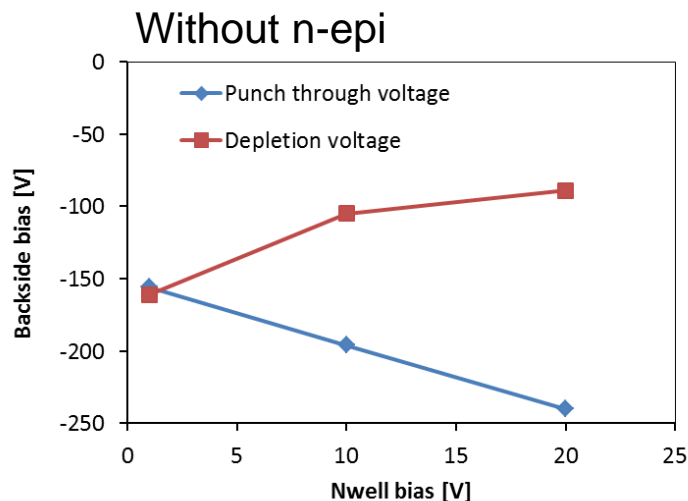
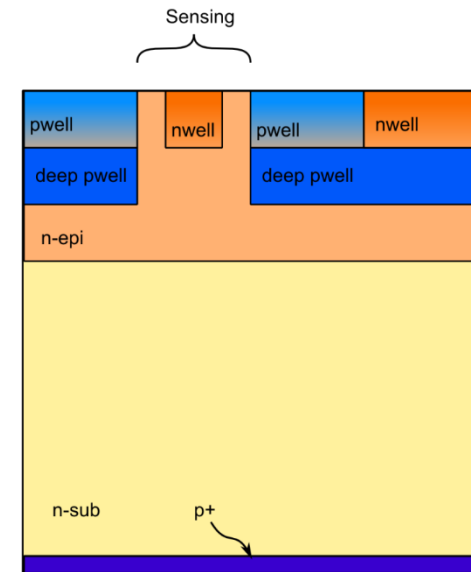
# Sensor bias

Backside bias:

- Large enough to reach **full depletion**
- Small enough to avoid **punch through**

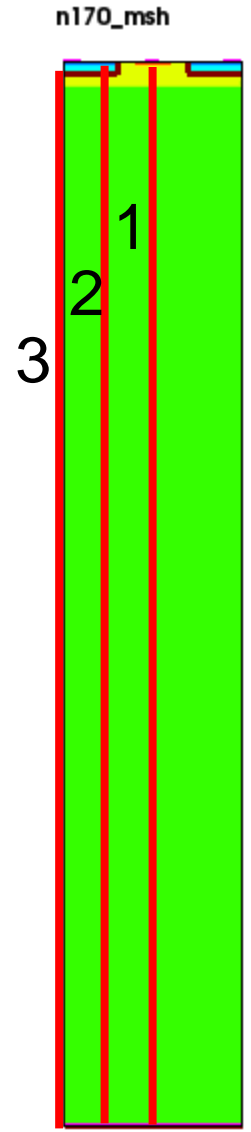
Constraint: maximum n-well voltage is 1.2V  
(available low voltage transistors)

N-type epitaxial layer with doping larger than substrate:  
increased control of the potential barrier below deep pwell



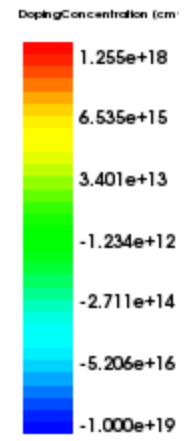


# Charge collection: 300um

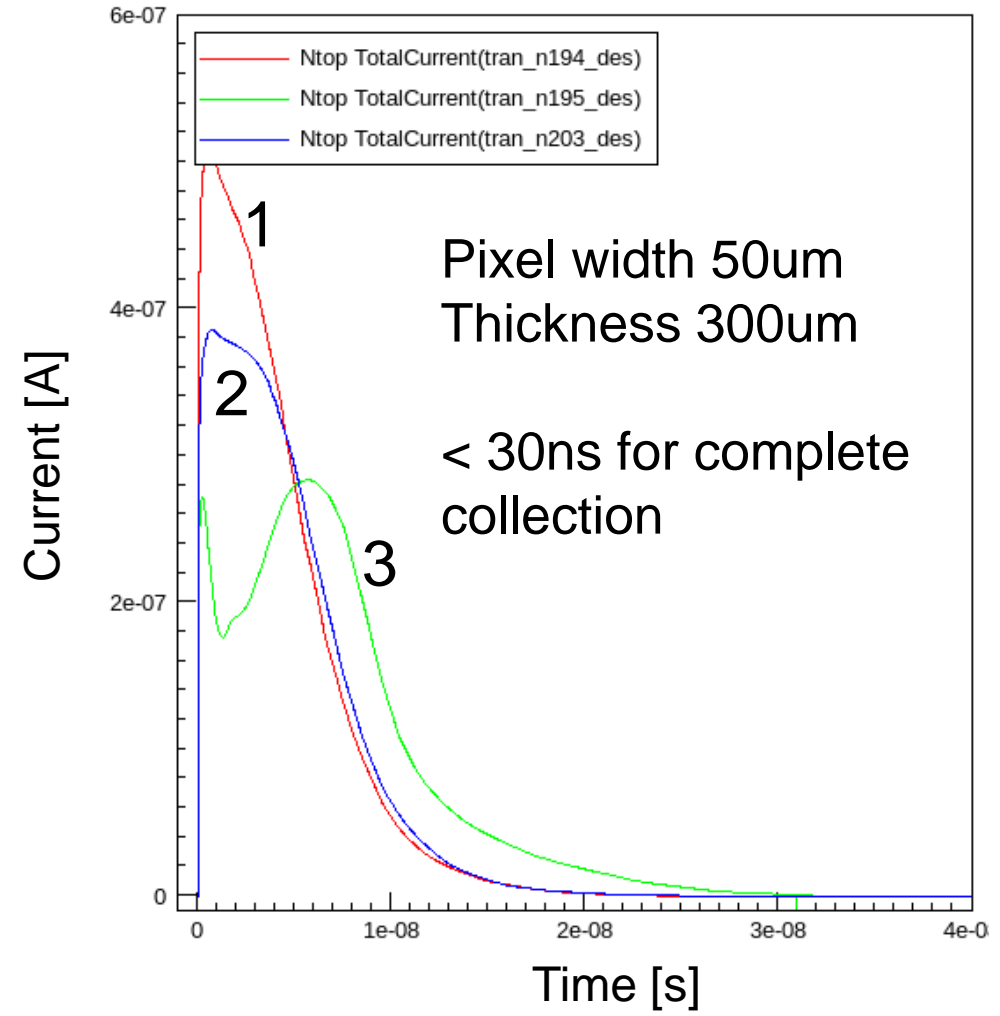


Vbias= -200V

MIP incident in  
3 different positions



W = 50um T = 300um



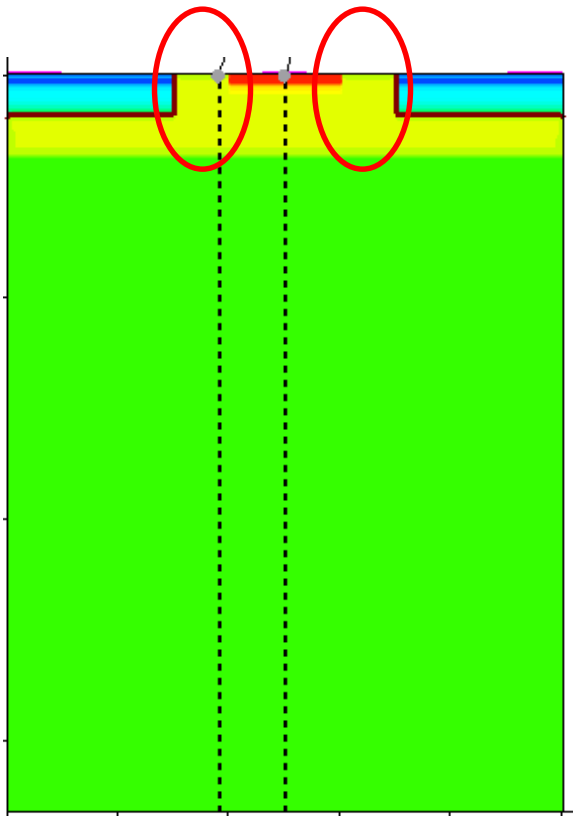


# Collection node capacitance

---

Dominant contribution:  
perimeter capacitance

Approximate perimeter cap:  
**0.25fF/um**

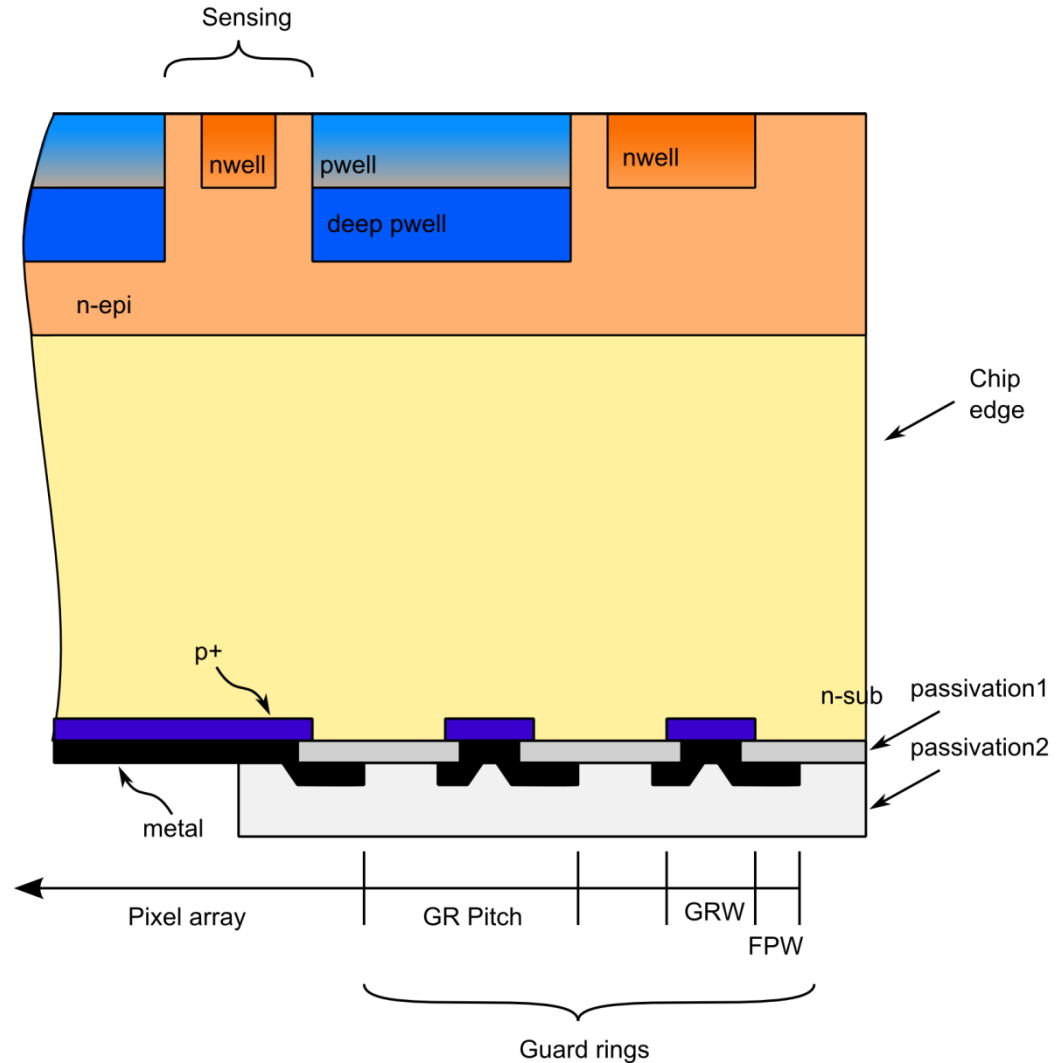


Capacitance for a 10um x 10um  
collection node = 10fF



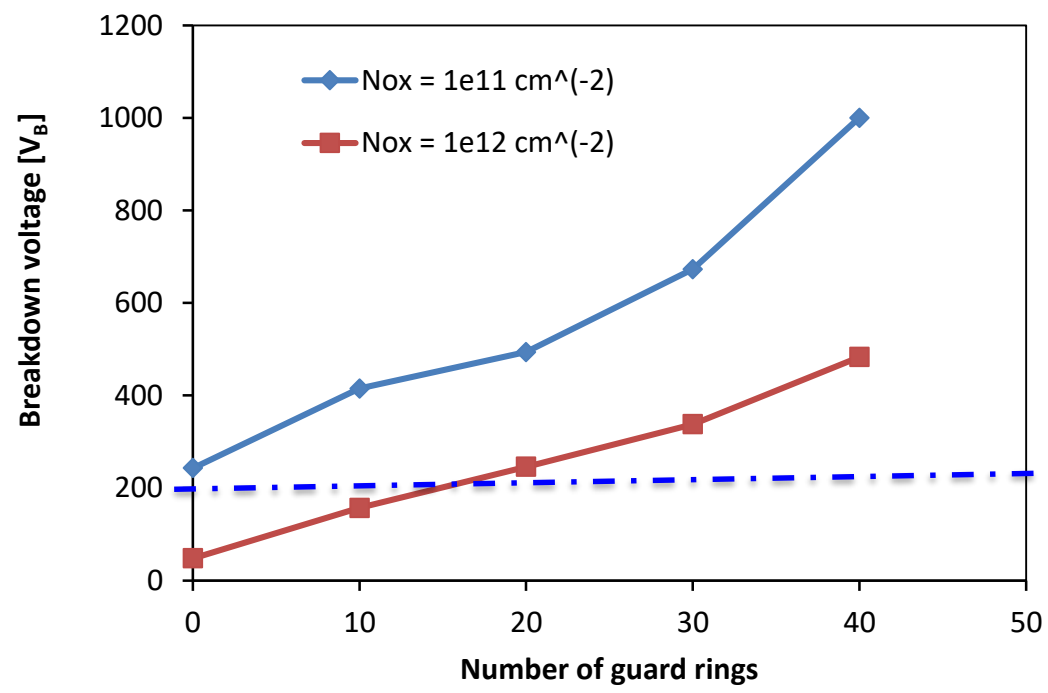
# Sensor periphery

- Nwell guard ring in the top plane
- Pwell ring termination structures in the back plane

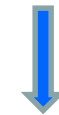




# Breakdown voltage simulations



GR pitch = 6μm



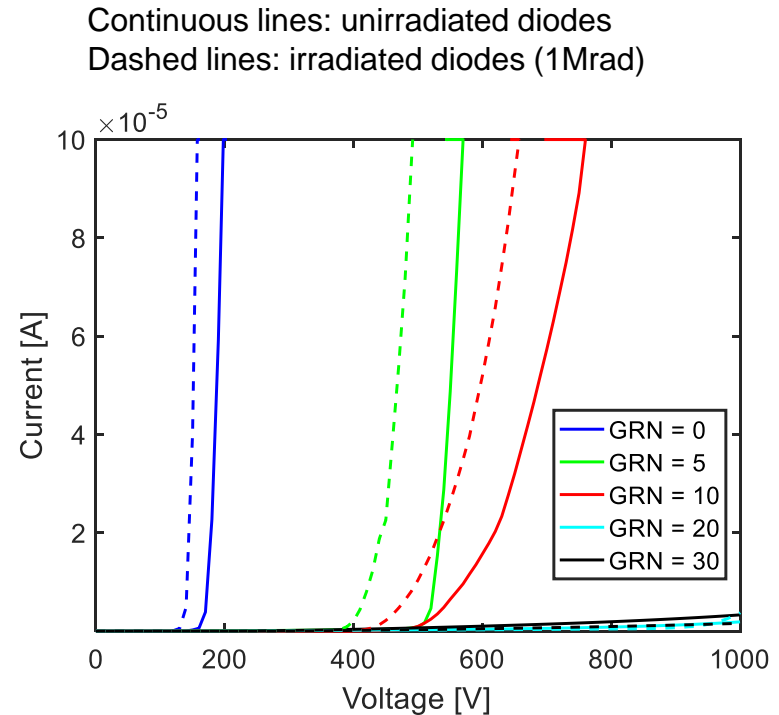
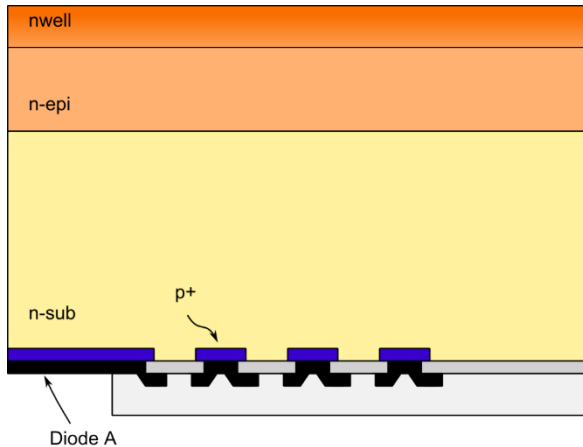
20 GR termination structure size = 120μm

- P+ shallow junction: many guard rings are needed
- Simulations with low ( $10^{11} \text{ cm}^{-3}$ ) and high ( $10^{12} \text{ cm}^{-3}$ ) positive oxide charge density
- At least 20 GR are needed to bias the sensor at 200V in the worst case



# Test structures: breakdown voltage

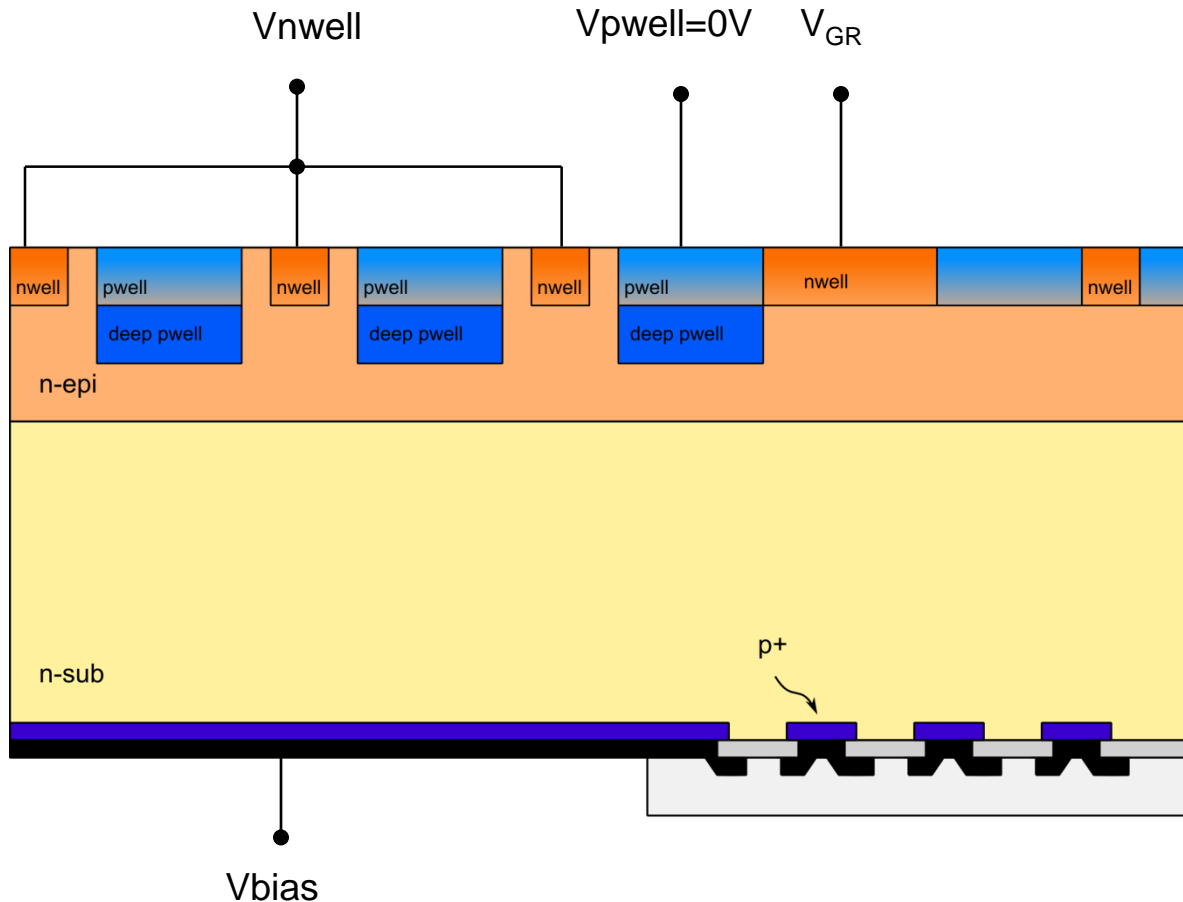
- Test diodes with different guard ring number (GRN)
- Breakdown voltage increases with GRN
- Test on unirradiated diodes and after 1Mrad irradiation (X-rays)
- Diodes with 20 and 30 guard rings have a breakdown voltage larger than 1000V





# Test structure: pseudo-pixel array

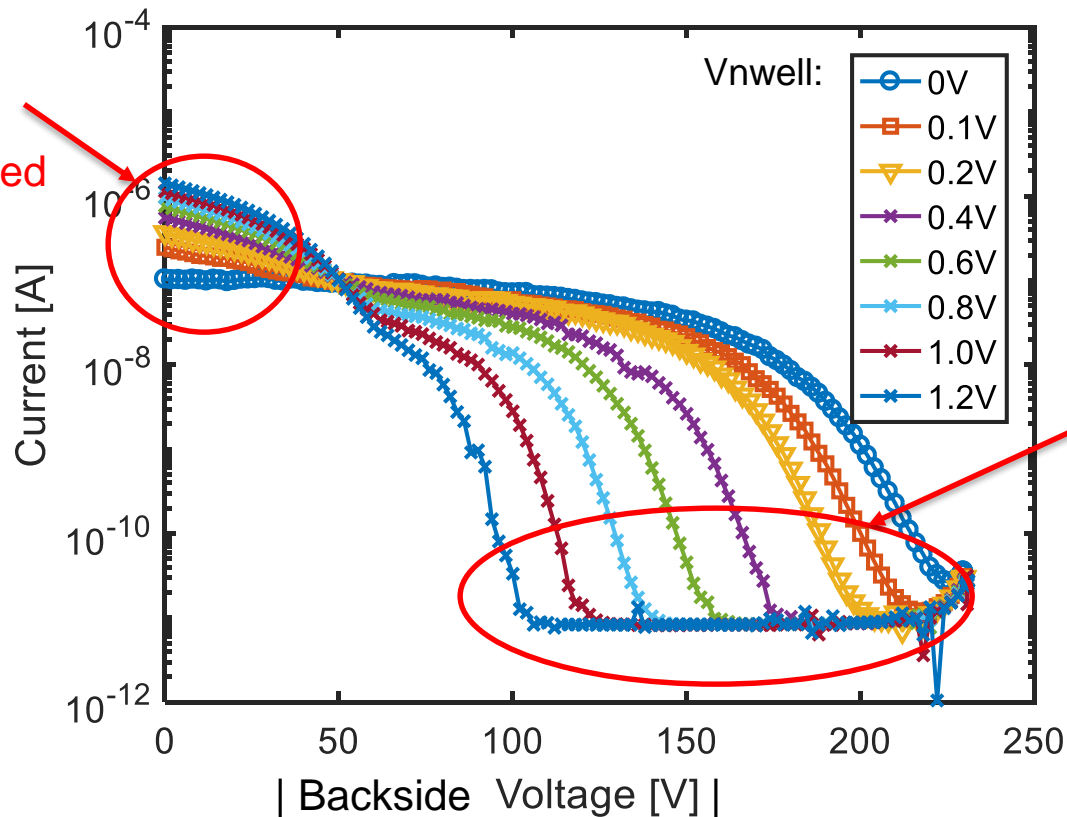
- Small (8x8) pixel array in parallel without electronics with external readout. Pixel size 50 $\mu$ m x 50 $\mu$ m





# Test pixels dark current

- Dark current can be measured only if the sensor is depleted
- Strong depletion dependence on small applied nwell voltage



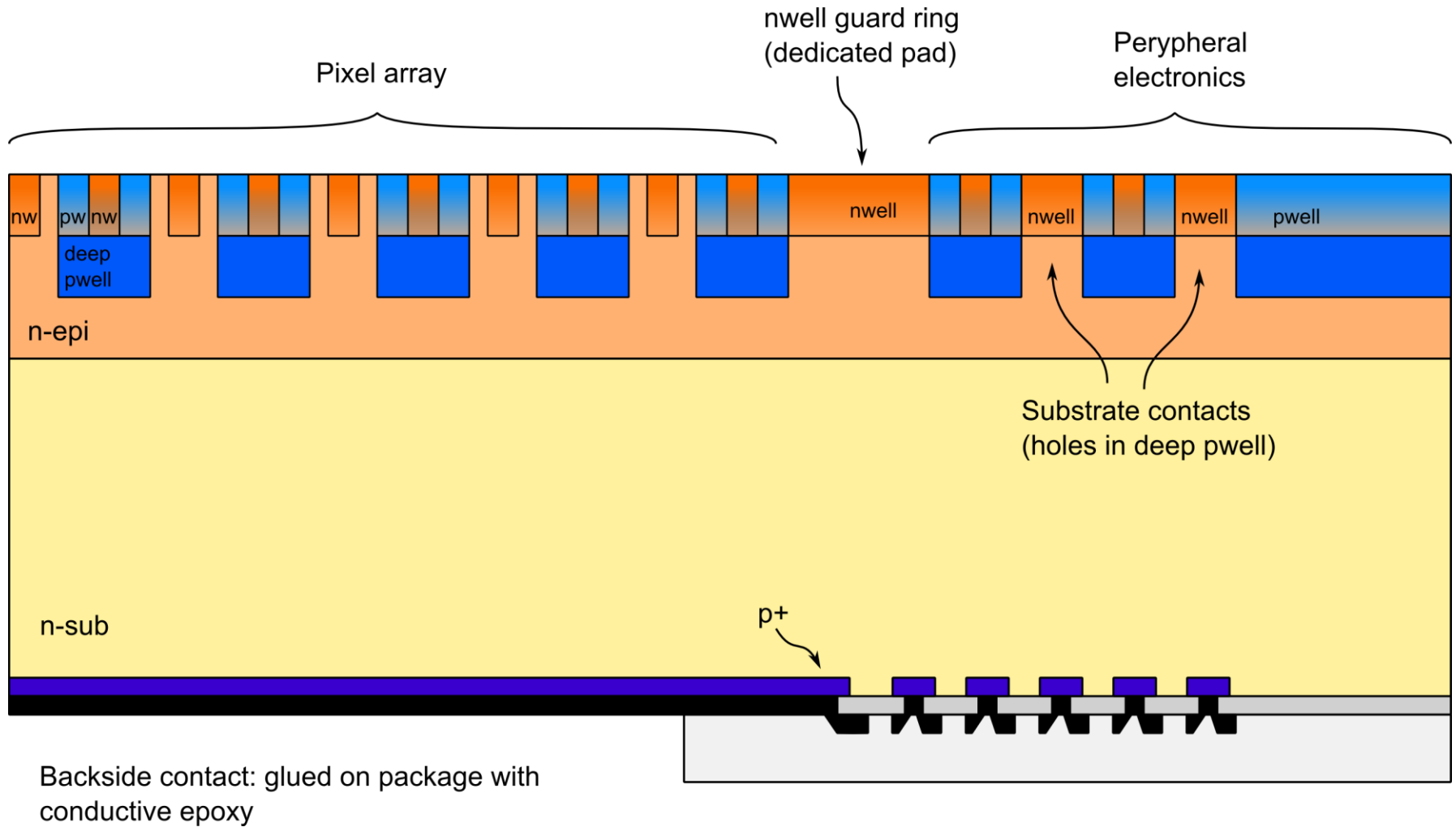
Current between guard ring and pixels in undepleted sensor

Depleted sensor: pixels isolated from guard ring



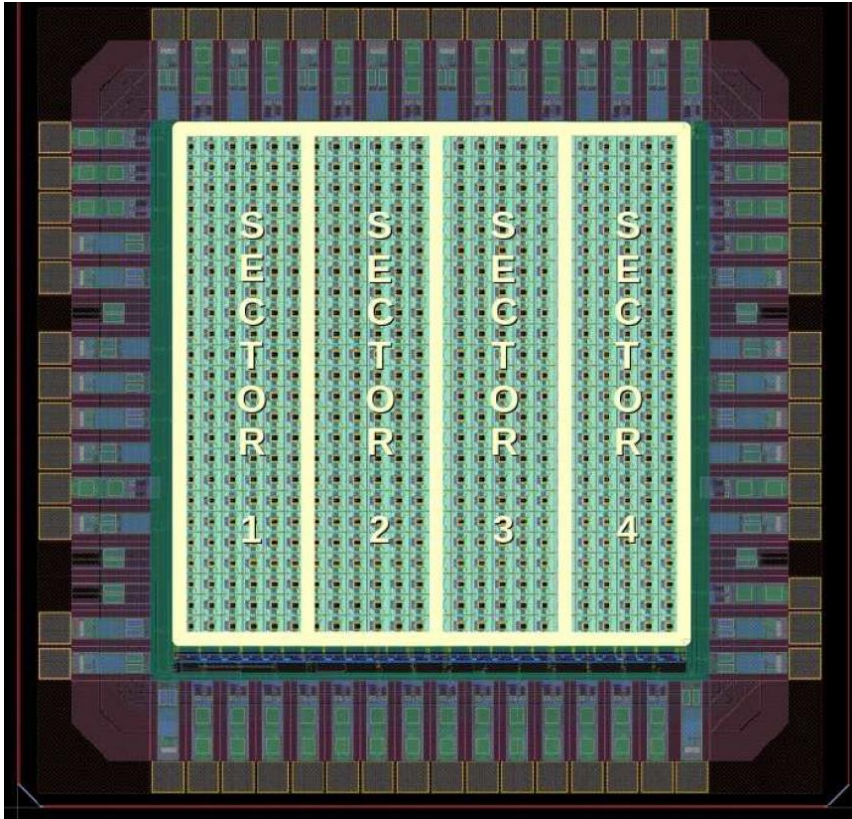


# Array cross section



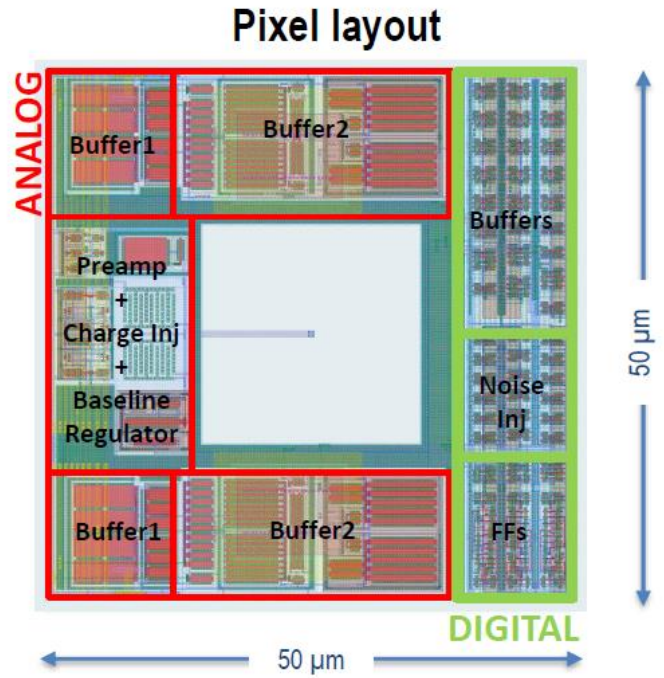
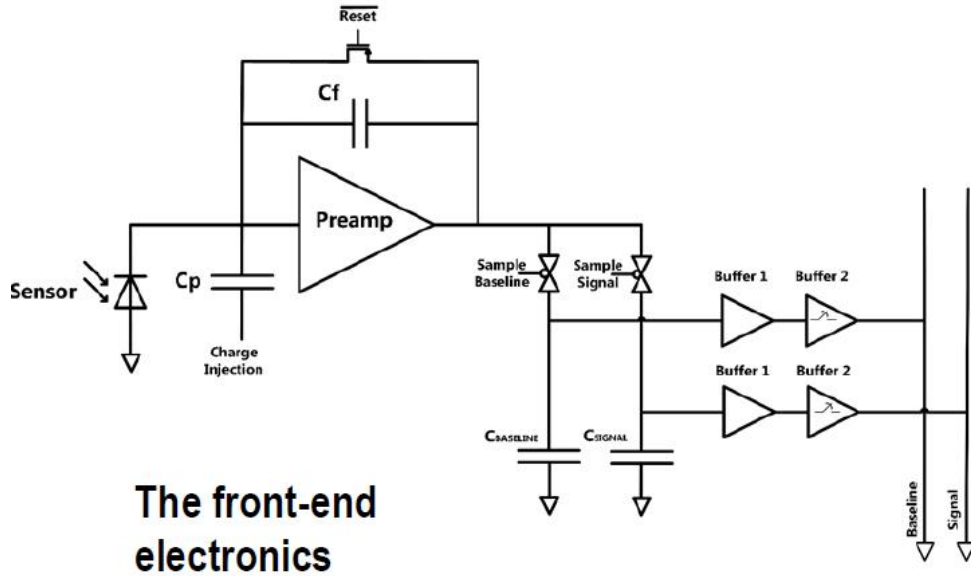


# Pixel array



- Die area:  $2 \times 2 \text{ mm}^2$
- low voltage operation: 1.2 V
- matrix of  $24 \times 24$  pixel units organized in 4 independent sectors
- 6 columns x 24 rows in each sector

# Pixel schematic and layout



- Both NMOS and PMOS transistors are used
- The electronics fits an area of  $30 \mu\text{m} \times 30 \mu\text{m}$
- Digital in-pixel logic



# Chip parameters

---

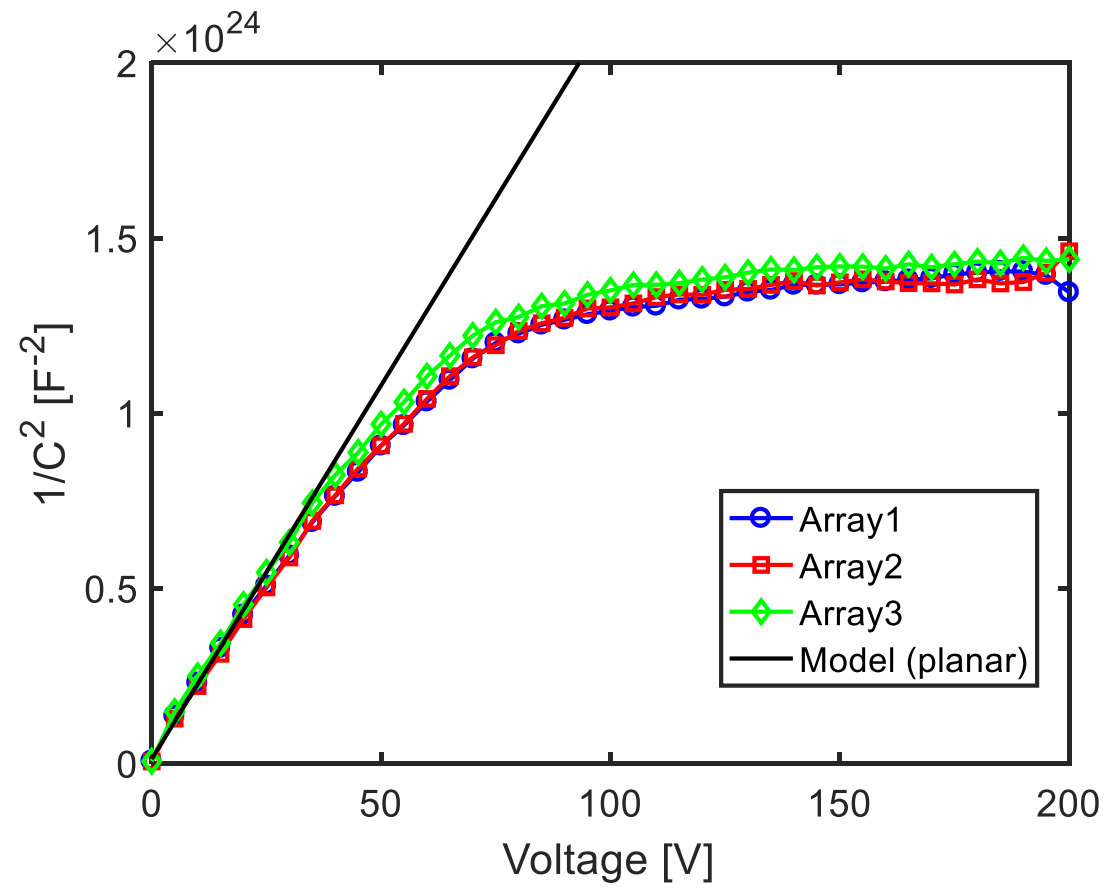
---

Parameter	Value
Analog gain	$\approx 130 \text{ mV/fC}$ ( $2.1 \text{ mV}/100 \text{ e}^-$ ) Transmission $\approx 370 \mu\text{W}$
Sensor Cap	40 fF
Storage Cap	$\approx 70 \text{ fF}$ (MIM CAPS)
Linearity Range	400 mV - 950 mV
Readout Speed	Up to 5 MHz
Other features	Internal Test Pulse Mask Mode Baseline Regulator
Shutter type	Snapshot Shutter
Readout Type	Correlated Double Sampling [3]

---



# Array backside measurements - CV

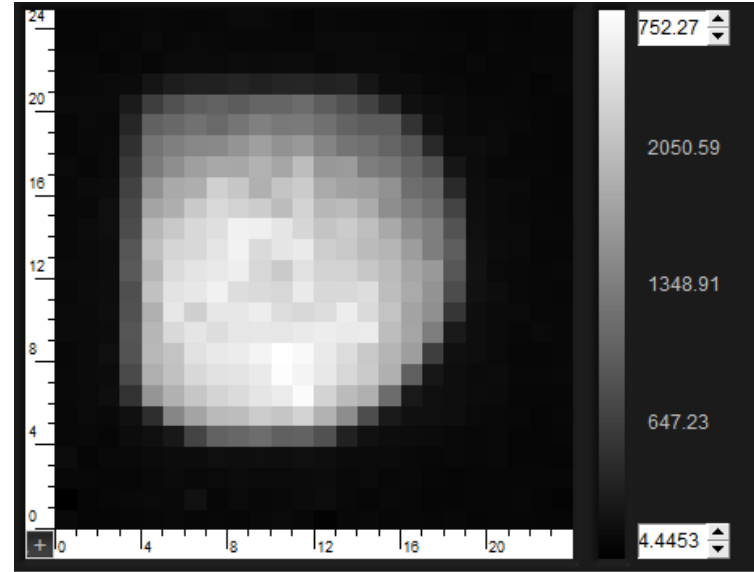
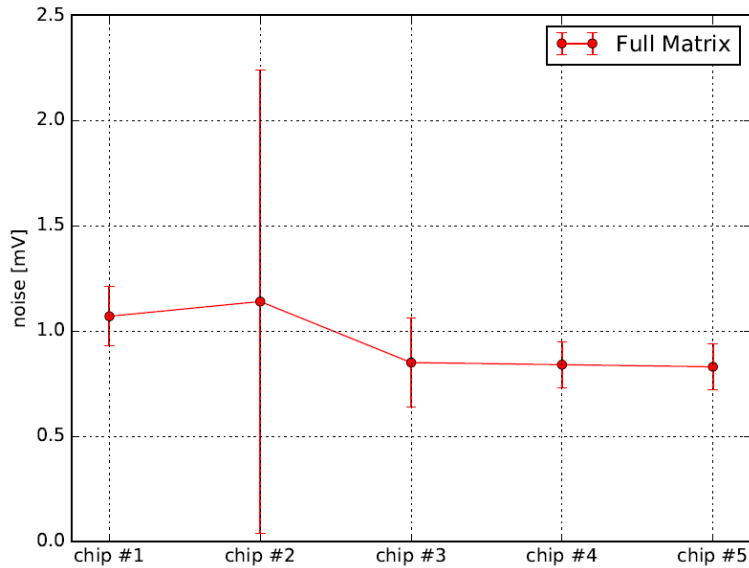


Doping  $2.4 \times 10^{12} \text{ cm}^{-3}$  – same as wafer specification

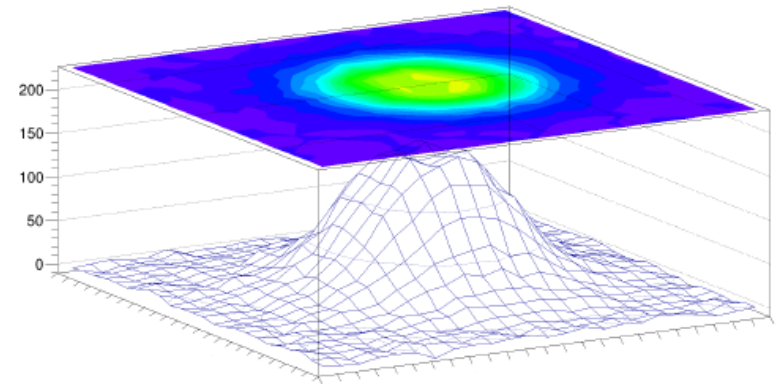


# Pixel array characterization

## IR laser pulse intensity map



## LASER PULSE RECONSTRUCTION

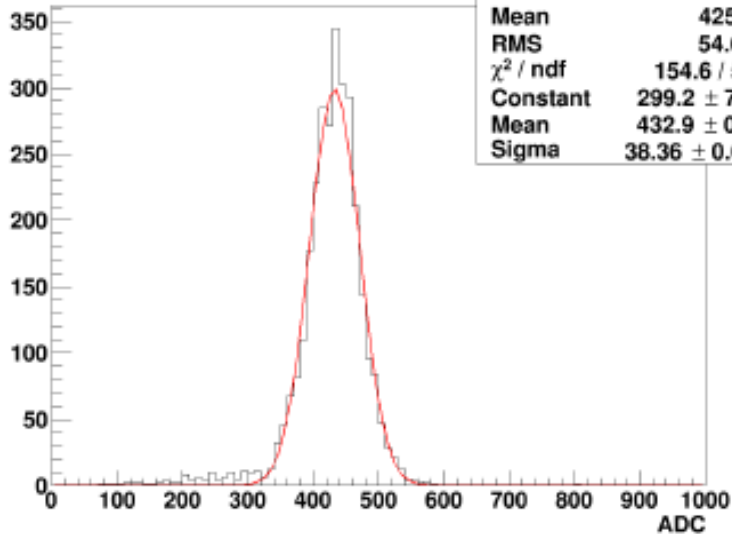


Average noise  $\sim 1\text{mV}$ :  
ENC  $< 50\text{e}^-$  rms at RT

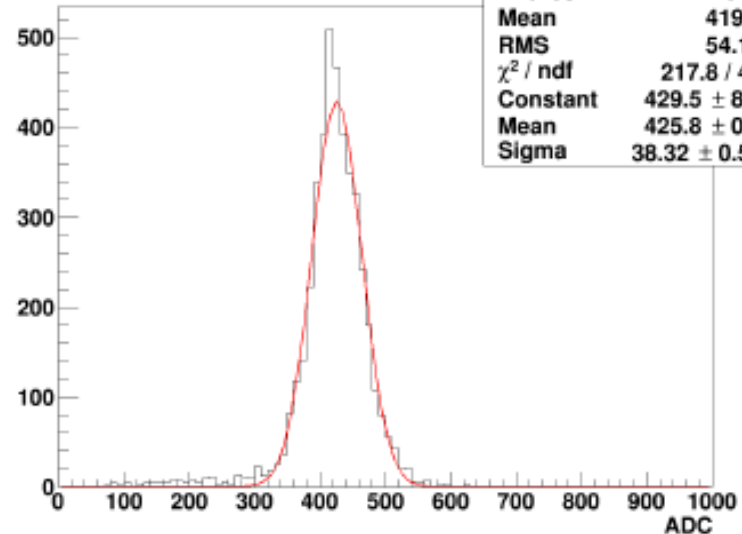


# Measurements with $^{55}\text{Fe}$

Cluster signal, Channel 0



Cluster signal, Channel 1



- Expected energy for the  $^{55}\text{Fe}$  peak: 5.9 keV (1650 e $^-$ )
- Standard deviation: 520 eV at RT
- Measured energy value: 420 counts used to estimate analog gain (117mV/fC)



# SEED: on-going and future plans

---

- Measurements on more chips and test structures (information on tech. variability)
- Radiation damage (IEL and NIEL)
- Charge collection speed (laser)
  
- New run with different substrate thickness:
  - 100 – 150um: particle tracking
  - 500um: X-ray imaging